SPLICE RESEARCH

Progress Report

ANALYTICAL AND EXPERIMENTAL INVESTIGATION OF STIFFENED FLUSH END-PLATE CONNECTIONS WITH FOUR BOLTS AT THE TENSION FLANGE

by

David Hendrick
and
Anant R. Kukreti
Thomas M. Murray
Co-Principal Investigators

Sponsored by

Metal Building Manufacturers Association
and
American Institute of Steel Construction

Report No. FSEL/MBMA 84-02

September 1984

FEARS STRUCTURAL ENGINEERING LABORATORY
School of Civil Engineering and Environmental Science
University of Oklahoma
Norman, Oklahoma 73019

TABLE OF CONTENTS

LIST OF FIGURES

LIST OF TABLES

ANALYTICAL AND EXPERIMENTAL INVESTIGATION OF STIFFENED FLUSH END-PLATE CONNECTIONS WITH FOUR BOLTS AT THE TENSION FLANGE

CHAPTER I

INTRODUCTION

1.1 Background

A research program to investigate the behavior of stiffened flush end-plate connections is being conducted at the Fears Structural Engineering Laboratory, University of Oklahoma under sponsorship of the Metal Building Manufacturing Association (MBMA) and the American Institute of Steel Construction (AISC). The purpose of this research is to develop design procedures for particular types of stiffened flush end-plate connections. Such connections, as shown in Figure 1.1, are primarily used for moment-resistant connections in portal frame construction. In the connection configuration shown in Figure 1.1(a), a gusset plate is placed between the tension bolt rows on both sides of the web. In Figure 1.1(b), the gusset plate is shown below the two rows of tension bolts.

The purpose of this study is to develop a rational method of design for the two stiffened flush end-plate connection configurations and to verify the results through extensive experimental testing. Both connection strength and flexibility are considered in the study. A design procedure is proposed and experimental evidence presented to justify the accuracy of the proposed method. Test results are also compared with the four bolt, unstiffened flush end-plate connection test results reported by Srouji(1).

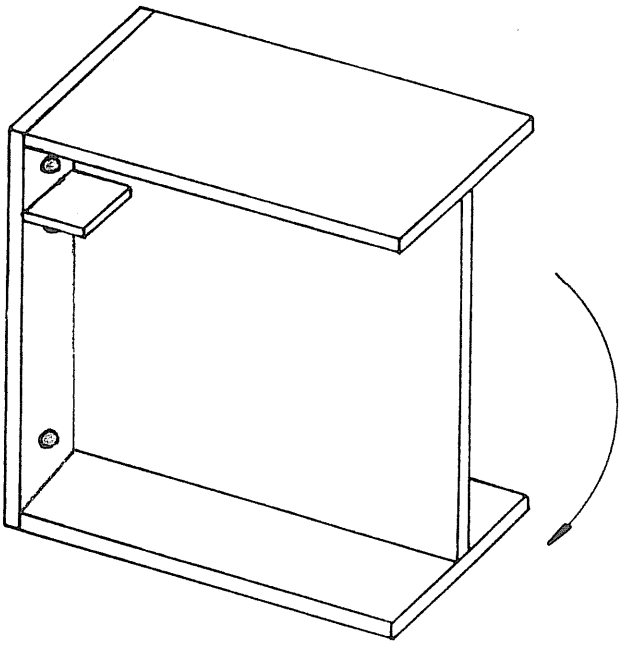

a) Gusset Plate Between Bolt Rows

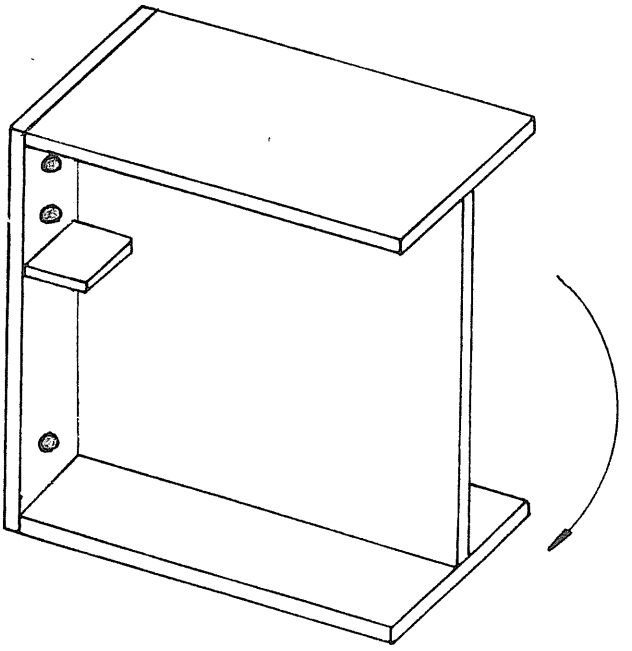

b) Gusset Plate Outside Bolt Rows

Figure 1.1 Typical Stiffened Flush End-Plate Connections

1.2 Literature Review

An extensive review of end-plate connection literature was reported by Srouji[1]. In his review he briefly discussed design procedures by various authors and determined end-plate thicknesses for a number of configurations based on the recommended design procedures. Because the variation in end-plate thicknesses was as large as 100%, a research program was undertaken to study unstiffened flush end-plate connections. The result was design procedures for two and four bolt at the tension flange flush end-plate connections based on yield-line analysis with bolt force predictions based on a method proposed by Kennedy[2]. Srouji's work is reported in Reference 1. The following research program is an extension of Srouji's research for stiffened flush end-plate connections of the configurations shown in Figure 1.1.

1.3 Scope of Research

The purpose of the research described here is to develop design procedures for stiffened flush end-plate connections with two rows of two bolts at the tension flange. A complete design procedure must provide criteria for:

1. Determination of end-plate thickness using given geometry and material yield stress, e.g. strength criterion.

2. Determination of required bolt diameter including prying effects, if any, using given end-plate geometry and thickness, and bolt pretension and proof load forces, e.g. bolt force criterion.

3. Determination of the moment-curvature relationship of the entire connection so that possible effects of connection flexibility can be accounted for in the frame design, e.g. stiffness criterion.

Yield-line theory is used here to develop strength criteria from which end-plate thickness is determined. A modification of the procedure suggested by Kennedy et al.[2] is used to develop bolt strength requirements. Development of a stiffness criterion is not addressed in this report. The analytical developments for the strength and bolt force criteria are described in Sections 2.1 and 2.2, respectively.

Eight full-scale tests were conducted to verify the analytical results, four tests of each configuration shown in Figure 1.1. The test specimens, set-up and procedures are described in Section 3.1. Comparisons are made with the yield-line strength and bolt force analytical predictions in Section 3.2. Finally, design procedures for end-plate thickness and bolt strength are presented in Chapter IV.

CHAPTER II

ANALYTICAL STUDY

2.1 Yield-Line Theory

2.1.1 General

Yield-line theory was first introduced to analyze reinforced concrete slabs. A yield-line is a continuous formation of plastic hinges along a straight or curved line. The failure mechanism of the slab is assumed to exist when the yield-lines form a kinematically valid collapse mechanism. Since the elastic deformations are negligible compared to the plastic deformations, it has been proven acceptable to assume that the yield-lines divide the slab into rigid plane regions. Most of the development of this theory is related to reinforced concrete; however, the principles and findings are applicable to steel plates.

Generally, yield-line patterns are assumed to be a series of straight lines; however, some work has been done with curved yield lines. To establish the location of a yield line, the following guidelines should be followed:

1. Axes of rotation generally lie along lines of support.

2. Yield lines pass through the intersection of the axes of rotation of adjacent plate segments.

3. Along every yield line, the bending moment is assumed to be constant and is taken as the plastic moment of the plate.

The analysis of a yield-line mechanism can be performed by two different methods, the equilibrium method and the virtual work or energy method. The latter method is comparatively simple and straight-forward and is preferred. In this method, the external work done by the applied loads from a small arbitrary virtual deflection is set equal to the internal work done as the plate rotates at the yield lines to accommodate this virtual deflection. For a specified yield-line pattern and loading, a certain plastic moment will be required along the hinge lines. For the same loading, other patterns may result in a larger required plastic moment capacity. Hence, the controlling pattern is the one pattern which requires the largest required plastic moment. Or conversely, for a given plastic moment capacity, the controlling mechanism is the one which produces the lowest failure load. This implies that the yield-line theory is an upper bound procedure and the least upper bound must be found.

To determine the required plastic moment capacity or the failure load, an arbitrary succession of possible yield-line mechanisms must be selected. By equating the internal and external work, the relation between the applied loads and the ultimate resisting moments is obtained. The resulting equation is then solved for either the unknown loads or unknown moments, and by comparing the different values obtained from the various mechanisms the controlling minimum load (or maximum required plastic moment) obtained.

The internal energy stored in a particular yield-line mechanism is the sum of the internal energy stored in each yield line forming the mechanism. The internal energy stored in any given yield line is obtained by multiplying the normal moment on the yield line with the normal rotation

of the yield line. Thus the energy stored in the n-th yield line of length L_n is

$$w_{in} = \int_{L_n} m_p \theta_n ds \tag{2.1}$$

where θ_n is the relative rotation of line n, and ds is the elemental length of line n. The internal energy stored by a yield-line mechanism can be written as

$$W_i = \sum_{n=1}^{N} \int_{L_n} m_p \theta_n ds$$

$$= \sum_{n=1}^{N} m_p \theta_n L_n \tag{2.2}$$

where N is the number of yield lines in the mechanism.

In complicated yield-line patterns the values of the relative rotation are somewhat tedious to obtain, therefore it is more convenient to resolve the slopes and moments in the x- and y- directions. This results in the following form of Equation 2.2

$$W_i = \sum_{n=1}^{N} (m_{px} \theta_{nx} L_x + m_{py} \theta_{ny} L_y) \tag{2.3}$$

in which m_{px} and m_{py} are the x- and y-components of the normal moment capacity per unit length, L_x and L_y are the x- and y-components of the yield line length, and θ_{nx} and θ_{ny} are the x- and y- components of the relative normal rotation of yield line n.

To calculate the values of θ_{nx} and θ_{ny}, convenient straight lines

parallel to the x- and y- axis in the two segments intersecting at the yield-line are selected and their relative rotation calculated by selecting straight lines with known displacements at the ends.

2.1.2 Application to Stiffened Flush End-Plates

A number of yield-line patterns are possible for the stiffened flush end-plate geometries defined in Figure 2.1. The controlling yield-line mechanisms used in this study are shown in Figures 2.2 and 2.3. These patterns were determined from a study of possible yield-line patterns and predict the least moment capacity of the sets analyzed. The resulting virtual work expressions are found in Appendix B.

For both patterns, the external work done due to a unit displacement at the top of the beam flange, resulting in a rotation of the beam cross-section about the outside of the compression flange is given by

$$W_e = M_u \theta \tag{2.4}$$

where M_u = factored beam moment at the end-plate, and θ = the rotation at the connection, equal to 1/h, where h = beam depth. The internal energy stored in the line mechanism shown in Figure 2.2 (see Appendix B) is

$$W_i = 4m_p \left\{ \left[\frac{b_f}{2} \left(\frac{1}{P_f} + \frac{1}{P_s} \right) + (P_f + P_s) \left(\frac{2}{g} \right) \right] \left(\frac{h - p_t}{h} \right) + \left[\frac{b_f}{2} \left(\frac{1}{P_s} + \frac{1}{s} \right) + (P_s + s) \left(\frac{2}{g} \right) \right] \left(\frac{h - P_t - P_b}{h} \right) \right\} \tag{2.5}$$

where p_f = the distance from the bolt centerline to the face of the flange, equal to $(p_t - t_f)$, and s = the distance between parallel yield lines, to be determined. The unknown quantity s in Equation 2.5 is obtained by differentiating the internal work equation with respect to s and equating to

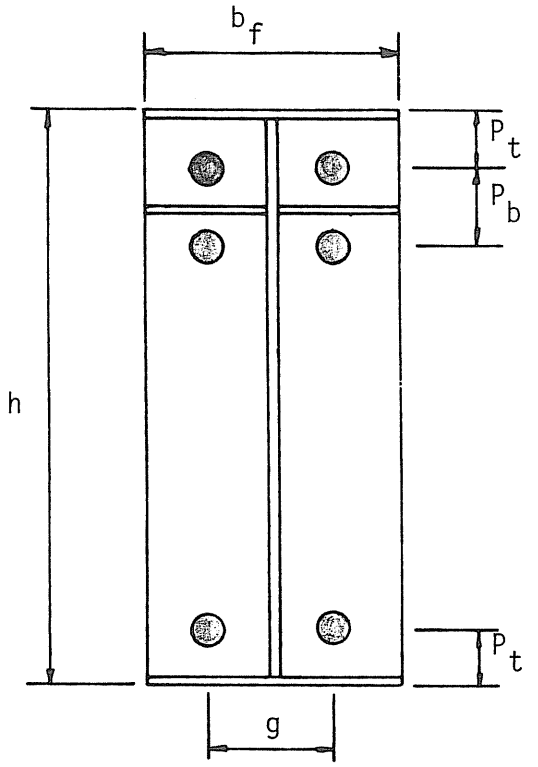

a) Gusset Plate Between Bolt Rows

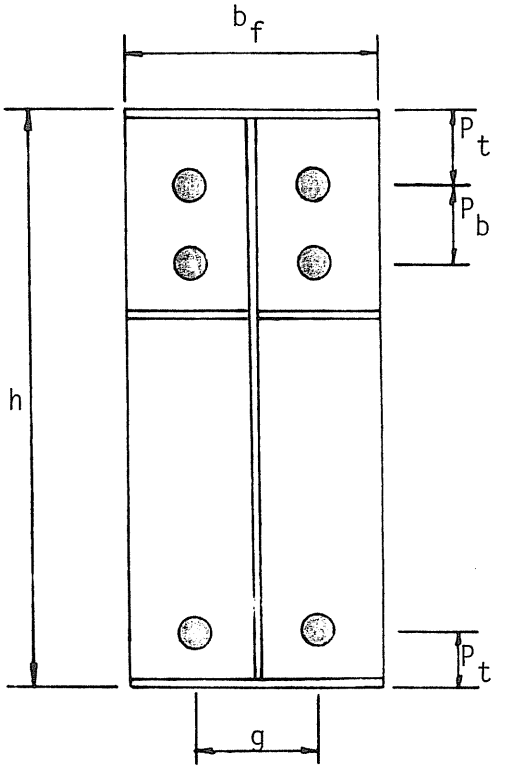

b) Gusset Plate Outside Bolt Rows

Figure 2.1 Definition of End Plate Geometry

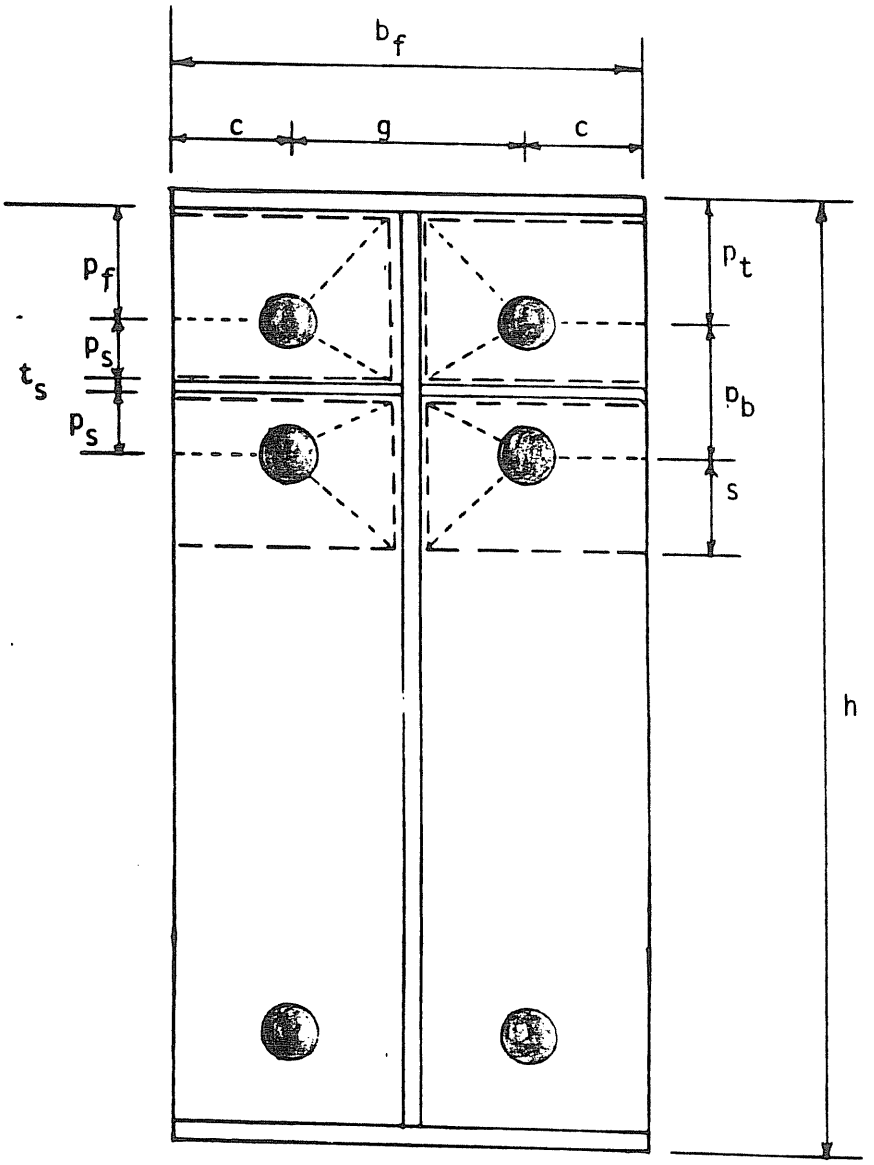

Figure 2.2 Controlling Yield-Line Mechansim for Gusset Plate Between the Tension Bolt Rows

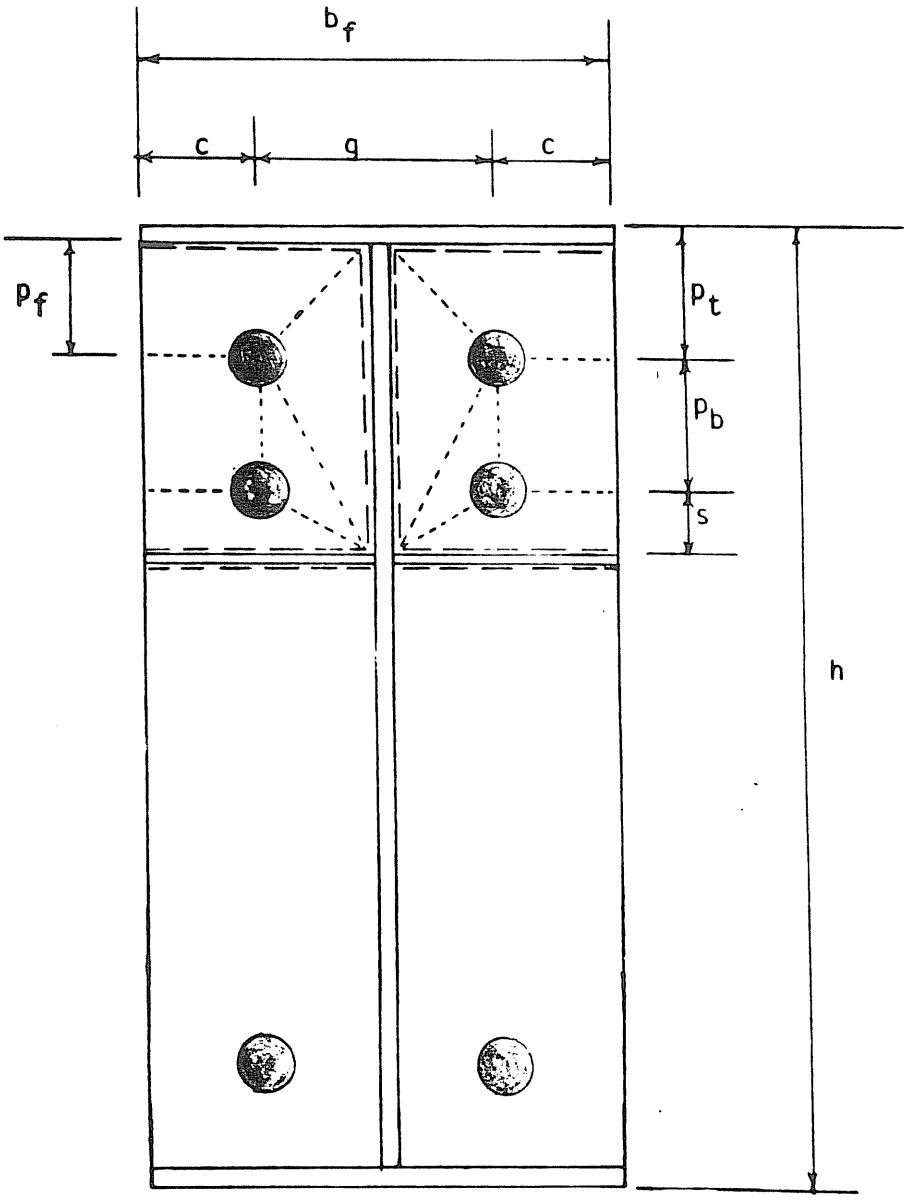

Figure 2.3 Controlling Yield-Line Mechanisms for Gusset Plate Outside the Tension Bolt Rows

zero, resulting in

$$s = \frac{1}{2}\sqrt{b_f g} \tag{2.6}$$

On equating the internal and external work terms and cancelling θ, the following expression is obtained

$$M_u = F_{py}\, t_p^2 \left\{ \left[\frac{b_f}{2}\left(\frac{1}{p_f} + \frac{1}{p_s}\right) + (p_f + p_s)\left(\frac{2}{g}\right) \right] (h - p_t) + \left[\frac{b_f}{2}\left(\frac{1}{p_s} + \frac{1}{s}\right) + (p_s + s)\left(\frac{2}{g}\right) \right] (h - p_t - p_b) \right\} \tag{2.7}$$

where $m_p = t_p^2 F_y/4$. Equation 2.7 can be solved for t_p, the end-plate thickness, in terms of the beam moment, M_u,

$$t_p = \left\{ \frac{M_u/F_{py}}{\left[\frac{b_f}{2}\left(\frac{1}{p_f} + \frac{1}{p_s}\right) + (p_f+p_s)\left(\frac{2}{g}\right) \right] (h-p_t) + \left[\frac{b_f}{2}\left(\frac{1}{p_s} + \frac{1}{s}\right) + (p_s+s)\left(\frac{2}{g}\right) \right] (h-p_t-p_b)} \right\}^{1/2} \tag{2.8}$$

The controlling mechanism for the two row flush end-plate with the stiffener outside the bolt rows, Figure 2.3, is calculated in a similar manner. The internal energy stored in the mechanism is (see Appendix B):

$$w_i = 4m_p \left[\frac{b_f}{2h}\left(\frac{h-p_t}{p_f}\right) + \frac{h-p_t-p_b}{s} + \frac{1}{2}\right) + \frac{2(h-p_t)}{gh}(p_f+p_b+s) + \frac{2p_b}{g}\left(\frac{h-p_t-p_b}{h}\right) \right] \tag{2.9}$$

where p_f equals $(p_t - t_f)$ as before. On the other hand, s = the distance from the center line of the inner bolt to the inner edge of the stiffener.

On equating the internal and external work terms and cancelling θ, the following expression is obtained

$$M_u = F_{py}\, t_p^2 \left[\frac{b_f}{2} \left(\frac{h-p_t}{p_f} + \frac{h-p_t-p_b}{s} + \frac{1}{2} \right) + \frac{2(h-p_t)}{g} (p_f+p_b+s) \right.$$

$$\left. \frac{2p_b}{g} (h-p_t-p_b) \right] \qquad (2.10)$$

Solving Equation 2.10 for t_p yields,

$$t_p = \left[\frac{M_u/F_{py}}{\frac{b_f}{2} \left(\frac{h-p_t}{p_f} + \frac{h-p_t-p_b}{s} + \frac{1}{2} \right) + \frac{2(h-p_t)}{g} (p_f+p_b+s) + \frac{2p_b}{g} (h-p_t-p_b)} \right]^{\frac{1}{2}}$$

(2.11)

Results from the above analyses are compared to experimental data in Chapter III.

2.2 Estimation of Bolt Forces

Basic yield-line analysis procedures do not result in bolt forces if prying action is to be considered. Therefore, it was necessary to use a different method to obtain the desired bolt forces. A method suggested by Kennedy et al.[2] can be used to estimate the bolt forces due to both applied force and prying action. The basic assumption in the method is that the end-plate goes through three different stages of behavior. During the first stage, plastic hinges have not developed and the plate is referred to as "thick". The prying force is taken as zero in this stage. When the plastic hinge forms at the beam flange, the plate becomes "intermediate" and the prying force is somewhere between zero and the maximum prying force that can occur. The last stage begins when a second plastic hinge forms at the bolt line. The end-plate in that stage is called "thin" and the prying force is at its maximum. For the two row flush end-plate, the model used for analysis is shown in Figure 2.4. Further assumptions

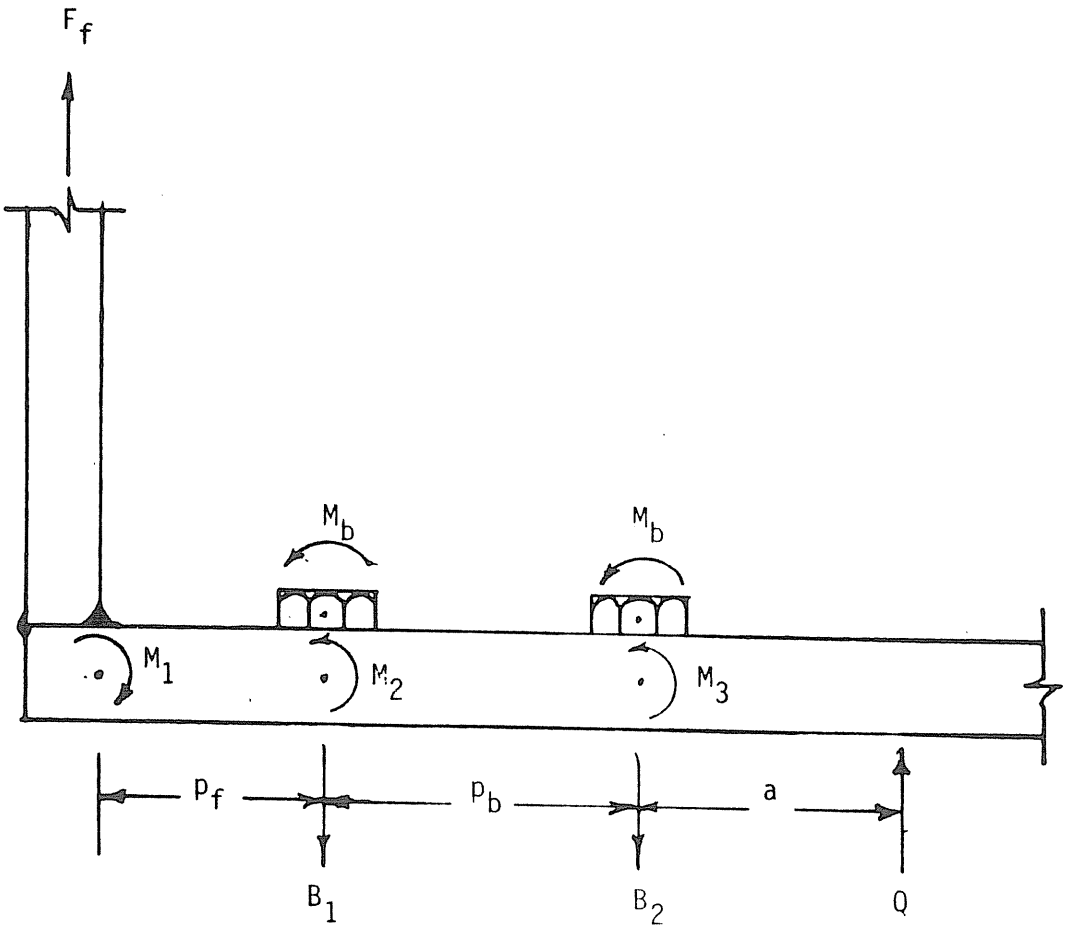

Figure 2.4 Modified Kennedy Model for Four-Bolt Flush End-Plate

have been made in order to obtain the bolt forces for this particular end-plate configuration. It is assumed that the inner bolt force, B_2, is a function of the flange force, F_f. For thick end-plates, B_2 is assumed to be zero. For intermediate end-plates, the inner bolt force, $B_2 = F_f/10$, and for thin end-plates, $B_2 = F_f/6$.

Following are the steps used in this method:

1. Select the load level, or moment at end-plate, at which the bolt forces are desired. Calculate the resulting flange force, F_f, and flange stress, σ_f.

2. Find the thick plate limit, t_1, for this load level using the following approximate equation:

$$t_1 = \sqrt{2.11\ p_f t_f\ \sigma_f / F_{by}} \tag{2.12}$$

Then using the following exact iterative equation:

$$t_1 = \sqrt{\frac{2t_f\sigma_f p_f}{\sqrt{F_{py}^2 - 3(t_f\sigma_f/2t_1)^2}}} \tag{2.13}$$

Once the thick plate limit is determined, the actual end-plate thickness, t_p, is compared to it. If $t_p > t_1$, then the prying force, Q, is taken as 0, otherwise, $Q \neq 0$ and the next step is used.

3. Find the thin plate limit, t_{11}, using the following approximate equation

$$t_{11} = \sqrt{\frac{2(b_f t_f \sigma_f p_f - (\pi/16) d_b^3 F_{yb})}{F_{py}(0.85 b_f + 0.80\ w')}} \tag{2.14}$$

where F_{yb} = yield stress of the bolt. Then using the iterative exact equation

$$t_{11} = \left(\frac{2(b_f t_f \sigma_f p_f - (\pi/16) d_b^3 F_{yb})}{b_f \sqrt{F_{py}^2 - 3\left(\frac{t_f}{2t_{11}} \sigma_f\right)^2} + w' \sqrt{F_{py}^2 - 3\left(\frac{b_f t_f}{2w' t_{11}} \sigma_f\right)^2}} \right)^{\frac{1}{2}} \quad (2.15)$$

Again, the end-plate thickness is compared to t_{11}. If $t_p > t_{11}$, then the plate is intermediate and the following equation for prying force is used

$$Q = F_2 \frac{(p_f + 0.1)}{(a + p_b)} - \frac{b_f t_p^2}{4(a+p_b)} \sqrt{F_{py}^2 - 3\left(\frac{F_2}{b_f t_p}\right)^2} - \frac{\pi d_b^3 F_{yb}}{16(a+p_b)} \quad (2.16)$$

where $a = t_p$ if $t_p/d_b < 2/3$ and $a = 2t_p$ otherwise, F = flange force per bolt and $F_2 = F_f/2$.

The bolt force in the two-row flush end-plates is given by

$$B_1 = \frac{F_2}{1.25} + Q \quad (2.17)$$

where B_1 = the outer row bolt force. Again, B_1 must be greater than the pretension force.

4. If $t_p < t_{11}$ the end-plate is said to be thin and the prying force is at its maximum.

$$Q_{max} = \frac{w' t_p^2}{4a} \sqrt{F_{py}^2 - 3\left(\frac{F'}{w' t_p}\right)^2} \quad (2.18)$$

where F' is the lesser of the following:

$$F_{limit} = \frac{t_p^2 F_{py}(0.85 b_f + 0.80 w') + (/16) d_b^3 F_{yb}}{4 p_f} \quad (2.19)$$

or

$$F_{max} = (F_f)_{max}/2$$

The bolt force is then

$$B_1 = \frac{F_2}{1.25} + Q \tag{2.20}$$

Bolt forces calculated using the above procedure are compared to experimentally obtained forces in Chapter III.

CHAPTER III

EXPERIMENTAL INVESTIGATION

3.1 Testing Program

3.1.1 Test Set-up and Procedure

To verify the analytical procedures described in Chapter II, eight tests were conducted. Four tests consisted of gusset plates between the tension bolt rows and four tests had gusset plates outside the tension bolt rows. The test set-up was as shown in Figures 3.1, 3.2 and 3.3. The end-plates and web gusset plates were welded to two beams and tested as splice connections under pure moment. All beam and end-plate material was A572 Gr50 steel and bolts were A325. Table 3.1 lists the nominal geometry of the eight end-plates and the measured yield stress obtained using coupons cut from identical material. The test designations shown in Table 3.1 are to be interpreted as follows: FB2-3/4-3/8-16 designates a stiffened flush end-plate test with two rows of 3/4 in. diameter bolts at the tension flange. The 'B' designates that a gusset plate is placed between the two rows of bolts. The end-plate thickness is 3/8 in. and the beam depth is 16 in. For tests where a stiffener was placed outside of the two bolt rows, an 'O' replaced the 'B' in the test designation. Tests were conducted using 16 in., 23 in. and 24 in. deep beams. The 23 in. beam used in tests 7 and 8 was to allow more space for the lateral brace mechanisms. Bolt pitch, gage, and diameter were varied within the limits shown in Table 3.2.

In the test setup, the load was applied using a closed-loop

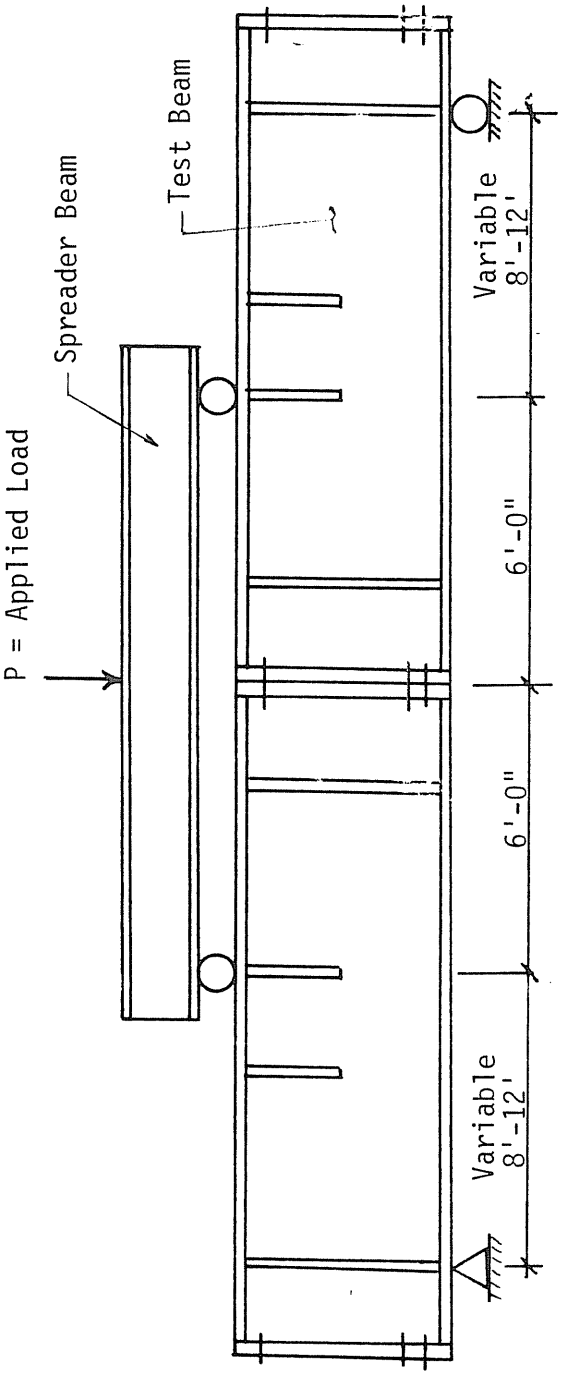

Figure 3.1 Elevation of Test Set-up

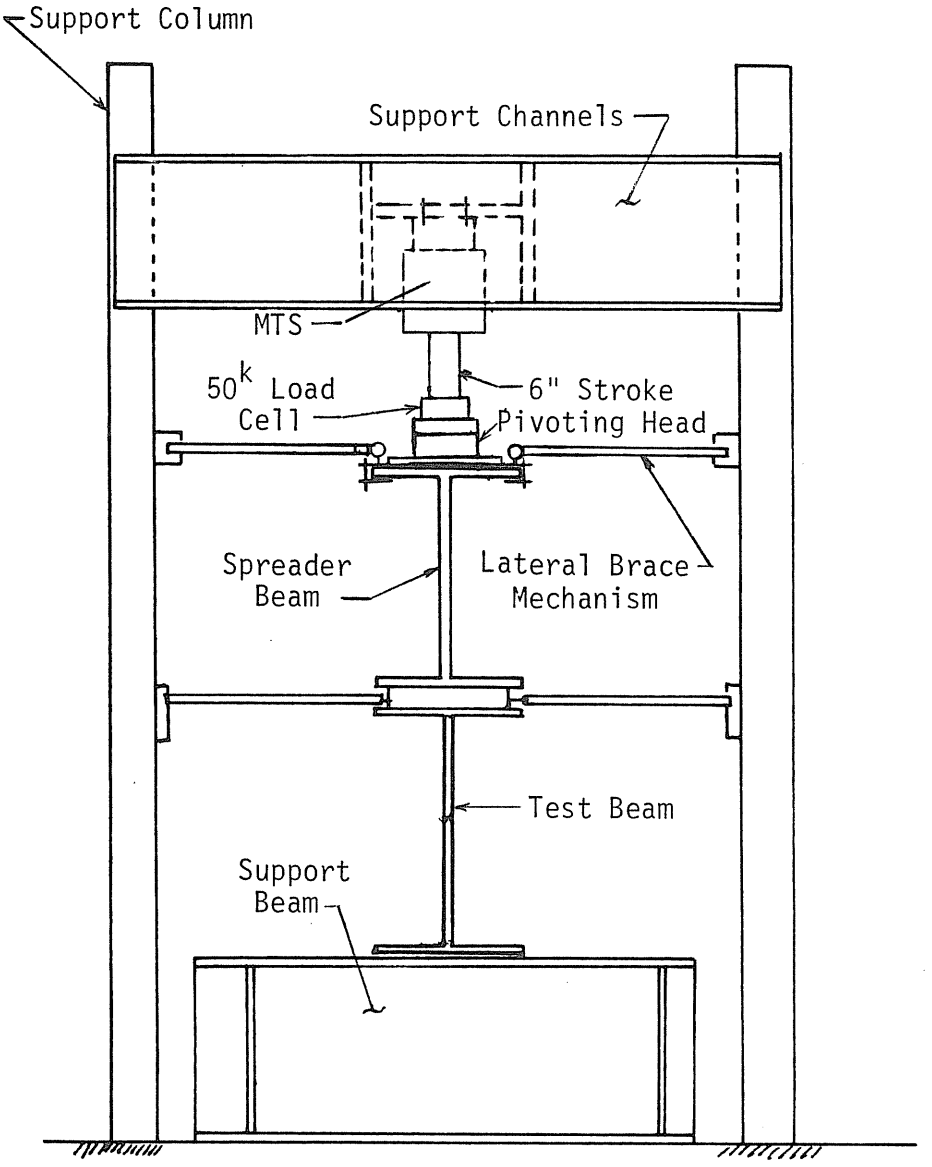

Figure 3.2 Cross-Section of Test Set-up

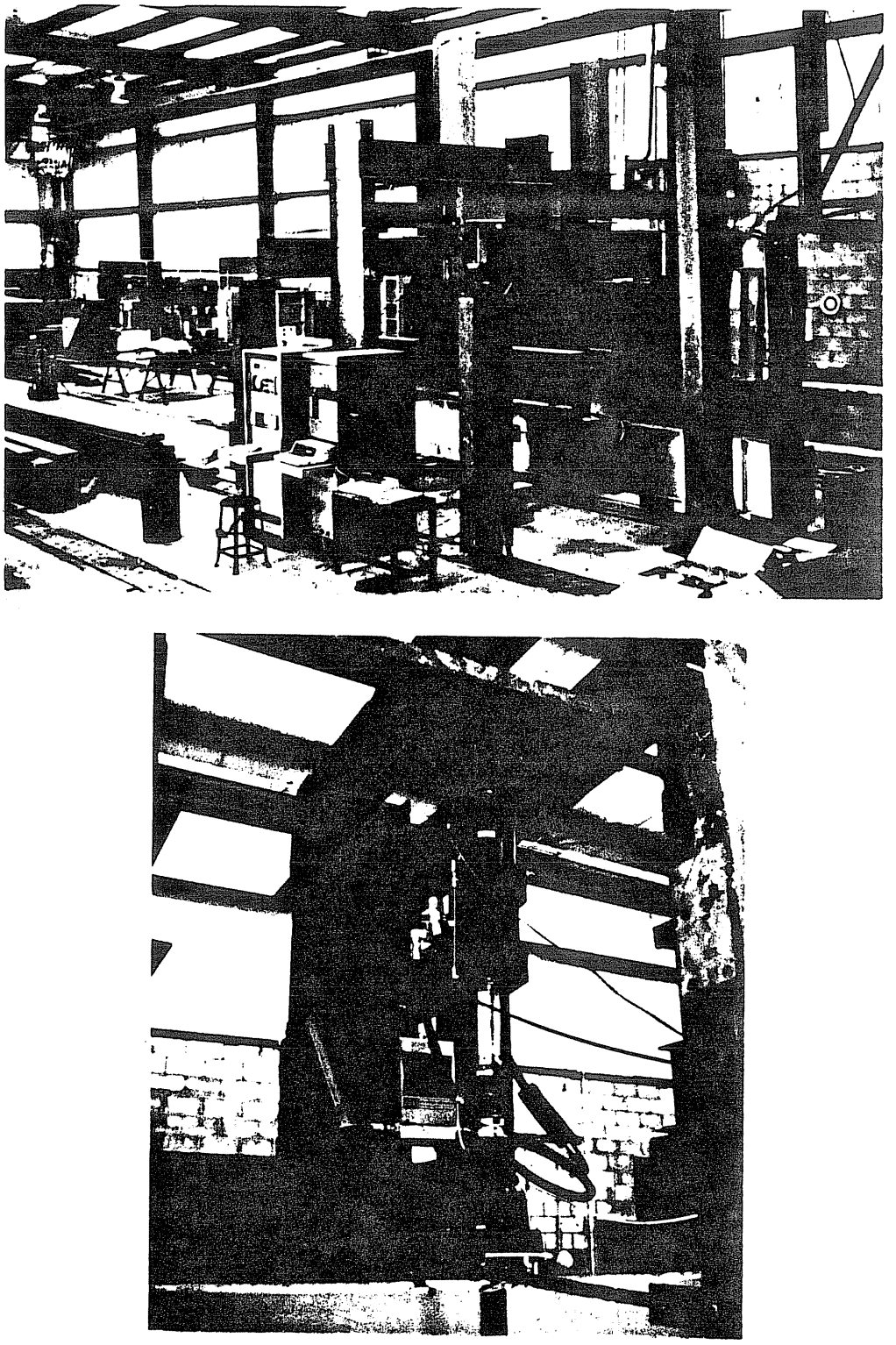

Figure 3.3 Photographs of Test Set-up and MTS Loading System

Table 3.1
Four Bolt Stiffened Flush End-Plate Parameters

Test No.	Test Designation	Bolt Diameter d_b (in.)	End-Plate Thickness t_p (in.)	Beam Depth h (in.)	Flange Width b_f (in.)	Pitch p_f (in.)	Gage g (in.)	Yield Stress (ksi)
1	FB2-3/4-3/8-16	3/4	3/8 (.379)	16	6	1 1/2	3 1/2	55.48
2	FO2-3/4-3/8-16	3/4	3/8 (.379)	16	6	1 1/2	3 1/2	55.48
3	FB2-3/4-3/8-24	3/4	3/8 (.366)	24	6	1 3/4	3 1/4	52.82
4	FO2-3/4-3/8-24	3/4	3/8 (.366)	24	6	1 3/4	3 1/4	52.82
5	FB2-5/8-3/8-16	5/8	3/8 (.381)	16	6	1 3/8	2 3/4	55.90
6	FO2-5/8-3/8-16	5/8	3/8 (.381)	16	6	1 3/8	2 3/4	55.90
7	FB2-3/4-1/2-23	3/4	1/2 (.507)	23	6	1 3/4	3 1/4	50.07
8	FO2-3/4-1/2-23	3/4	1/2 (.507)	23	6	1 3/4	3 1/4	50.07

Notes: FB2: a 3/8" stiffener was placed between the two rows of tension bolts.
FO2: a 3/8" stiffener was placed outside the two rows of tension bolts.
(.XXX): Measured thickness.

Table 3.2
Limits of Geometric Parameters

Parameter	Low	Intermediate	High
g	2 1/4	2 3/4	3 1/2
d_b	5/8	3/4	1
p_f	1 1/8	1 3/4	2 1/2
p_b	1 7/8	2 3/4	4
b_f	5	7	10
t_p	5/16	1/2	3/4
t_f	.18	.375	.50
t_w	.10	.1875	.375

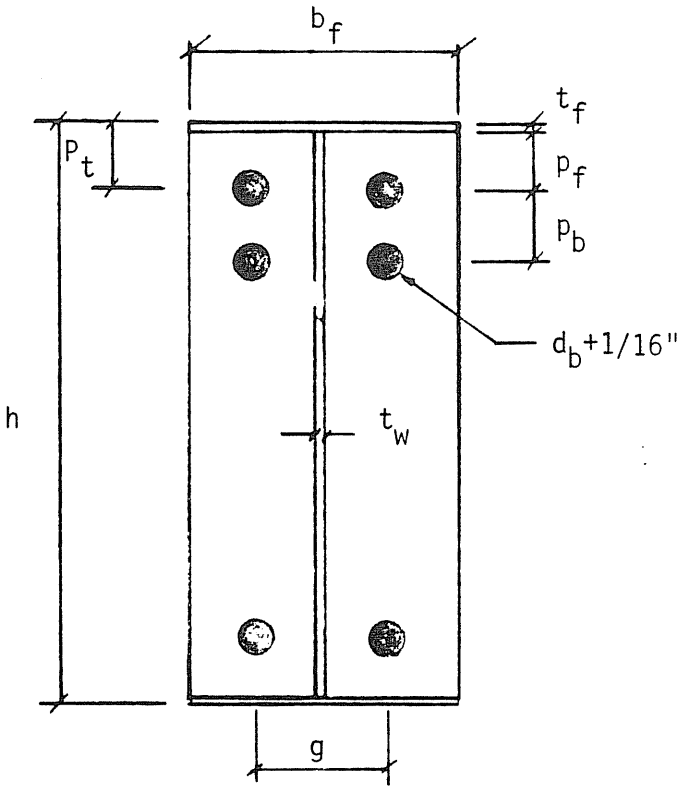

hydraulic testing (MTS) system. The test beams were laterally supported at three locations using lateral brace mechanisms. The spreader beam was also laterally braced at the centerline (see Figures 3.1, 3.2 and 3.3).

The weight of the spreader beam, the pivoting head and the other equipment on top of the test beam produced a moment of approximately 3 ft.-kips at the end-plate connection. The loads or moments indicated throughout the following discussion are applied loads or moments and include the dead load moment.

3.1.2 Instrumentation

Instrumentation consisted of wire displacement transducers, calipers, strain gages and instrumented bolts. For all eight tests a Hewlett-Packard 3497 data acquisition/control unit was used with an HP 85 desktop computer to collect and record the data. One wire displacement transducer was placed at the end-plate to measure the vertical deflection, two more were placed on the top and bottom flange of the test beam to measure the lateral displacement close to the end-plate. Two calipers were used to measure the plate separation at two locations on the end-plate. One of the calipers was placed on the centerline of the plate while the other was attached to the edge.

Strain gages were used to measure web and flange strains at approximately 2 in. from the face of the end-plate. Figure 3.4 shows the typical location of the strain gages; gages were placed on the top and bottom of both the tension and compression flanges and at the web centerline. Gages were also located on the web opposite each bolt row. The instrumented bolts were used on the tension side to monitor the bolt

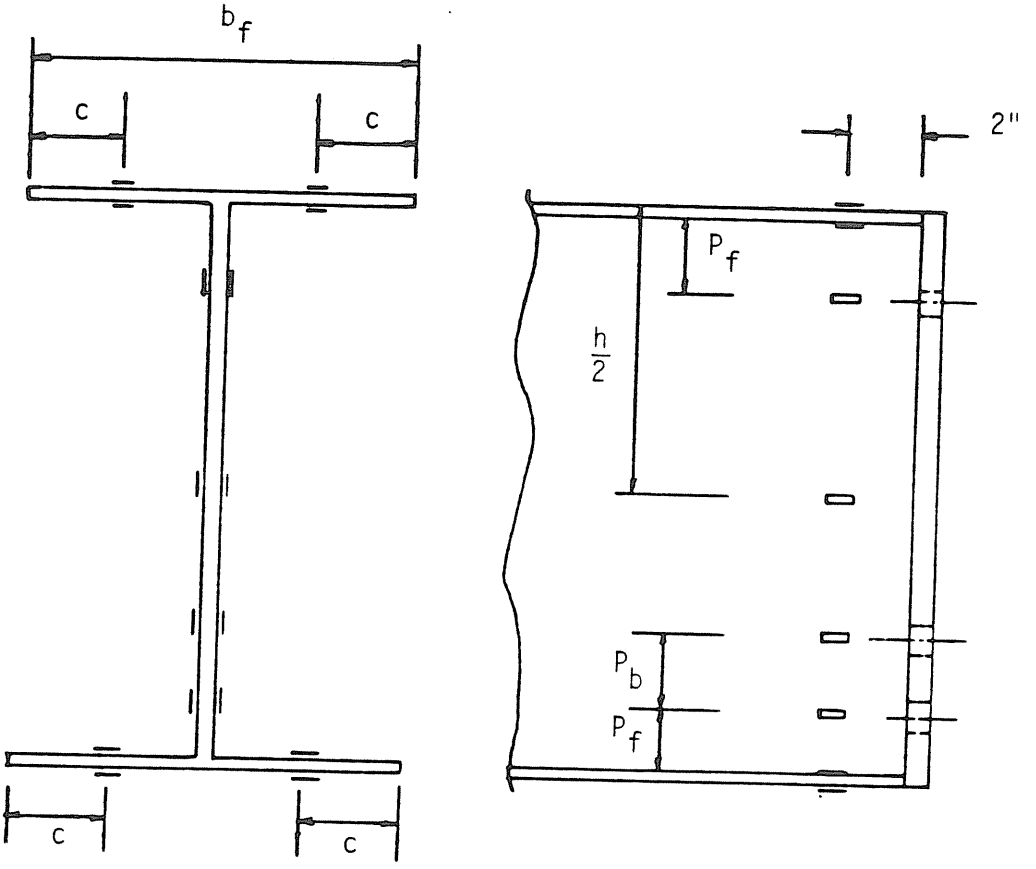

Figure 3.4 Typical Strain Gage Locations

strains resulting from the applied loads. The bolts were pretensioned after the spreader beam was placed on top of the test beam. Measured strains were converted to stresses assuming a modulus of elasticity of 29,000 ksi, but not to exceed the yield stress of the material.

3.1.3 Loading Procedures

At the beginning of each test the specimen was loaded to approximately 20% of the expected maximum load to check the test setup and instrumentation. Load-deflection and load-plate separation curves were plotted simultaneously using an HP 7470A graphics plotter. The specimen was then unloaded and initial readings recorded at zero load.

The specimens were then loaded at varying increments depending on the expected failure load of each test to approximately 2/3 of the failure load. The specimens were then unloaded at increments of 5 kips or more to a load of 2 or 5 kips, taking readings at every step while unloading. The load was then increased to the previous load, which was then increased 5 to 10%. The process was repeated with resulting load versus deflection curves as shown for a typical test in Figure 3.5.

3.2 Experimental Results and Comparisons

3.2.1 Results of Stiffened Four-Bolt Flush End-plate Tests

The test results consist of load versus vertical deflection, load versus plate separation, load versus bolt forces, and stress distribution at the instrumented cross-sections. Failure moment and the failure mode were also noted and recorded during the tests. Data packages for each of the eight tests, including a test summary sheet, are found in Appendices C through J.

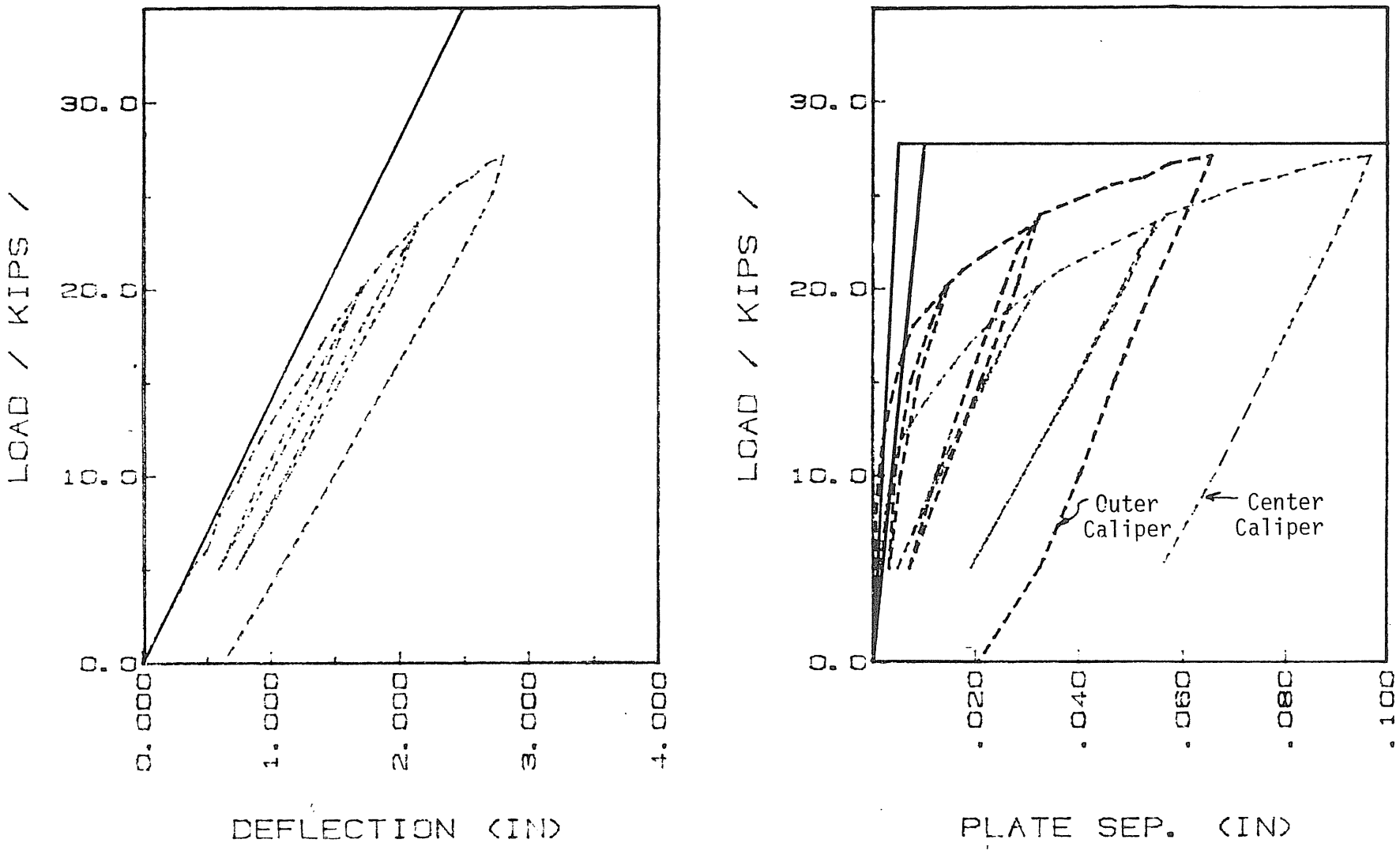

a) Load vs. Vertical Deflection

b) Load vs. Plate Separation

Figure 3.5 Typical Loading versus Deflection Curves

The load versus vertical deflection data includes a theoretical line obtained using the following equation

$$\delta_{max} = \frac{Pa}{24EI}(3L^2-4a^2) \qquad (3.1)$$

where a is the distance from the beam support to the point of load application. The predicted strength using the previously described straight line yield-line mechanism for the measured yield stress is also indicated on these plots. Bolt force versus moment figures include predictions using the modified Kennedy et al. procedures described in Section 2.2. The cross-section stress distribution plots include a theoretical line based on the flexure formula.

Figure 3.6 shows the moment versus vertical displacement relationships for all eight tests. From these plots it is noted that the test beams always deflected as predicted to a certain moment whereupon the curve softened. The moment at this load level is defined here as M_{yv} and is taken at the level when the measured deflection exceeded the theoretical deflection by approximately 10%. The predicted failure moments from the yield-line mechanisms are also shown in the plots.

Moment versus plate separation relationships are shown in Figure 3.7. In each test, the plate separation is linear up to 40-60% of failure load at which point the curve begins to lean over and a yield plateau forms near the failure moment.

Figure 3.8 shows bolt force versus moment relationships for the eight tests. Predicted bolt forces using the Kennedy et al. method are also shown in the figures. The measured bolt forces were calculated from strain data assuming elastic material properties and a modulus of

elasticity of 29,000 ksi. The measured bolt forces were close to the predicted values to near the bolt proof load (twice the allowable tension capacity given in the AISC Manual[3]). The corresponding moment is designated as M_{yb}.

For all tests, the loading was increased until a yield plateau was reached in either the moment versus vertical deflection curve or moment versus plate separation curve or the bolt forces became excessive. Figure 3.9 shows typical end-plate yielding in the vicinity of the tension bolts after loading.

Stress distribution, calculated from measured strains, at a cross-section 2 in. from the end-plate and at various load levels, is found for each test in the respective appendix. Figure 3.10 shows a typical set (from Test FB2-3/4-1/2-23). In all load vs. stress plots, the tension flange of the beam is at the top.

Table 3.3 summarizes the strength data. The ratio of maximum applied moment to predicted failure moment using the straight yield-line mechanism varied from 0.92 to 1.08. Table 3.4 presents ratios of vertical yield moment, M_{yv}, and bolt proof load moment, M_{yb}, to the maximum applied moment for all tests. The moment governed by the bolt proof load exceeds in all cases the yield moments defined by vertical deflection and plate separation. The ratio of the vertical deflection yield moment to the maximum moment varied from 0.34 to 0.92. The ratio of the bolt proof moment to the maximum moment varied from 0.71 to 1.10.

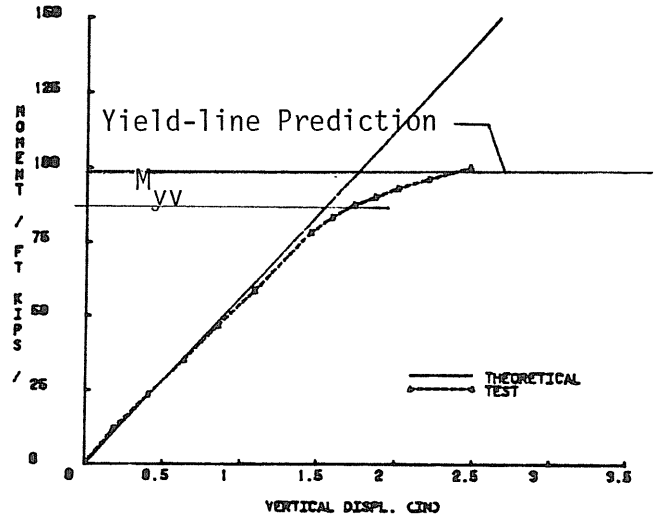

a) Moment vs. Vert. Displacement, FB2-3/4-3/8-16

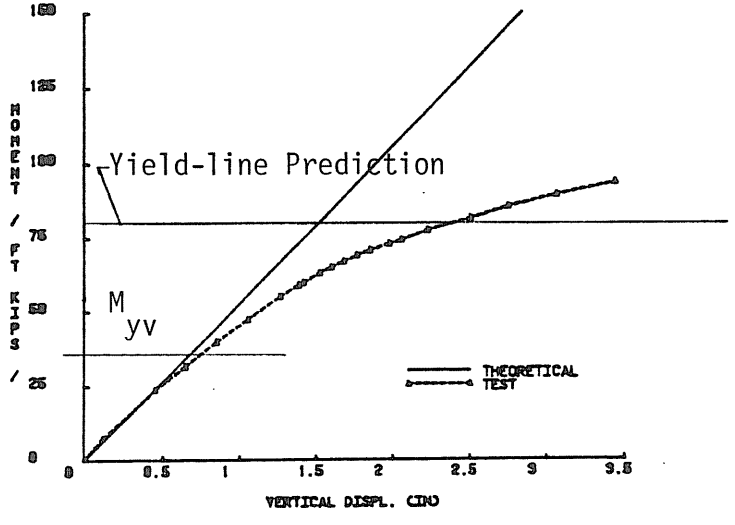

b) Moment vs. Vert. Displacement, FO2-3/4-3/8-16

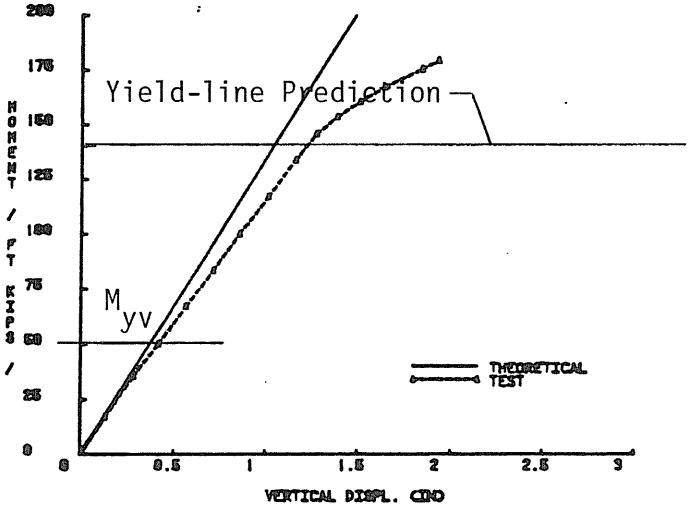

c) Moment vs. Vert. Displacement, FB2-3/4-3/8-24

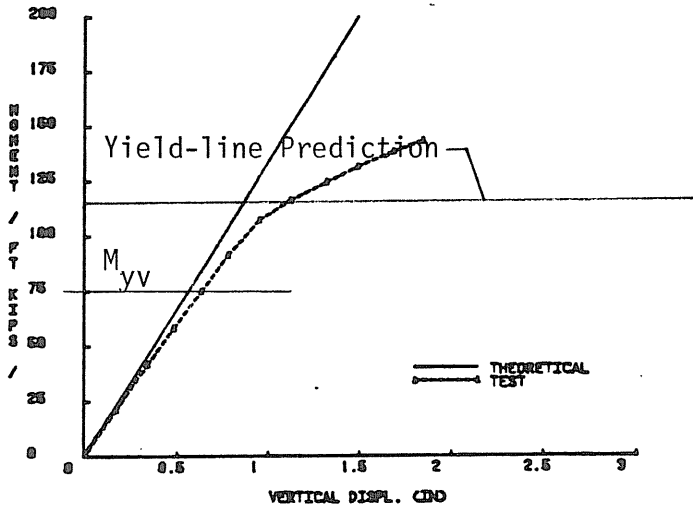

d) Moment vs. Vert. Displacement, FO2-3/4-3/8-24

Figure 3.6 Moment versus Vertical Displacement Relationships

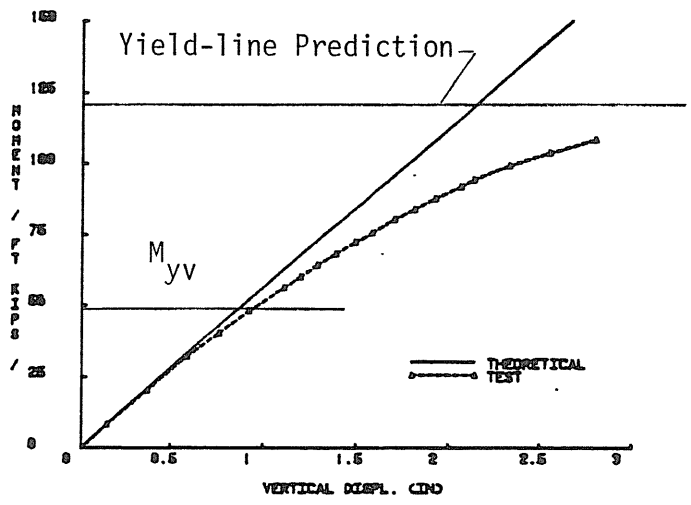

e) Moment vs. Vert. Displacement, FB2-5/8-3/8-16

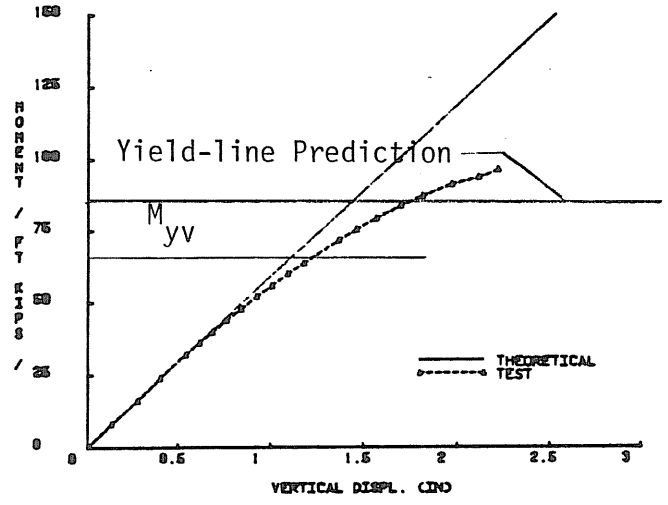

f) Moment vs. Vert. Displacement, FO2-5/8-3/8-16

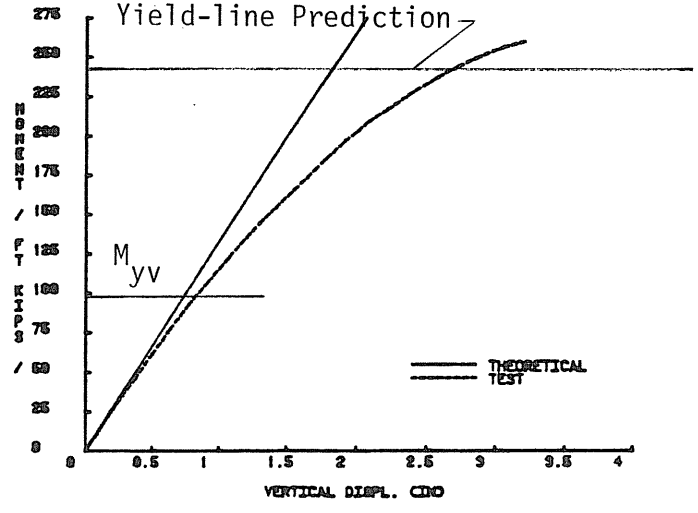

g) Moment vs. Vert. Displacement, FB2-3/4-1/2-23

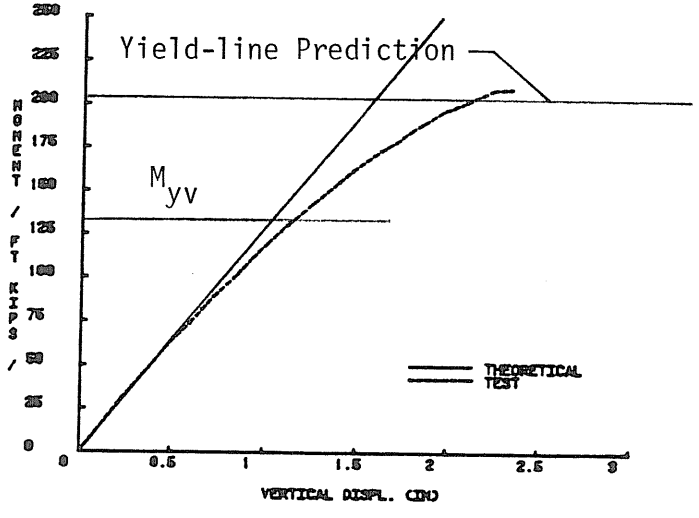

h) Moment vs. Vert. Displacement, FO2-3/4-1/2-23

Figure 3.6 Moment versus Vertical Displacement Relationships, Cont.

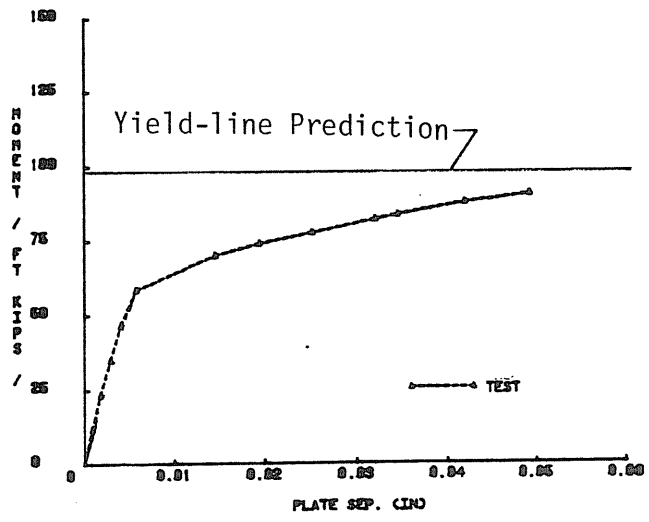

a) Moment vs. Plate Separation, FB2-3/4-3/8-16

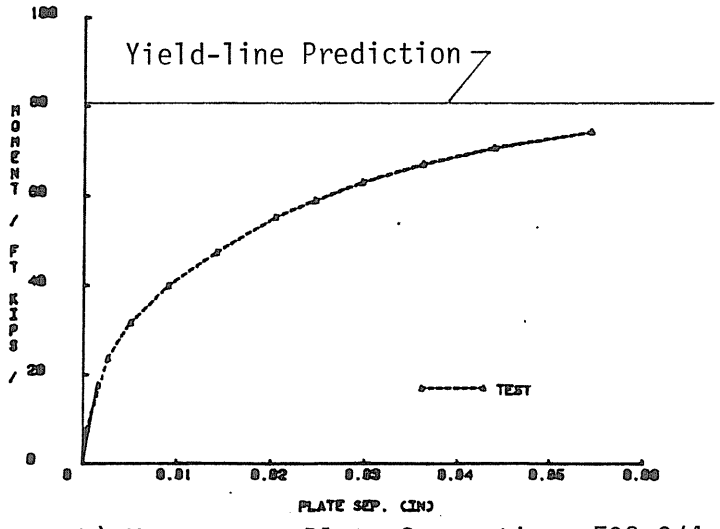

b) Moment vs. Plate Separation, FO2-3/4-3/8-16

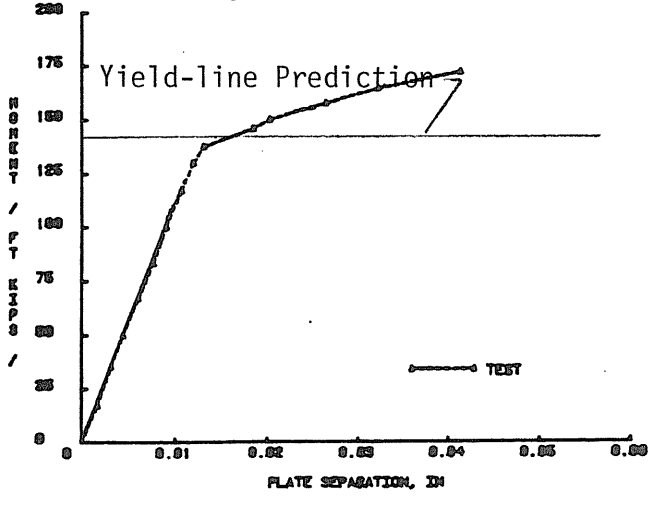

c) Moment vs. Plate Separation, FB2-3/4-3/8-24

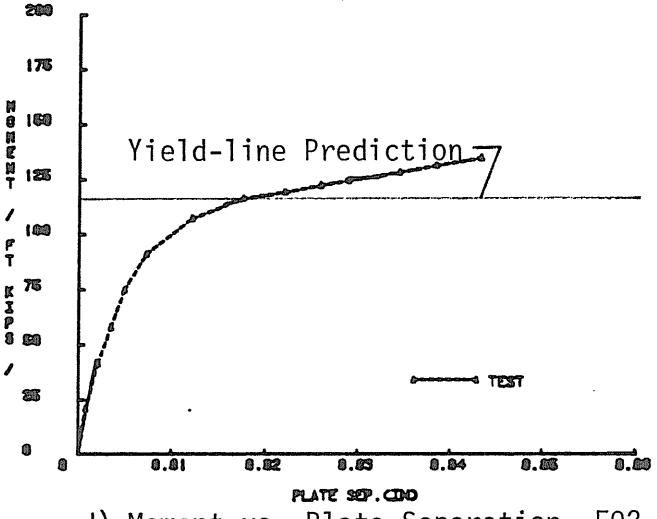

d) Moment vs. Plate Separation, FO2-3/4-3/8-24

Figure 3.7 Moment versus Plate Separation Relationships

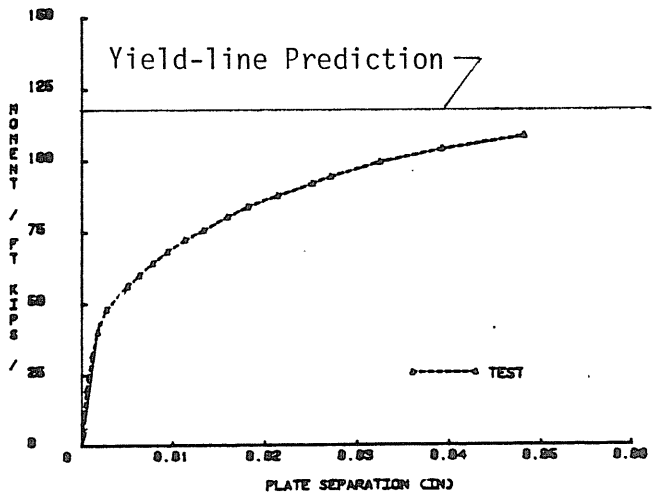

e) Moment vs. Plate Separation, FB2-5/8-3/8-16

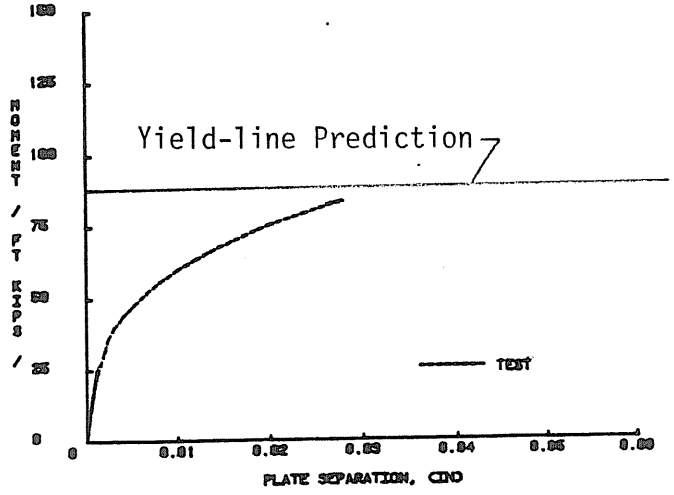

f) Moment vs. Plate Separation, FO2-5/8-3/8-16

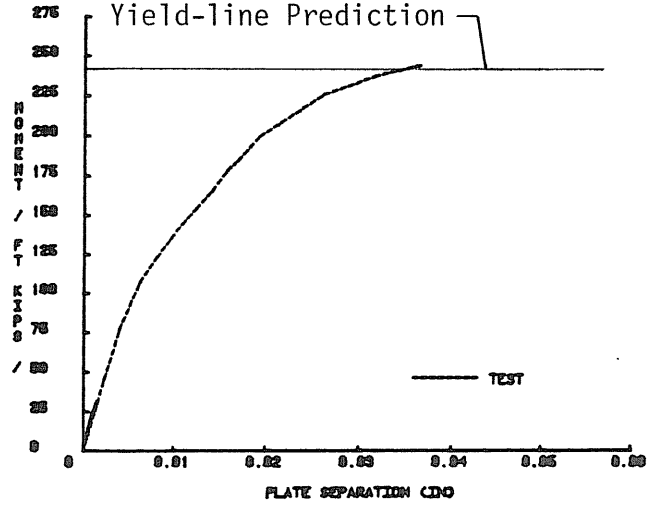

g) Moment vs. Plate Separation, FB2-3/4-1/2-23

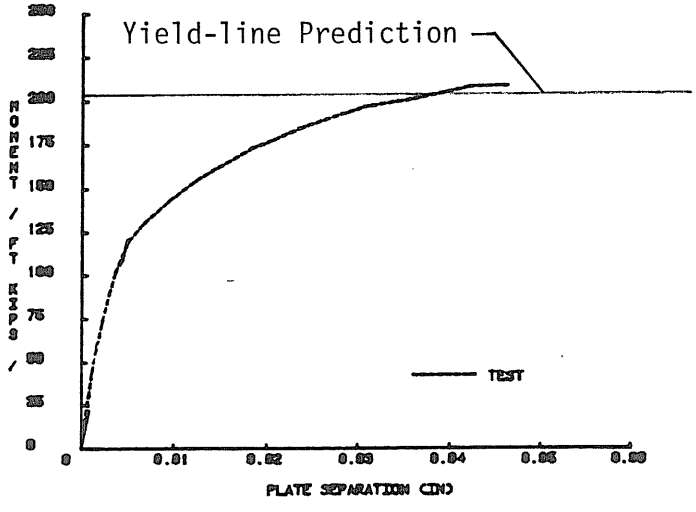

h) Moment vs. Plate Separation, FO2-3/4-1/2-23

Figure 3.7 Moment versus Plate Separation Relationships, Cont.

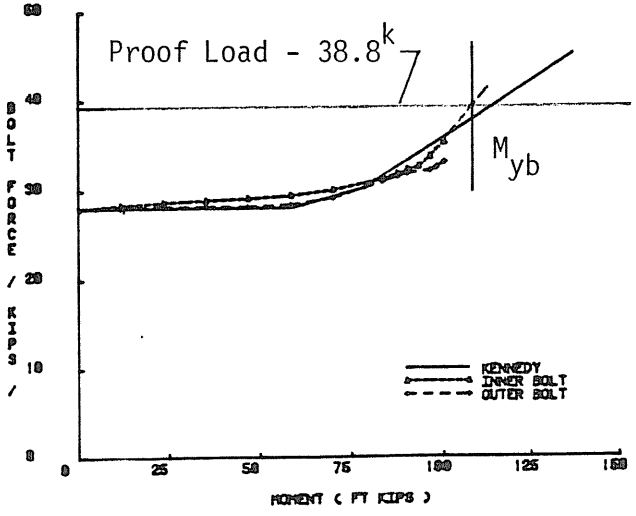

a) Bolt Force vs. Moment, FB2-3/4-3/8-16

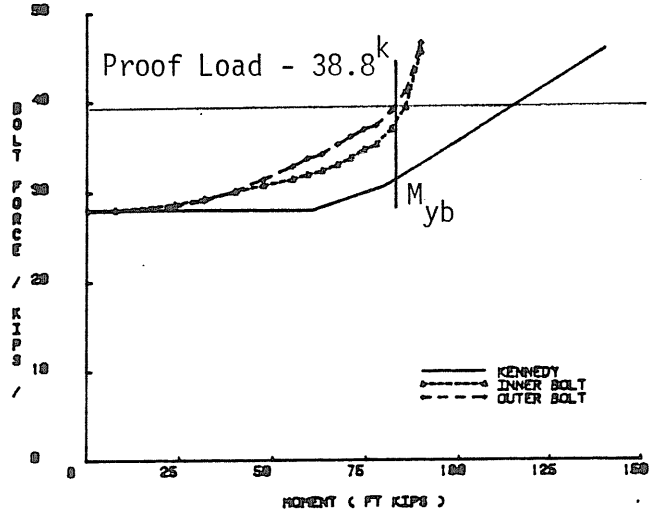

b) Bolt Force vs. Moment, FO2-3/4-3/8-16

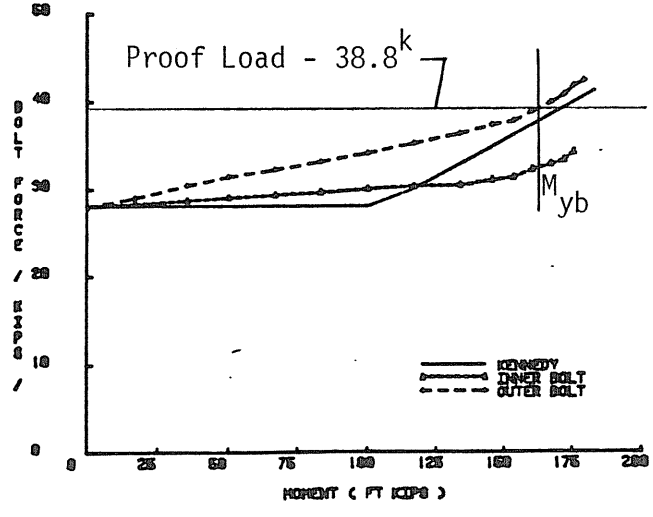

c) Bolt Force vs. Moment, FB2-3/4-3/8-24

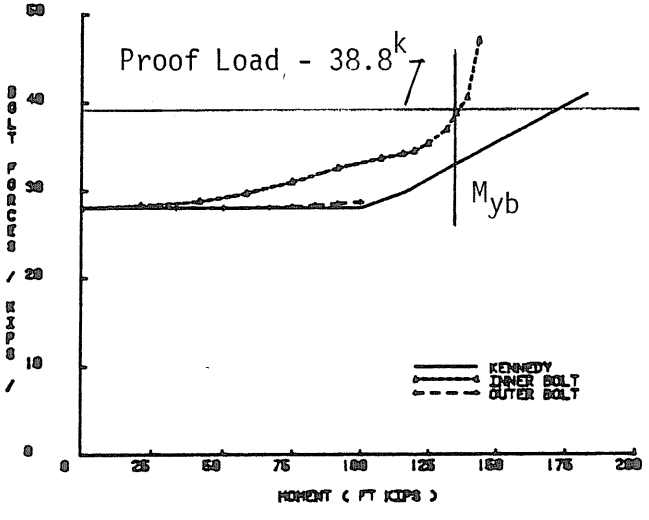

d) Bolt Force vs. Moment, FO2-3/4-3/8-24

Figure 3.8 Bolt Force versus Moment Relationships

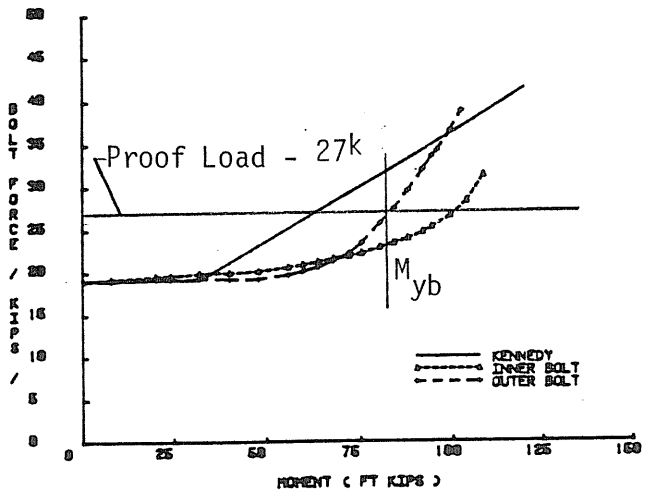

e) Bolt Force vs. Moment, FB2-5/8-3/8-16

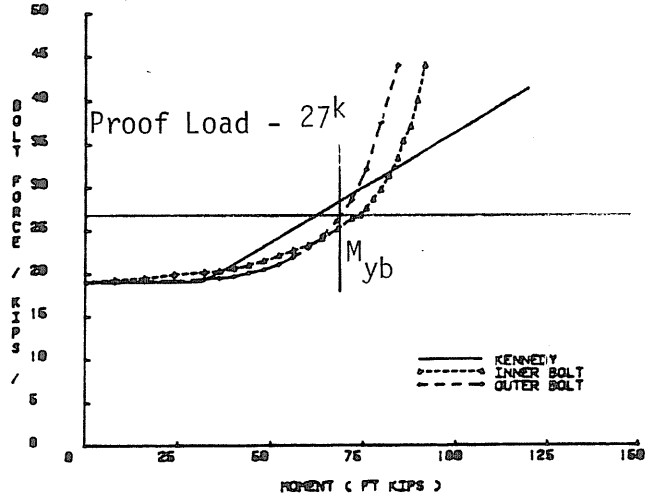

f) Bolt Force vs. Moment, FO2-5/8-3/8-16

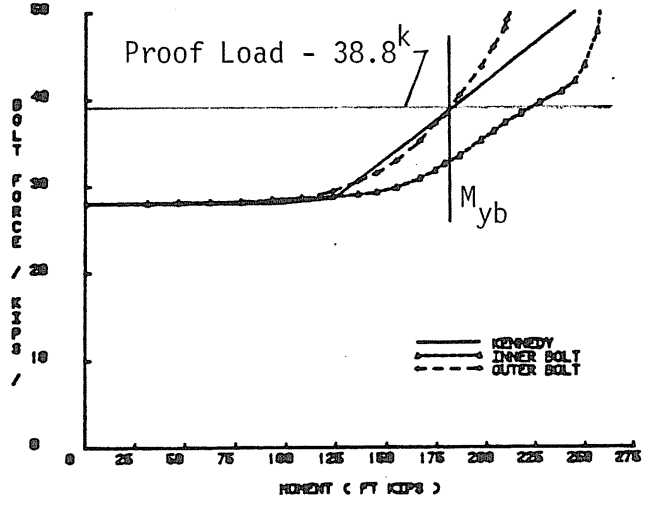

g) Bolt Force vs. Moment, FB2-3/4-1/2-23

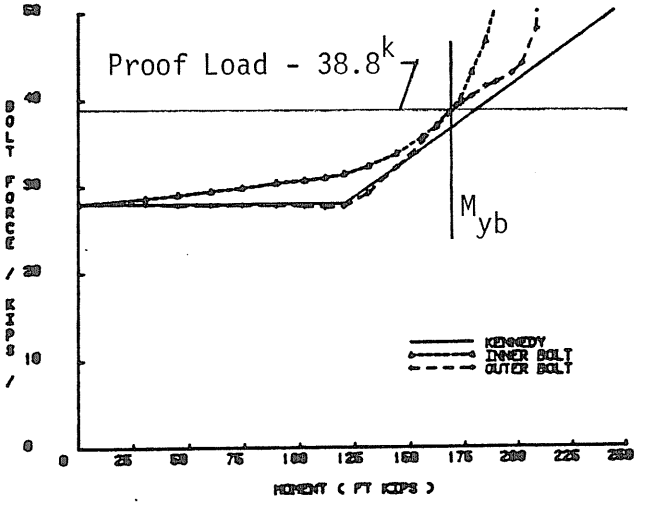

h) Bolt Force vs. Moment, FO2-3/4-1/2-23

Figure 3.8 Bolt Force versus Moment Relationships, Cont.

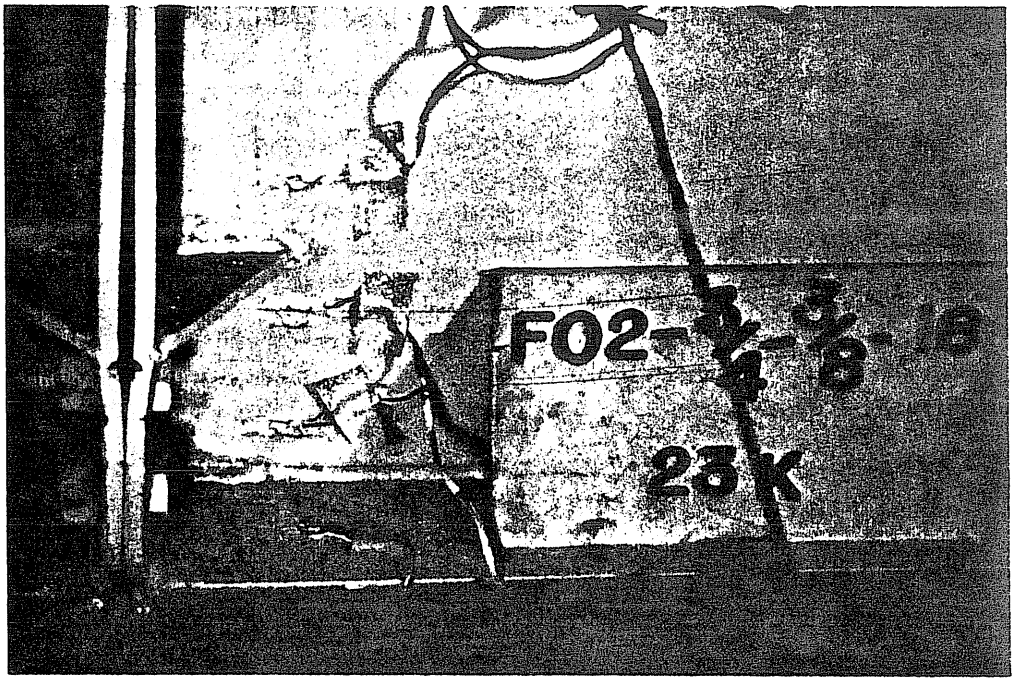

a) Plate Separation, Test FO2-3/4-3/8-16

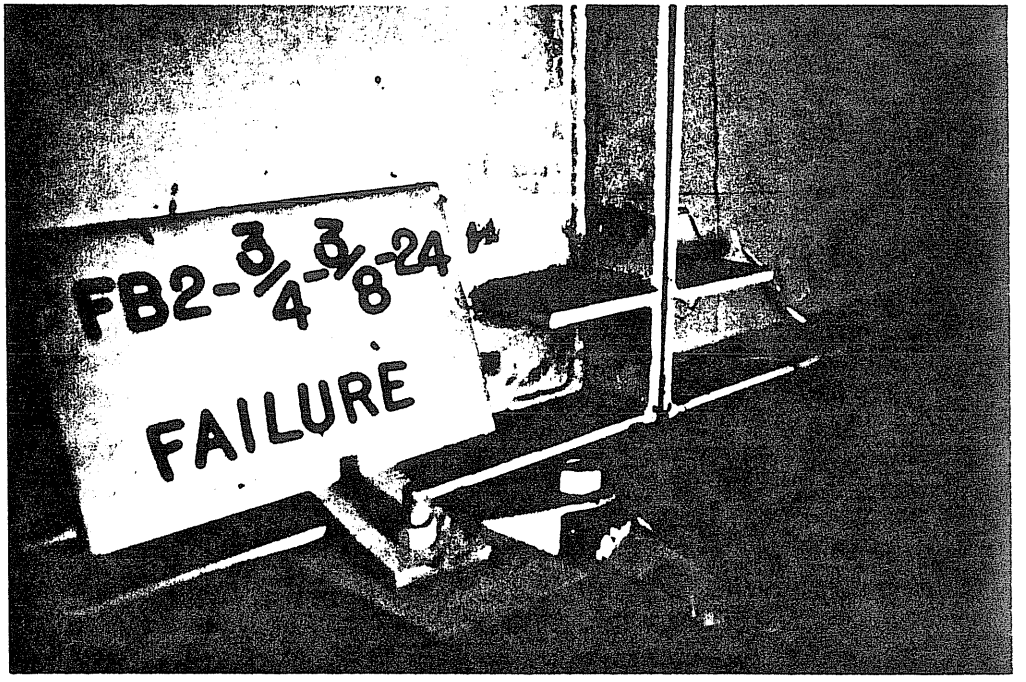

b) Failure Mechanism, Test FB2-3/4-3/8-24

Figure 3.9 Photographs Showing End-Plate Yielding

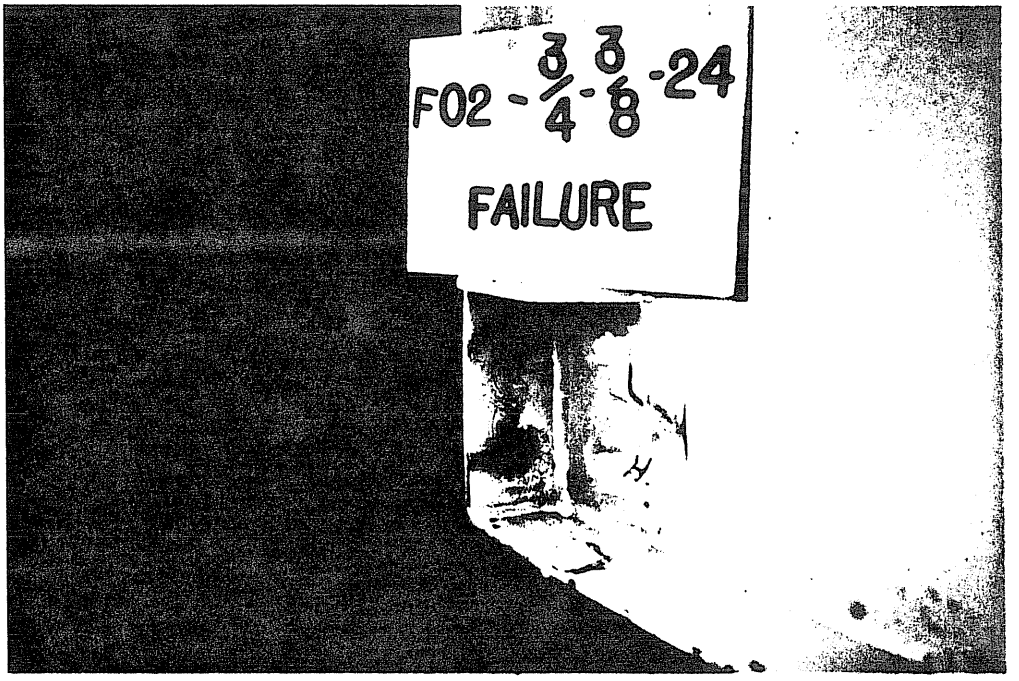

c) Failure Mechanism, Test F02-3/4-3/8-24

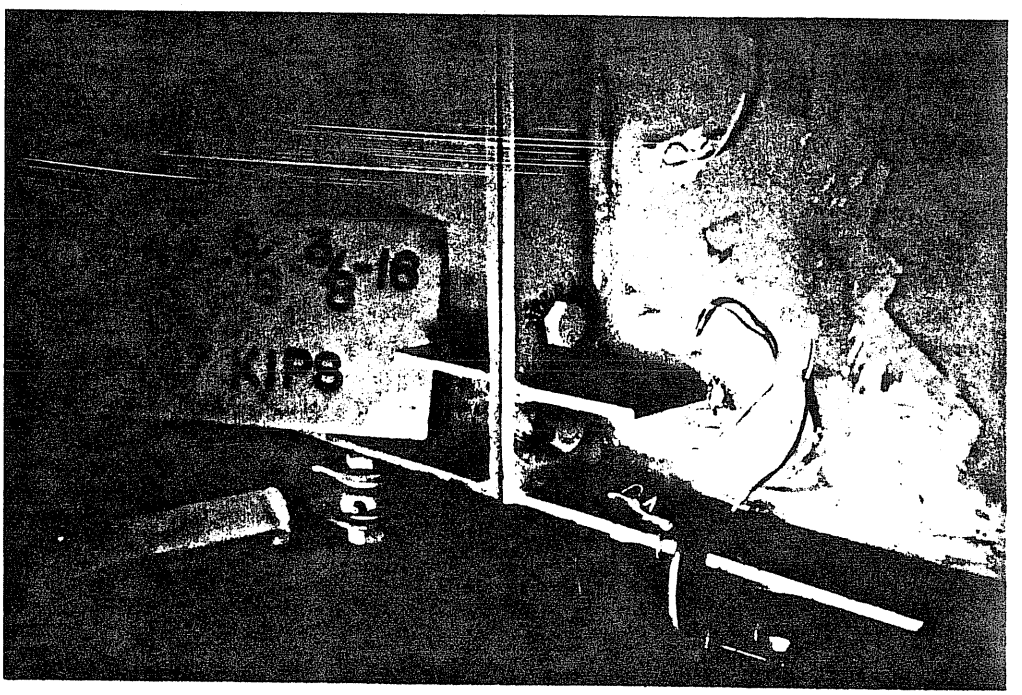

d) Failure Mechanism, Test FB2-5/8-3/8-16

Figure 3.9 Photographs Showing End-Plate Yielding (cont.)

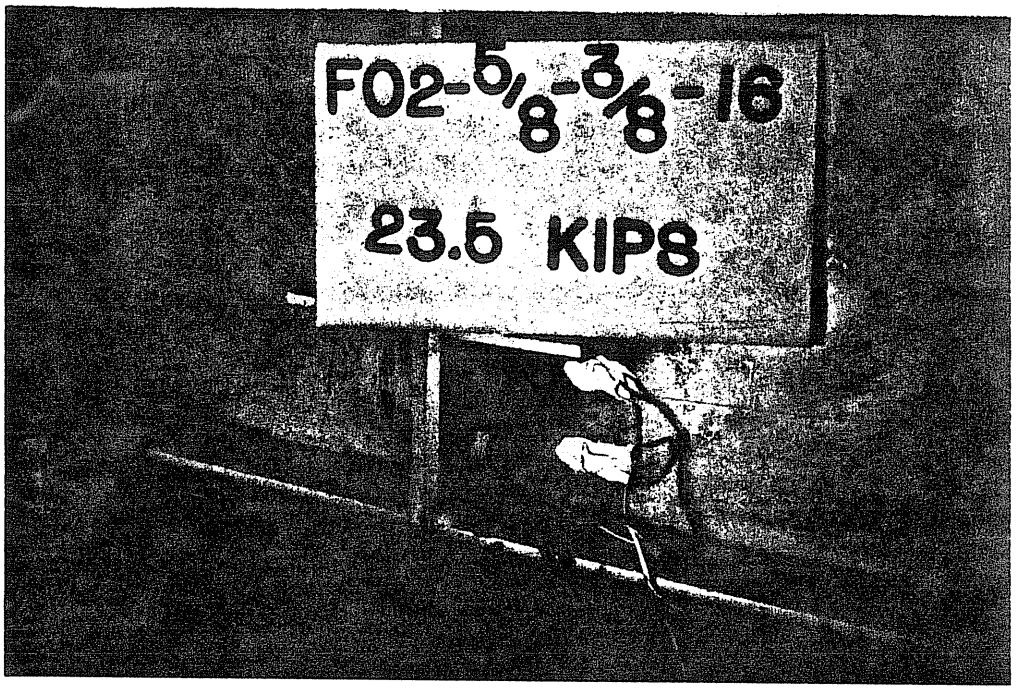

e) Failure Mechanism, Test F02-5/8-3/8-16

Figure 3.9 Photographs Showing End-Plate Yielding (cont.)

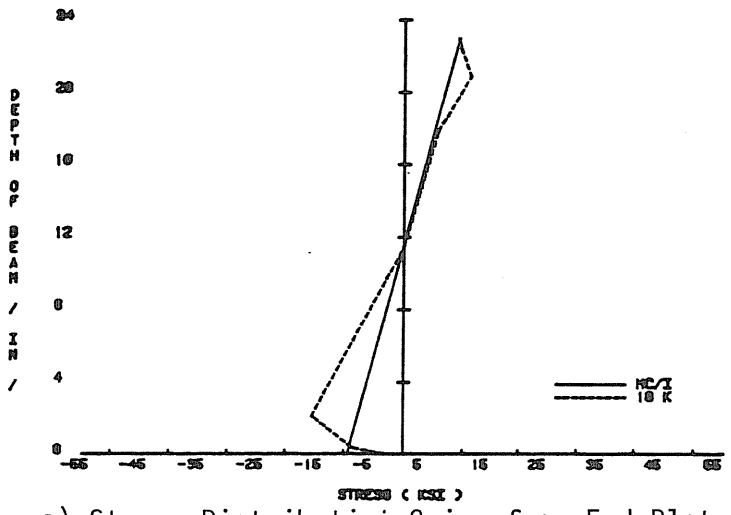

a) Stress Distribution 2 in. from End-Plate at 25% of Maximum Moment

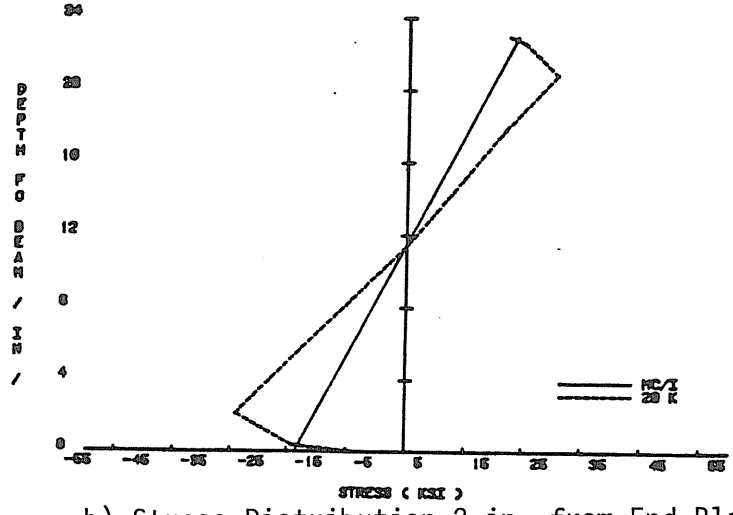

b) Stress Distribution 2 in. from End-Plate at 50% of Maximum Moment

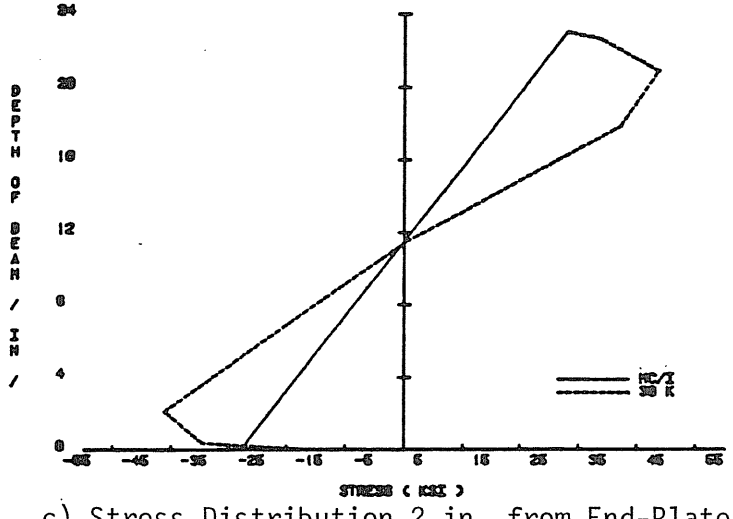

c) Stress Distribution 2 in. from End-Plate at 75% of Maximum Moment

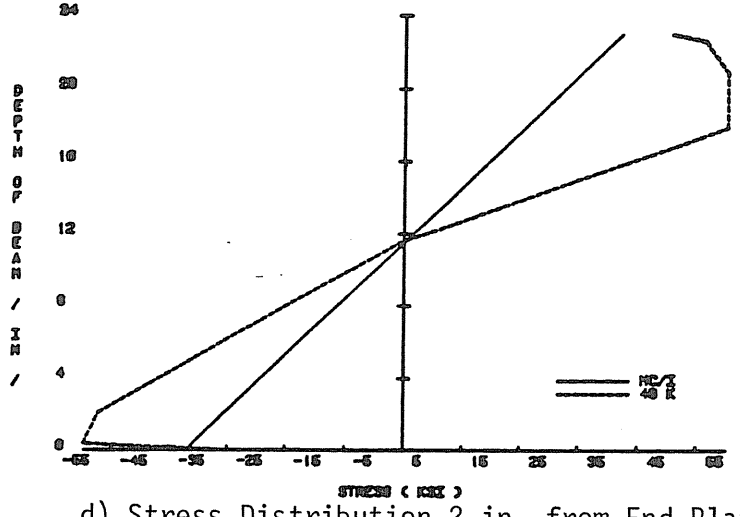

d) Stress Distribution 2 in. from End-Plate at 98% of Maximum Moment

Figure 3.10 Typical Cross-Section Stress Distribution

Table 3.3
Summary of Strength Data for Four-Bolt Stiffened Flush End-Plate Tests

Test Number	Actual Failure Moment (ft.-k)	Predicted Failure Moment (ft.-k)	$\frac{M_{act.}}{M_{pred.}}$	Percent Error
FB2-3/4-3/8-16	95.8	98.1	.98	2%
FO2-3/4-3/8-16	77.4	80.8	.96	4%
FB2-3/4-3/8-24	149.2	141.5	1.05	5%
FO2-3/4-3/8-24	123.2	114.5	1.08	8%
FB2-5/8-3/8-16	111.4	121.5	.92	8%
FO2-5/8-3/8-16	88.0	87.2	1.01	1%
FB2-3/4-1/2-23	257.0	243.3	1.06	6%
FO2-3/4-1/2-23	210.0	203.9	1.03	3%

Table 3.4
Yield Moment Comparisons for Four-Bolt Flush End-Plate Tests

Test	Maximum Applied Moment (ft.-k)	Strength M_{yv} (ft.-k)	Bolt M_{yb} (ft.-k)	$\frac{M_{yv}}{M_{max}}$	$\frac{M_{yb}}{M_{max}}$
FB2-3/4-3/8-16	95.8	88	104*	.92	1.09
FO2-3/4-3/8-16	77.4	35	80	.45	1.03
FB2-3/4-3/8-24	149.2	50	161	.34	1.08
FO2-3/4-3/8-24	123.2	75	135	.61	1.10
FB2-5/8-3/8-16	111.4	48.8	82.7	.44	.74
FO2-5/8-3/8-16	88.0	66.3	69.2	.75	.79
FB2-3/4-1/2-23	257.0	98	183	.38	.71
FO2-3/4-1/2-23	210.0	134	171	.64	.81

*Extrapolated

M_{yv} = moment at which the experimental vertical deflection exceeds the predicted deflection by 10%.

M_{yb} = moment at which the experimental bolt force is at the proof load (twice the allowable) of the bolt.

3.2.2 Comparison of Stiffened Four-Bolt Flush End-Plate Tests

Figure 3.11 shows comparisons between results from Tests FB2-3/4-1/2-23 and FO2-3/4-1/2-23. These two tests are geometrically identical, except for the location of the gusset plate. From the moment versus vertical displacement curves shown in Figure 3.11, it can be seen that the four-bolt flush end-plate with a stiffener between the tension row of bolts provides a slightly stiffer connection than when the stiffener is outside the bolt rows. However from the moment versus plate separation curves, Figure 3.12, the stiffener outside provided a slightly stiffer connection only at low loads. From the bolt force comparisons, Figures 3.13 and 3.14, it can be seen that when the stiffener is placed outside the tension rows of bolts, the inner bolt force reaches the proof load (38.8 kips) at a lower moment than when the stiffener is placed between the tension rows of bolts. For the outer bolt, the two configurations reached the proof load at approximately the same applied moment.

Addtional comparisons of the data from the eight tests are presented in Tables 3.5 and 3.6. Only six tests, three of each configuration, are compared because the pitch between bolt rows differs in the FX2-5/8-3/8-16 series. Table 3.5 presents strength and comparison data for the configurations. Strength data includes maximum applied moment, predicted failure moment and ratios. The comparisons include the ratio of maximum applied moments for the gusset plate between the tension bolt rows to the maximum applied moment for the gusset plate outside the tension bolt rows, the ratios of the predicted failure moments, and the ratios of the maximum to predicted failure moment ratios.

The maximum moment ratios vary from 1.21 to 1.24, which indicates that the four-bolt flush end plates with a stiffener between the tension row of bolts are 21% to 24% stronger than when the stiffener is outside the tension row of bolts. The predicted failure moment ratios ranges from 1.19 to 1.24, showing that the predicted increase in strength is 19% to 24%. The ratios of the ratios varied from 0.97 to 1.03 and show that the prediction equations are consistent in accuracy between the two configurations.

Table 3.6 presents comparisons of the yield moment, M_{yv} and M_{yb}, for the two configurations. Again, only three sets of tests are compared. The ratios shown for the stiffness yield moment (vertical displacement) are not consistent. The ratios of the bolt proof load moments, $(M_{yb})_B/(M_{yb})_0$, show that the proof load is reached at a 7% to 30% higher moment when the gusset plate is placed between the tension row of bolts.

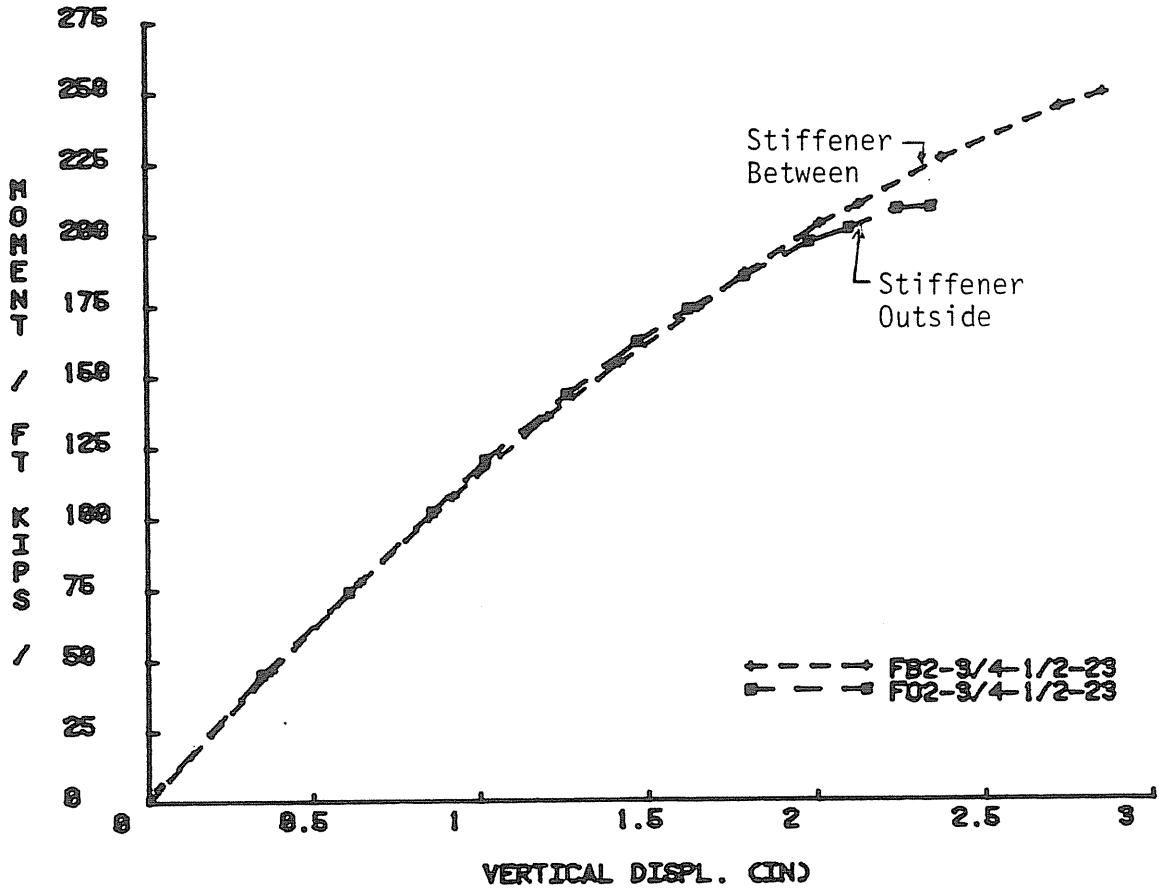

Figure 3.11 Comparison of Stiffened Four-Bolt Flush End-Plate Moment vs. Vertical Deflection Relationships

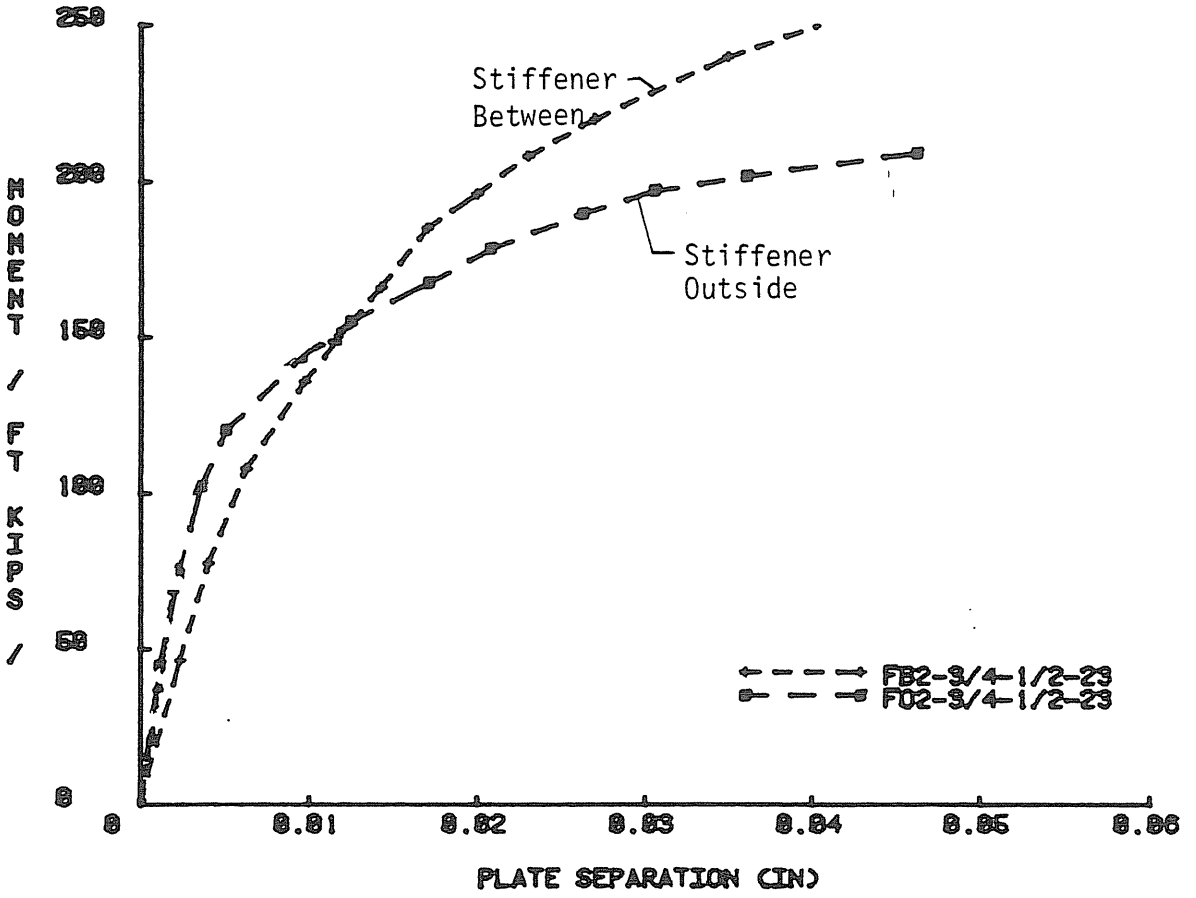

Figure 3.12 Comparison of Stiffened Four-Bolt Flush End-Plate Moment vs. Plate Separation Relationships

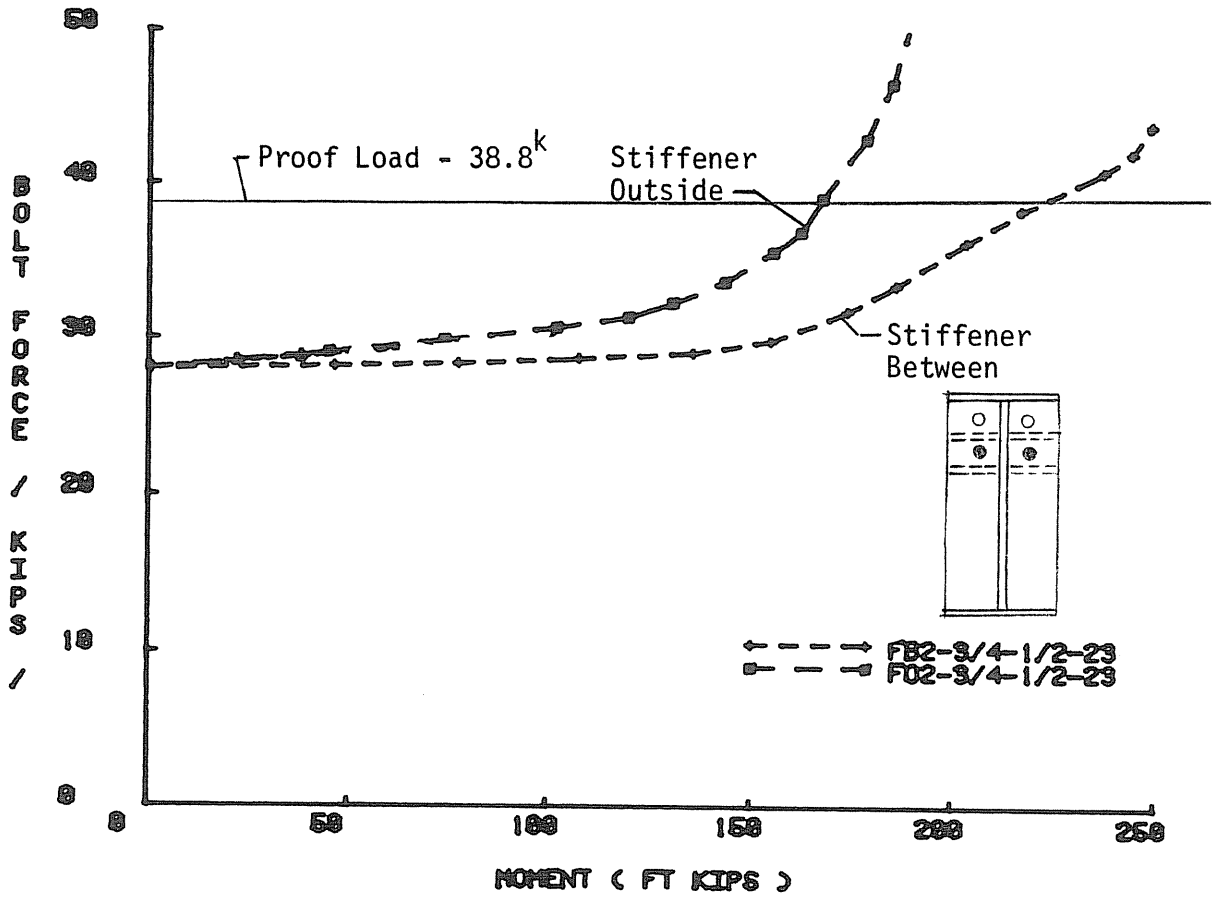

Figure 3.13 Comparison of Stiffened Four-Bolt Flush End-Plate Inner Bolt Force vs. Moment Relationships

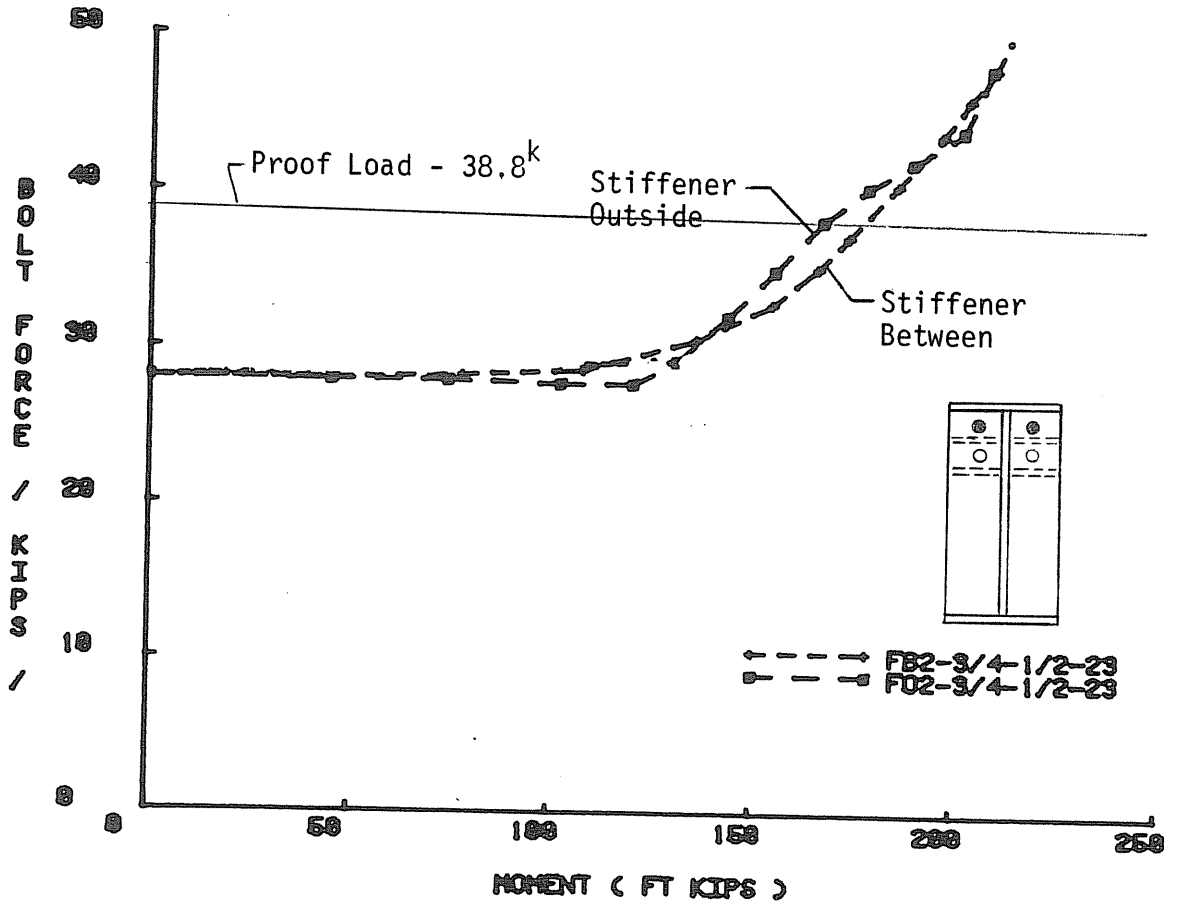

Figure 3.14 Comparison of Stiffened Four-Bolt Flush End-Plate Outer Bolt Force vs. Moment Relationships

Table 3.5 Comparisons of Stiffened Four-Bolt Flush End-Plate Strength Data

Gusset Plate Between Bolt Rows				Gusset Plate Outside Bolt Rows				Comparison		
Test No.	Maximum Applied Moment (ft.-k)	Predicted Failure Moment (ft.-k)	$\frac{M_{max}}{M_{pred}}$	Test No.	Maximum Applied Moment (ft.-k)	Predicted Failure Moment (ft.-k)	$\frac{M_{max}}{M_{pred}}$	$\frac{(M_{max})_B}{(M_{max})_o}$	$\frac{(M_{pred})_B}{(M_{max})_o}$	$\frac{(Ratio)_B}{(Ratio)_o}$
FB2-3/4-3/8-16	95.8	98.1	0.98	FO2-3/4-3/8-16	77.4	80.8	0.96	1.24	1.21	1.02
FB2-3/4-3/8-24	149.2	141.5	1.05	FO2-3/4-3/8-24	123.2	114.5	1.08	1.21	1.24	0.97
FB2-5/8-3/8-16	111.4	121.5	0.92	FO2-5/8-3/8-16	88.0	87.2	1.01	*	*	*
FB2-3/4-1/2-23	257.0	243.3	1.06	FO2-3/4-1/2-23	210.0	203.9	1.03	1.22	1.19	1.03

*Note: The 5/8-3/8-16 tests had different geometric configurations. Thus, no comparison was made.

Table 3.6 Comparisons of Stiffened Four-Bolt Flush End-Plate Yield Moments Data

Gusset Plate Between Bolt Rows	Gusset Plate Outside Bolt Rows	$\frac{(M_{yv})_B}{(M_{yv})_o}$	$\frac{(M_{yb})_B}{(M_{yb})_o}$	$\frac{(M_{yv}/M_{max})_B}{(M_{yv}/M_{max})_o}$	$\frac{(M_{yb}/M_{max})_B}{(M_{yb}/M_{max})_o}$
FB2-3/4-3/8-16	FO2-3/4-3/8-16	2.51	1.30	2.04	1.06
FB2-3/4-3/8-24	FO2-3/4-3/8-24	0.53	1.14	0.44	0.98
FB2-3/4-1/2-23	FO2-3/4-1/2-23	0.73	1.07	0.59	0.88

CHAPTER IV

SUMMARY COMPARISONS, CONCLUSIONS AND RECOMMENDATIONS

4.1 Summary Comparisons

The investigation of the behavior of stiffened flush end-plate connections, with two rows of tension bolts, has been described in the preceding chapters. The investigation included yield-line analyses and procedures to estimate bolt forces along with experimental testing to verify the analytical models. Eight specimens were tested and the data obtained was compared to the analytical predictions. The test results were all very similar and compared well with the predictions.

4.1.1 Comparison of Stiffened and Unstiffened Four-Bolt Flush End-plate Tests

Figures 4.1 thru 4.4 shows comparisons of results from Tests F2-3/4-3/8-16, FB2-3/4-3/8-16 and F02-3/4-3/8-16. These three tests are geometrically identical, except for the placement of the gusset plate in the stiffened tests. The moment versus rotation curves are shown in Figure 4.1. The rotation at centerline, ϕ, was determined from Equation 4.1 by solving

$$\Delta_{exp} = \Delta_{theor.} + \frac{\phi L}{2} \qquad (4.1)$$

for ϕ. In this equation, Δ_{exp} is the experimental centerline deflection at load P and Δ_{theor} is the centerline theoretical deflection at the same

load P. (Equation 4.1 was developed in Chapter III). From the moment rotation curves, it can be seen that the four bolt connection with the gusset plate between the tension rows of bolts provides a slightly stiffer connection than the other two configurations. A similar conclusion is reached from the moment versus plate separation curves shown in Figure 4.2.

Figures 4.3 and 4.4 provide bolt force comparisons for the inner and outer bolt forces, respectively. In bolt plots, the proof load is first reached in the unstiffened connection, followed by the stiffened outside connection and finally the stiffened between connection. Thus, the addition of the gusset plate reduces the force that is carried by the bolts.

A comparison of the strength data for the stiffened and unstiffened tests is presented in Table 4.1. The F2-3/4-3/8-16 tests are the only tests that have identical geometric configurations; thus, comparisons of experimental data for each set of tests cannot be made. However, predicted failure moments for each test can be calculated and comparisons made on this basis. This data and ratios of stiffened between and stiffened outside to unstiffened failure moments are found in Table 4.1. From the predicted ratios, the stiffened between connection is 42-56% stronger than the unstiffened connection, while the stiffened outside connection is 24-29% stronger than the unstiffened connection.

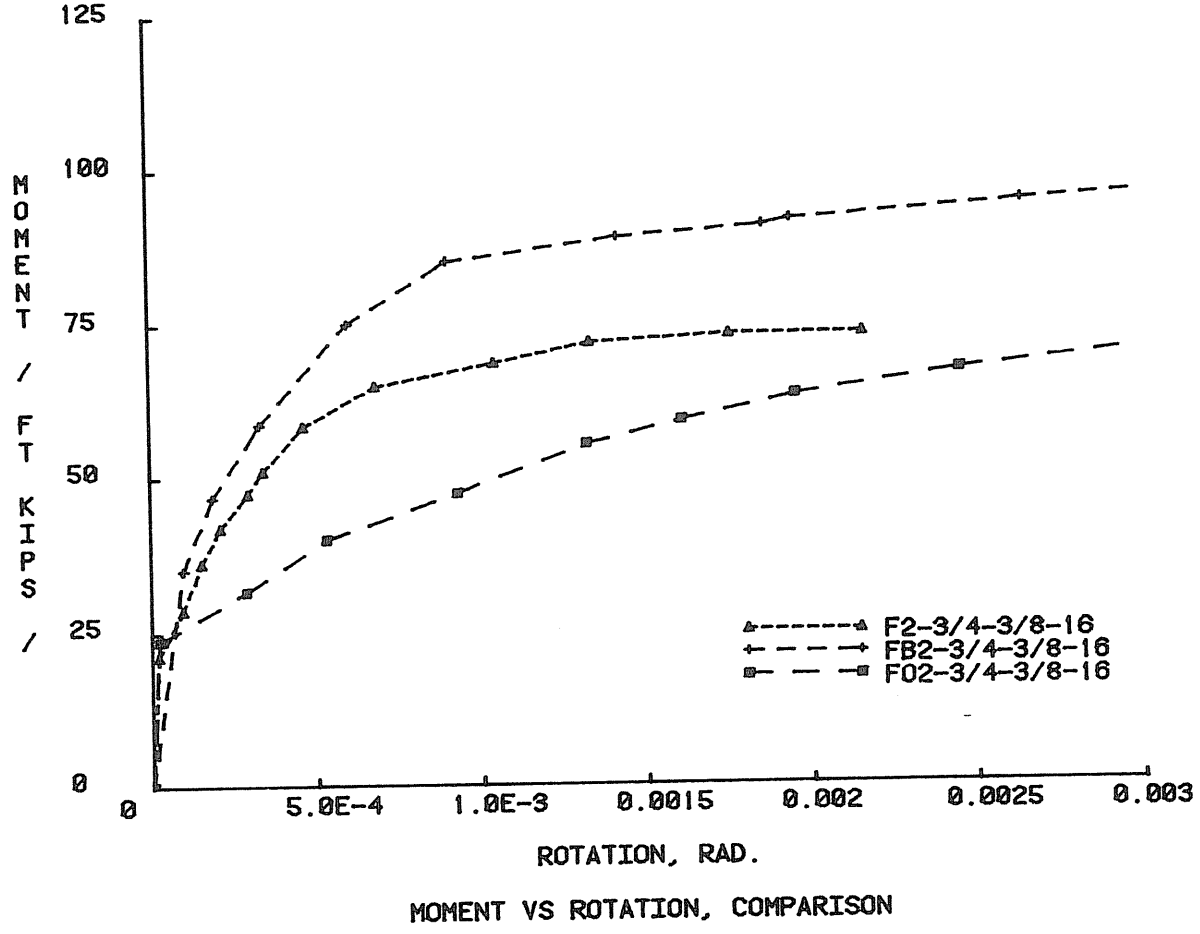

Figure 4.1 Comparison of Stiffened and Unstiffened Four-Bolt Flush End-Plate Load vs. Rotation Relationship

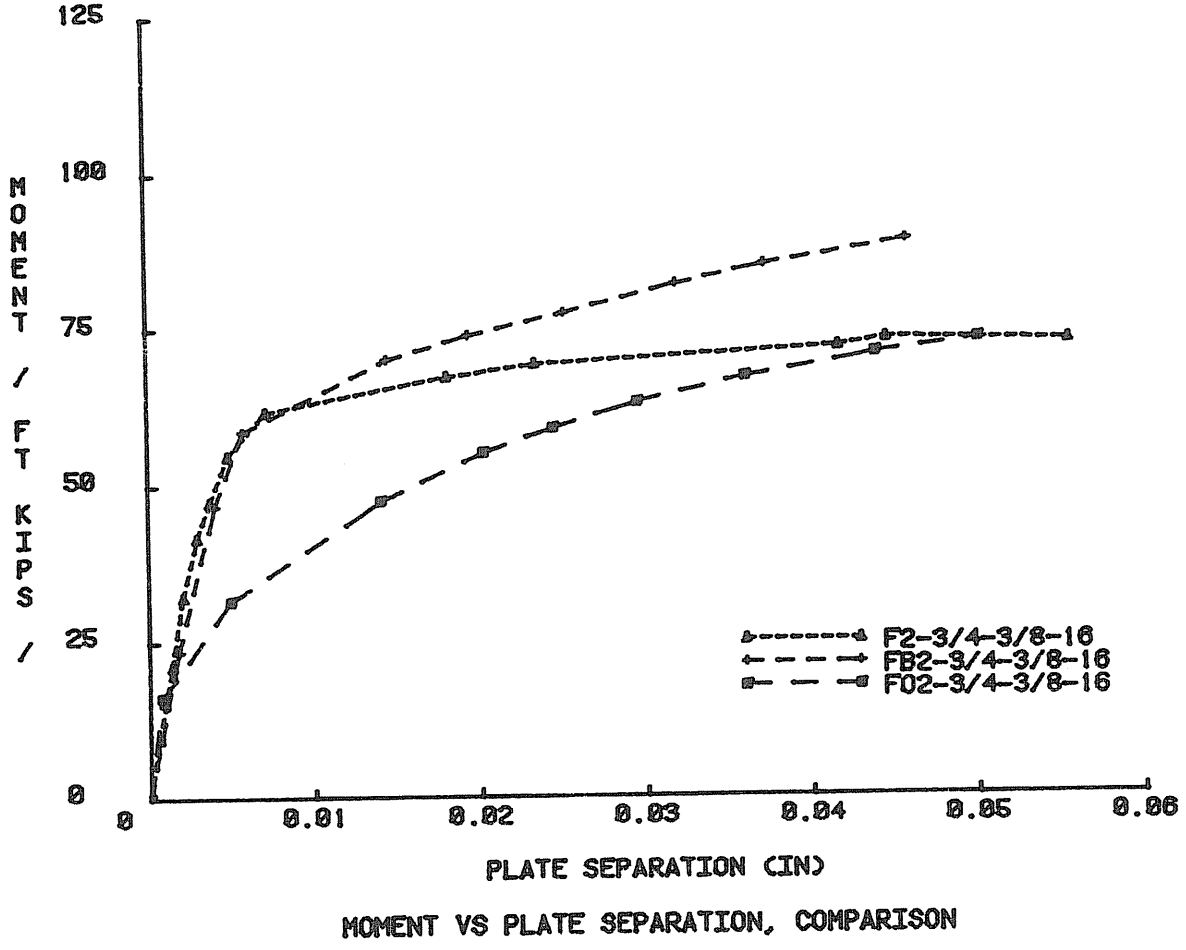

Figure 4.2 Comparison of Stiffened and Unstiffened Four-Bolt Flush End-Plate Inner Bolt Force vs. Moment Relationship

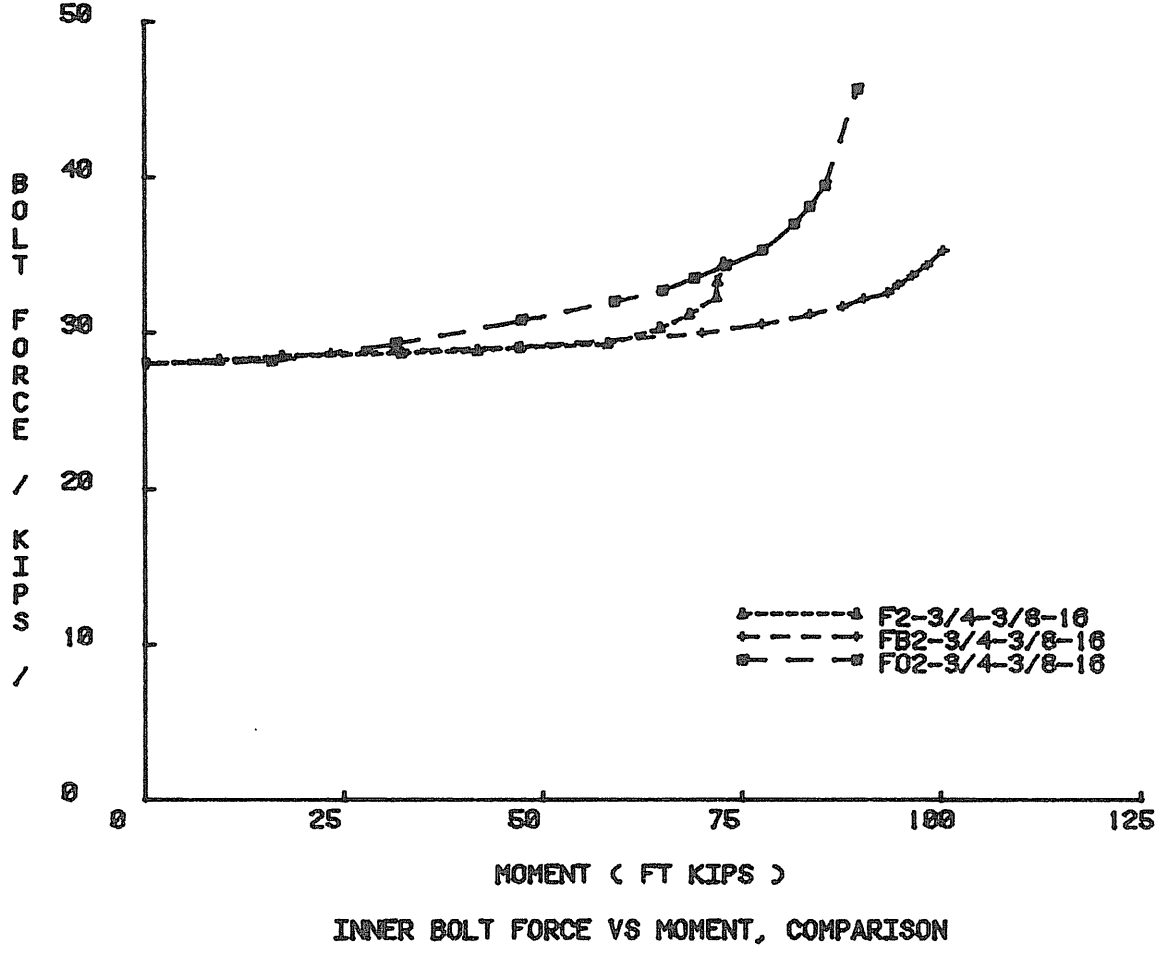

Figure 4.3 Comparison of Stiffened and Unstiffened Four-Bolt Flush End-Plate Inner Bolt Force vs. Moment Relationship

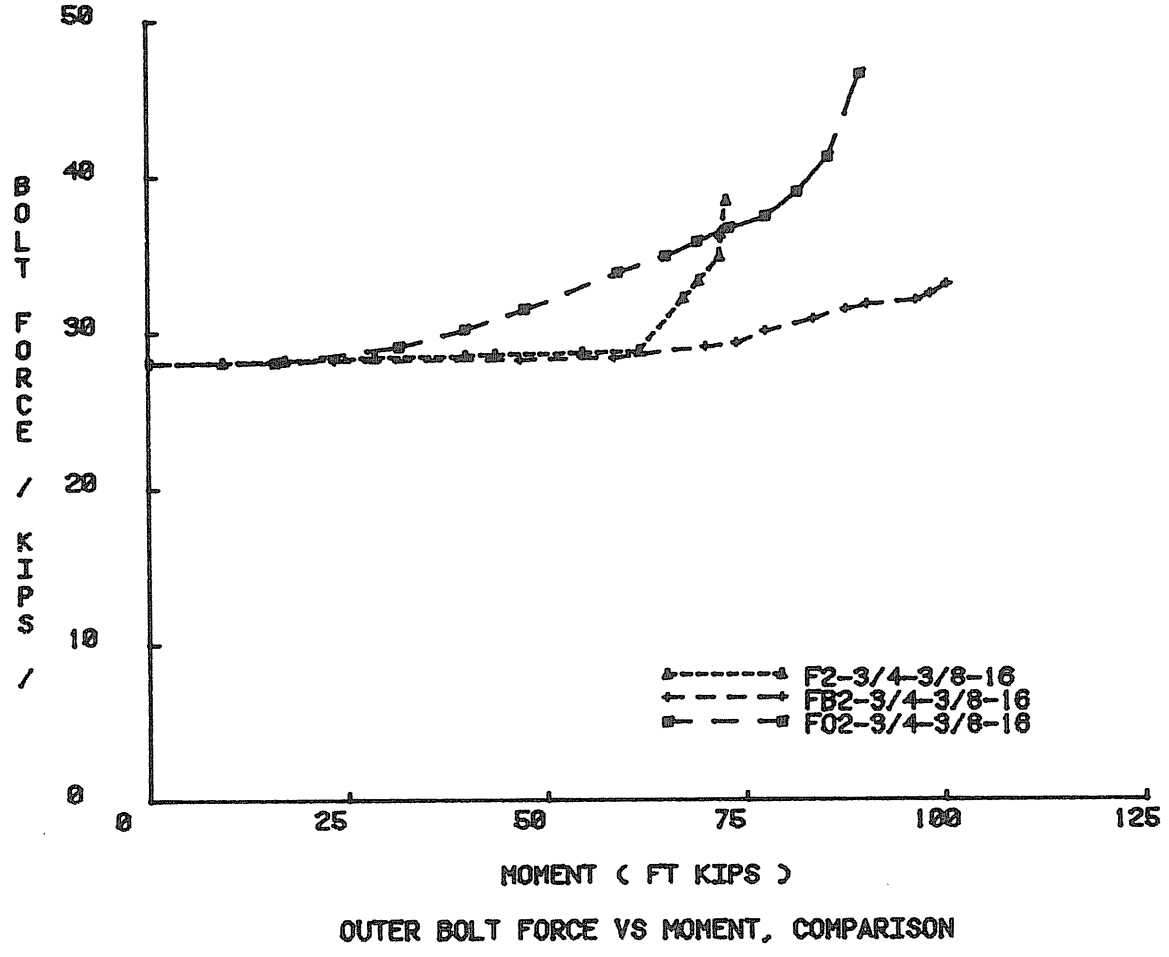

Figure 4.4 Comparison of Stiffened and Unstiffened Four-Bolt Flush End-Plate Outer Bolt Force vs. Moment Relationship

Table 4.1 Comparison of Stiffened and Unstiffened Four-Bolt Flush End-Plate Strength Data

		Test No.	Experimental	Predicted				
			Actual Failure Moment (ft.-k)	Unstiffened Failure Moment (ft.-k)	Stiffened Failure Moment (ft.-k) Between	Outside	$\frac{(Stiff.)_B}{(Unstiff.)}$	$\frac{(Stiff.)_O}{(Unstiff.)}$
Unstiffened Parameters		F2-3/4-3/8-16	73.2	63.4	95.1	78.4	1.50	1.24
		F2-3/4-3/8-24	144.7	117.0	170.0	151.5	1.45	1.29
		F2-5/8-3/8-16	85.5	74.1	104.9	93.8	1.42	1.27
		F2-3/4-1/2-24	171.8	180.6	274.9	230.5	1.52	1.28
Stiffened Parameters	Between	FB2-3/4-3/8-16	95.8	63.4	95.1	78.4	1.50	1.24
		FB2-3/4-3/8-24	149.2	101.6	154.6	129.6	1.52	1.28
		FB2-5/8-3/8-16	111.4	71.2	111.1	89.2	1.56	1.25
		FB2-3/4-1/2-23	257.0	170.0	259.8	218.0	1.53	1.28
	Outside	FO2-3/4-3/8-16	77.4	63.4	95.1	78.4	1.50	1.24
		FO2-3/4-3/8-24	123.2	101.6	154.6	129.6	1.52	1.28
		FO2-5/8-3/8-16	88.0	67.6	*	83.1	*	1.23
		FO2-3/4-1/2-23	210.0	170.0	259.8	218.0	1.53	1.28

Note: Predicted values are all based on F_y = 55 ksi.

*Geometry of this test does not permit placing a gusset plate between the tension row of bolts.

4.2 Conclusions

The major conclusions drawn from this study are:

1. The proposed yield-line mechanisms adequately predict the strength of stiffened flush end-plate connections with two rows of two bolts at the tension flange. For all eight tests where yielding of the end-plate governed the maximum applied moment, the ratio of applied to predicted moment varied from 0.92 to 1.08 (Table 3.3).

2. The modified Kennedy et al. procedure adequately predicts bolt forces to the proof load of the bolt, (Figure 3.8).

3. The applied moment corresponding to a measured bolt force equal to the published proof load varied from 72% to 112% of the maximum applied moment (Table 3.4).

4. The moment versus vertical displacement curves for the four-bolt flush end-plates were linear to 50-90% of the total strength.

5. The moment versus plate separation curve for the eight end-plates tested were linear to 40-60% of the total strength (Figure 3.7).

6. The applied moment corresponding to the bolt proof load always exceeded the "yield moment" based on plate separation (Table 3.4).

7. The useful strength of the stiffened flush end-plate connection studied here may be limited to 50% to 90% of the strength predicted by the straight yield-line mechanism because of excessive deformation due to end-plate yielding unless the connection is located at an assumed plastic hinge.

8. Stresses in the beam web of the four-bolt stiffened flush end-plate were not close to the flexure formula prediction line. The stresses near the tension bolts are the highest and in some tests the nominal yield stress was exceeded.

9. Analytical comparisons with unstiffened configurations, shows that a gusset plate between the tension row of bolts increases the predicted plate capacity by 40-50%. Placement of the gusset plate outside the tension bolts increased predicted plate capacity by 24-29%.

10. The proof load of the most highly stressed bolt is reached at a higher relative moment if the end-plate is stiffened.

11. Increasing the bolt pitch, p_f, and gage, g, decreases the capacity of the end-plate for both the stiffened and unstiffened configurations. Increasing the pitch between bolt rows, p_b, increases the capacity of unstiffened and outside stiffened connections and decreases plate capacity of between stiffened connections. However, as p_b is increased, the bolt forces also increase so no benefit is obtained. The ideal geometry is minimum values for p_t and g, and p_b between minimum p_b and approximately $4d_b$, where d_b = bolt diameter.

12. Use of a web gusset definitely increases the strength of the end-plate but only slightly increases the stiffness.

4.3 Recommendations

For the four-bolt stiffened flush end-plates with the range of geometries used in this research, it is recommended that Equations 2.8 and 2.11 be used to determine end-plate thickness for a given ultimate design moment. For stiffness requirements, the following design moments are recommended:

- Type III Construction (Semi-Rigid Framing)

$$M_w = 0.6M_u$$

- Type I Construction (Rigid or Continuous Framing)

$$M_w = 0.75\ M_y = 0.75(0.6\ M_u)$$
$$= 0.45\ M_u$$

The required bolt size can then be determined using Equations 2.12 to 2.20 and

$$d_b = \sqrt{2B_1/\pi Fa} \qquad (4.2)$$

where F_a = the allowable stress of the bolt material. In the AISC specification[4], the allowable tensile stress for A325 bolt material is 44 ksi with a factor of safety against yielding of 2.0. Equation 4.2 reflects this factor of safety. The recommended procedures are demonstrated in the following design examples.

Design Example (1). Determine end-plate thickness, for both Type III and Type I Construction and bolt size for a built-up beam with dimensions below. Assume a working moment of 55 ft-kips, A572 Gr50 Steel and A325 bolts. Use a 3/8 in. gusset plate between the tension row of bolts.

h=16 in. b_f=6 in. p_f=1 1/4 in. p_b=3.0 in.

t_w=1/4 in. t_f=1/4 in. g=2 3/4 in. t_s=3/8 in.

a). For Type III Construction

Step 1. Determine M_u and end-plate thickness (Equations 2.6 and 2.8):

$$M_u = 55/0.6 = 91.7 \text{ ft.-kips}$$

$$s = 1/2\ \sqrt{6 \times 2.75} = 2.03 \text{ in.}$$

$$P_t = 1.25 + 0.25 = 1.50 \text{ in.}$$

$$P_s = 1/2\ [3 - .375] = 1.3125$$

$$t_p = \left\{ \frac{91.7 \times 12/50}{\left[\frac{6}{2}\left(\frac{1}{1.25} + \frac{1}{1.3125}\right) + (1.25 + 1.3125)\left(\frac{2}{2.75}\right)\right](16-1.5) + \left[\frac{6}{2}\left(\frac{1}{1.3125} + \frac{1}{2.03}\right) + (1.3125+2.03)\left(\frac{2}{2.75}\right)\right](16-1.5-3)} \right\}^{1/2}$$

t_p = 0.364 in. Try PL 6 x 3/8.

Step 2. Compute flange force and flange stress.

$F_f = (91.7 \times 12)/(16 - 0.25) = 69.9$ kips

$\sigma_f = 69.9/(6 \times 0.25) = 46.6$ ksi

Step 3. Find the thick plate limit, t_1, (Equation 2.12 and 2.13).

Approximate thickness (Equation 2.12):

$t_1 = \sqrt{(2.11)(1.25)(0.25)(46.6)/50}$

$= 0.784 >> t_p = 0.375$ in.

Therefore $Q \neq 0$

Step 4. Determine the thin plate limit, t_{11}, (Equation 2.14 and 2.15).

Assume d_b = 3/4 in.

$w' = \frac{6}{2} - (3/4 + 1/16) = 2.188$ in.

F_{yb} = 120 ksi for A325 material

Approximate thickness (Equation 2.14):

$$t_{11} = \sqrt{\frac{2\{(6.0 \times 0.25 \times 46.6 \times 1.25) - \pi(0.75)^3(120)/16\}}{50(0.85 \times 6 + 0.8 \times 2.188)}}$$

$= 0.672$ in.

Using the exact equation (Equation 2.15):

$$t_{11}=\sqrt{\frac{2(6.0x0.25x46.6x1.25 - \pi (0.75)^3 (120)/16)}{6.0\sqrt{50^2-3(\frac{0.25x46.6}{2x0.672})^2} + 2.313 \sqrt{50^2-3(\frac{6.0x0.25x46.6}{2x2.188x0.672})^2}}}$$

$$= 0.664 \simeq 0.672 \text{ in.}$$

Since $t_{11} > t_p = 0.375$ in., $Q = Q_{max}$.

Step 5. Determine prying force, Q, (Equations 2.16 or 2.18)

F_{limit} from Equation 2.19:

$$F_{limit} = \frac{0.375^2 \times 50(0.85 \times 6.0 + 0.8 \times 2.188) + \pi(0.75)^3 120/16}{4 \times 1.25}$$

$$= 11.62 \text{ kips}$$

$(F_f)_{max}/2 = 6.0 \times 0.25 \times 50/2 = 37.5$ kips

Thus, F' = 11.62 kips and a = 0.375 in.

$$Q_{max} = \frac{(2.188)(0.375)^2}{4 \times 0.375}\sqrt{50^2 - 3(\frac{11.62}{2.188 \times 0.375})^2}$$

$$Q_{max} = 8.94 \text{ kips}$$

Step 6. Select bolt diameter

From Equation 2.20:

$$B_1 = \frac{69.9}{2(1.5)} + 8.94 = 32.2 \text{ kips} > P_T = 28 \text{ kips}$$

$$d_b = \sqrt{2 \times 32.2/(\pi \times 44.0)} = 0.683 \text{ in.} < 0.75 \text{ in.}$$

Use P_L 6 x 3/8 A572 Gr50, 4 - 3/4 in. diameter A325 bolts.

Connection Strength = 97.4 ft.-kips (Equation 2.7).

b). For Type I Construction

Step 1. Determine M_u and end-plate thickness (Equation 2.6 and 2.16).

$M_u = 55/0.45 = 122.2$ ft.-kips

$s = 1/2\ \sqrt{6.0 \times 2.75} = 2.03$ in.

From Equation 2.8.

$$t_p = \left\{ \frac{122.2 \times 12/50}{\left[\frac{6}{2}\left(\frac{1}{1.25} + \frac{1}{1.3125}\right) + (1.25 + 1.3125)\left(\frac{2}{2.75}\right)\right](16 - 1.5) + \left[\frac{6}{2}\left(\frac{1}{1.3125} + \frac{1}{2.03}\right) + (1.3125 + 2.03)\left(\frac{2}{2.79}\right)\right](16 - 1.5 - 3)} \right\}^{\frac{1}{2}}$$

$t_p = 0.42$ in. Try PL 6 x 1/2.

Step 2. Compute flange force and flange stress.

$F_f = 122.2 \times 12/(16 - 0.25) = 93.10$ kips

$\sigma_f = 93.10/(6.0 \times 0.25)$ 62.1 ksi

Step 3. Find the thick plate limit, t_1.

Approximate thickness (Equation 2.12):

$t_1 = \sqrt{2.11 \times 1.25 \times 0.25 \times 62.1/50} = 0.905$ in.

Exact thickness (Equation 2.13):

$$t_1 = \sqrt{\frac{2 \times 0.25 \times 62.1 \times 1.25}{50^2 - 3\left(\frac{0.25 \times 62.1}{.905}\right)^2}} = 0.982 \text{ in.}$$

$t_1 > t_p = 0.50$ in.

Therefore, $Q \neq 0$.

Step 4. Determine the thin plate limit, t_{11}.

Assume $d_b = 3/4$ in.

$w' = \frac{6}{2} - (3/4 + 1/16) = 2.188$ in.

Approximate thickness (Equation 2.14).

$$t_{11} = \sqrt{\frac{2(6.0 \times 0.25 \times 62.1 \times 1.25 - (\pi/16)0.75^3 \times 120)}{50(0.85 \times 6.0 + 0.80 \times 2.188)}}$$

$= 0.789$ in. >> 0.5 in.

Therefore $Q = Q_{max}$.

Step 5. Determine prying force, Q.

From Equation 2.19

$$F_{limit} = \frac{0.5^2 \times 50(0.85 \times 6.0 + 0.80 \times 2.188) + (\pi/16)0.75^3 \times 120}{4 \times 1.25}$$

$= 19.11$ kips

$(F_f)max/2 = 37.5$ kips

Thus $F' = 19.11$ kips and $a = 2 \times 0.5 = 1.0$ in.

$$Q_{max} = \frac{(2.188)(0.5)^2}{4 \times 1.0} \sqrt{50^2 - 3\left(\frac{19.11}{2.188 \times 0.5}\right)^2}$$

$= 5.44$ kips

Step 6. Select bolt diameter.

$B_1 = 93.1/2(1.5) + 5.44 = 36.47$ kips

$B_2 = F_f/6 = 15.5$ kips

$d_b = \sqrt{2 \times 36.47/(\pi \times 44.0)}$

$= 0.726$ in. < 0.75 in.

Use PL 6 x 1/2 A572 Gr50, 4 - 3/4 in. diameter A325 bolts.

Connection strength = 173.1 ft.-kips (Equation 2.7).

Design Example (2). For the working moment and geometry given in Example (1), determine the thickness for a stiffened four-bolt flush end-plate with a gusset plate outside the tension rows of bolts. Also size bolt.

a). For Type III Construction:

Step 1. Determine M_u end-plate thickness

$M_u = 55/0.6 = 91.7$ ft.-kips

$s = 1.25$ in.

From Equation 2.11:

$$t_p = \left[\frac{91.7 \times 12/50}{\frac{6}{2}\left(\frac{16-1.5}{1.25} + \frac{16-1.5-3}{1.25} + \frac{1}{2}\right) + \frac{2(16-1.5)}{2.75}(1.25+3+1.25) + \frac{2(3)}{2.75}(16-1.5-3)} \right]^{\frac{1}{2}}$$

$t_p = 0.387$ in. Try PL 6 x 1/2

Step 2. Compute flange force and flange stress.

$F_f = (91.7 \times 12)/(16 - 0.25) = 69.9$ kips

$\sigma_f = 69.9/(6 \times .25) = 46.6$ ksi

Step 3. Find the thick plate limit, t_1.

Same as Example (1-a), $t_1 = 0.784 >> t_p = 0.50$ in.

Therefore, $Q \neq 0$.

Step 4. Determine the thin plate limit, t_{11}.

Same as Example (1-a), assume $d_b = 3/4$ in.

$Q = Q_{max}$.

Step 5. Determine prying force, Q.

$Q = Q_{max} = 8.94$ kips

Step 6. Select bolt diameter.

From Equation 2.20:

$$B_1 = \frac{69.9}{2(1.5)} + 8.94 = 32.2 \text{ kips} > P_T = 28 \text{ kips}$$

$$B_2 = F_f/6 = 11.65 \text{ kips}$$

Select all bolts for B_1.

$$d_b = \sqrt{2 \times 32.2/\pi \times 44.0}$$

$$= 0.683 \text{ in.} < 0.75 \text{ in.}$$

Use PL 6 x 1/2 A572 Gr50, 4 - 3/4 in. diameter A325 bolts.

Connection strength = 153.1 ft.-kips (Equation 2.19).

b). For Type I Construction

Step 1. Determine M_u and end-plate thickness.

$M_u = 55/0.45 = 122.2$ ft.-kips

From Equation 2.11:

$$t_p = \left[\frac{122.2 \times 12/50}{\frac{6}{2}\left(\frac{16-1.5}{1.25} + \frac{16-1.5-3}{1.25} + \frac{1}{2}\right) + \frac{2(16-1.5)}{2.75}(1.25+3+1.25) + \frac{2(3)}{2.75}(16-1.5-3)} \right]^{\frac{1}{2}}$$

$$= 0.447 \text{ in.} \quad \text{Try PL 6 x 1/2}$$

Step 2. Compute flange force and flange stress.

$F_f = (122.2 \times 12)/(16 - 0.25) = 93.1$ kips

$\sigma_f = 93.1/(6 \times .25) = 62.1$ ksi

Step 3. Find the thick plate limit, t_1.

Same as example (1 - b), $t_1 = 0.905 >> 0.50$ in.

Therefore, $Q \neq 0$.

Step 4. Determine the thin plate limit, t_{11}.

Same as example (1 - b), assume $d_b = 3/4$ in.

$Q = Q_{max}$

Step 5. Determine prying force, Q.

$Q = Q_{max} = 5.44$ kips

Step 6. Select bolt diameter.

From Equation 2.20.

$$B_1 = \frac{93.10}{2(1.5)} + 5.44 = 36.5 \text{ kips} > P_T = 28 \text{ kips}$$

$d_b = 0.727$ in. < 0.75 in.

Use PL 6 x 1/2 A572 Gr50, 4 - 3/4 in. diameter A325 bolts.

Connection strength = 153.1 ft.-kips.

For comparison, the results of the previous examples are summarized in Table 4.2. Also presented in this table are end-plate thicknesses and bolt diameters for unstiffened flush end-plates with the same geometry as the previous examples based on design equations presented by Srouji[1].

Table 4.2

Summary of Flush End-Plate Design Examples

			Type	Bolt Diameter (in.)	Plate Thickness (in.)	Connection Strength (ft.-kips)
Stiffened	Four-Bolt	Between	I	3/4	1/2	173.1
			III	3/4	3/8	97.4
		Outside	I	3/4	1/2	153.1
			III	3/4	1/2	153.1
Unstiffened	Four-Bolt		I	3/4	1/2	122.7
			III	3/4	1/2	122.7
	Two-Bolt		I	7/8	5/8	147.8
			III	3/4	1/2	94.6

From Table 4.2, for Type I Construction (Rigid or Continuous Framing) with a working moment of 55 ft.-kips, a 3/4 in. diameter bolt and 1/2 in. end-plate is required for both stiffened and unstiffened four-bolt connections. However, the connection strength when the stiffener is placed between the tension rows of bolts is 41% stronger than the unstiffened connection and 13% stronger than the stiffened outside connection. For the two bolt connection , a 7/8 in. diameter bolt and 5/8 in. end-plate is required.

For Type III Construction (Semi-Rigid Framing) and a working moment of 55 ft.-kips, a 3/4 in. diameter bolt is required for both stiffened and unstiffened connections. However, a 3/8 in. end-plate

can be used when a stiffener is placed between the tension rows of bolts; whereas, the other connections require a 1/2 in. end-plate. If a 1/2 in. end-plate is used, by placing a stiffener outside the tension bolts the connection strength will be increased 25% over the unstiffened four-bolt connection and 62% over the two bolt connection.

The design procedures presented herein are based on specific yield-line mechanisms. Significant changes in the geometric relationships can affect the mechanism configuration and thus the predicted capacity. For these reasons the following limitations apply to the design procedures presented herein:

$$p_f \leq 2.0 \text{ in.} \qquad \frac{t_p}{d_b} \leq 1.0$$

$$g \leq 4.0 \text{ in.} \qquad \frac{b_f}{g} \leq 2.25$$

REFERENCES

1. Srouji, Ramzi, "Yield Line Analysis of End-Plate Connections With Bolt Force Predictions", A Thesis Submitted to the Graduate Faculty in Partial Fulfillment of the Requirement for the Degree of Master of Science, School of Civil Engineering and Environmental Science, University of Oklahoma, Norman, Oklahoma.

2. Kennedy, N.A., Vinnakota, S. and A.N. Sherbourne, "The Split-Tee Analogy in Bolted Splices and Beam-Column Connections", Joints in Structural Steelwork, Proceedings of the International Conference on Joints in Steelwork, held at Middlesbrough, Cleveland, John Wiley and Sons, New York - Toronto, 1981, pp. 2.138-2.157.

3. Manual of Steel Construction, 8th ed., American Institute of Steel Construction, Chicago, Illinois, 1980.

4. "Specification for the Design, Fabrication and Erection of Structural Steel for Buildings", American Institute of Steel Construction, New York, 1978.

APPENDIX A

NOMENCLATURE

NOMENCLATURE

a = distance from edge of end-plate to the bolt line

a_1 = distance from bolt centerline to edge of web root fillet

a_5 = distance from top bolt row centerline to edge of flange root fillet

B = bolt force

B_1 = outer bolt force

B_2 = inner bolt force

b_f = beam flange width

$c = (b_f - g)/2$ = end-plate bolt edge distance

$c_1 = (p_f - 3/2t_f - t_p/2$ - diameter of washer/4)

d_b = bolt diameter

d_e = distance from bolt line above tension flange to edge of plate

d_h = bolt hole diameter

ds = elemental length of line n

ds_x = the x-component of the elemental length ds

ds_y = the y-component of the elemental length ds

E = Young's modulus of elasticity

F = flange force per bolt

F_a = allowable bolt stress

f_b = bending stress

F_{by} = yield stress of beam material

F_f = flange force = $Mu/(d-t_f)$

F_{limit} = flange force at which the end-plate becomes "thin"

F_{py} = yield stress of plate material

F_t = tensile strength of bolt material

F_{yb} = yield stress of bolt material

g = gage distance between bolts

h = beam depth

h_s = distance between bolt centerline and compression flange

I = moment of inertia

L = length of beam

Ln = length of yield line n

M_u = ultimate moment at end-plate

M_{yb} = moment at which the experimental bolt force is at the proof load (twice the allowable)

M_{ys} = moment at which the experimental plate separation exceeds the predicted separation by 10%

M_{yv} = moment at which the experimental vertical deflection exceeds the predicted deflection by 10%

m_p = plastic moment capacity of plate per unit length, equal to $F_{py}t_p^2/4$

m_{px} (m_{py}) = the x(y)-component of the normal moment capacity per unit length

m_{px} = the y-component of the normal moment capacity per unit length

N = number of yield lines in a mechanism

P_b = pitch between upper and lower rows of the tension bolts

P_f = pitch measured from bottom of flange to centerline of first bolt row

P_p = bolt proof load

p_T = Pretension force

P_t = pitch measured from top of flange to centerline of the first bolt row

Q = prying force

s = distance from bolt centerline to the lower yield line

s_t = stiffener thickness

t_f = flange thickness

t_p = end-plate thickness

t_1 = thick plate limit

t_{11} = thin plate limit

w_i = total internal energy stored

w = width of end-plate per bolt pair

w_{in} = internal work done in the nth yield line

w' = width of end-plate per bolt at bolt line minus bolt hole diameter

x = distance from the edge of the bolt head to the beam web

α_s = plate separation correction factor

σ = coefficient depending on bolt arrangement (Zoetermeijer)

β = angle between the edges

δ = normalized displacement at bolt line

Δ_c = vertical displacement

δ_{max} = maximum vertical deflection (at centerline of beam)

δ_p = plate separation

θ_n = relative normal rotation of yield line n

θ_{nx} = the x-component of the relative normal rotation of the yield line n

θ_{ny} = the y-component of the relative normal rotation of the yield line n

σ_f = stress in beam flange

σ_{yb} = yield stress of bolt material

APPENDIX B

YIELD-LINE PATTERNS

Four Bolt with Stiffener Between the Bolt Holes

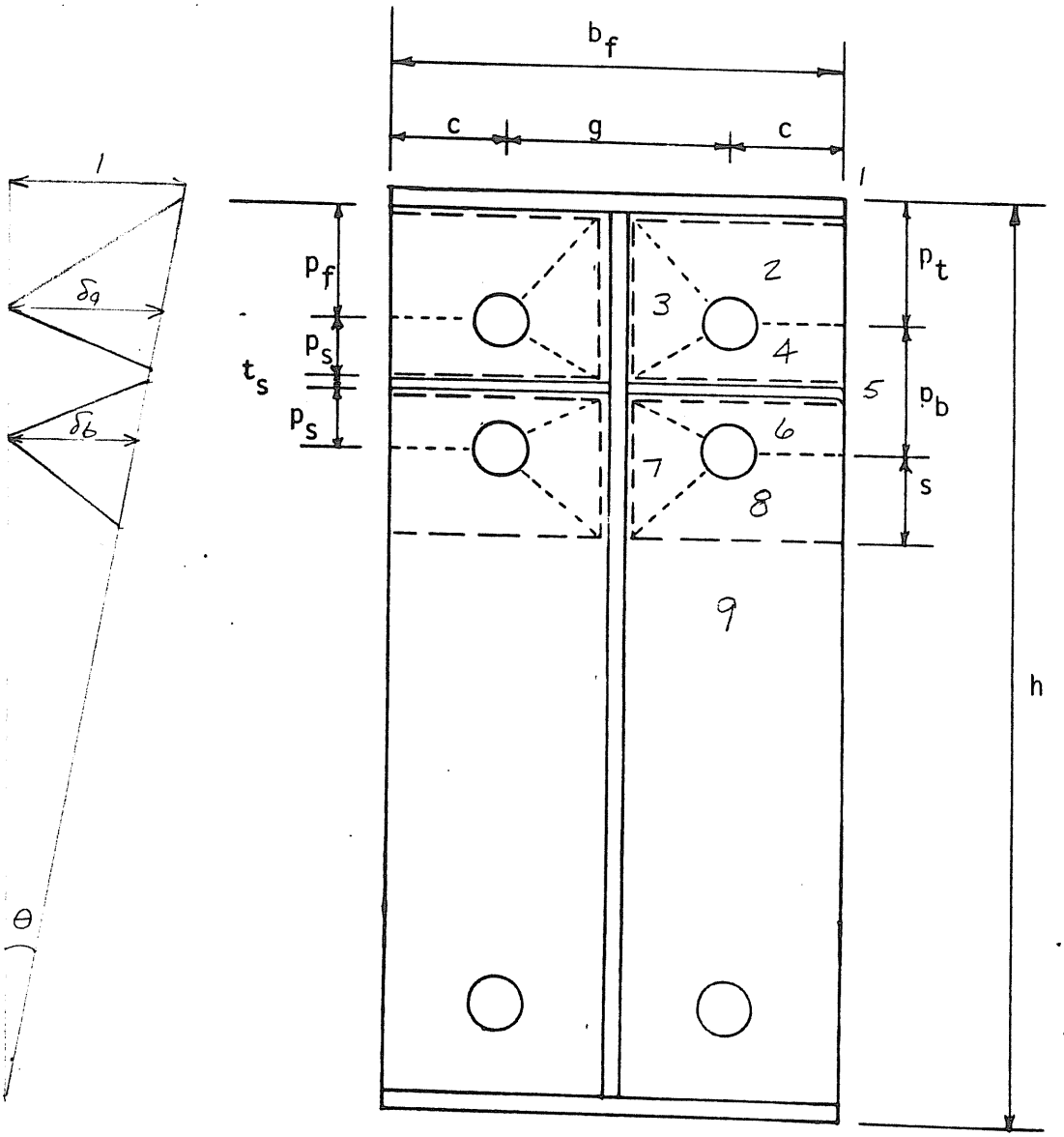

$$t_p = \left[\frac{M_u/F_{py}}{\left[\frac{b_f}{2}\left(\frac{1}{p_f}+\frac{1}{p_s}\right) + (p_f+p_s)\left(\frac{2}{g}\right)\right](h-p_t) + \left[\frac{b_f}{2}\left(\frac{1}{p_s}+\frac{1}{s}\right) + (p_s+s)\left(\frac{2}{g}\right)\right](h-p_t-p_b)} \right]^{\frac{1}{2}}$$

Mechanism I - Stiffener Between Bolt Lines

m_p = plastic moment capacity of the plate per unit length

line i/j denotes the line of intersection between the rigid segments i and j.

Slopes in Panels in Mechanism-I

Panel	Slope Normal to x-axis	Slope Normal to y-axis
1	$\theta = 1/h$	0
2	$(\delta_a + \rho_f\theta)/\rho_f$	0
3	$\theta = 1/h$	$2\delta_a/g$
4	$-(\delta_a - \rho_s\theta)/\rho_s$	0
5	θ	0
6	$(\delta_b + \rho_s\theta)/\rho_s$	0
7	$\theta = 1/h$	$2\delta_b/g$
8	$-(\delta_b - s\theta)/s$	0
9	θ	0

$$\delta_a = \frac{h-\rho_t}{h} \quad ; \quad \delta_b = \frac{h-\rho_t-\rho_s}{h}$$

Energy stored in line 1/2

$$= m_p \frac{b_f}{2}\left((\delta_a + \rho_f\theta)/\rho_f - 1/h\right) = \frac{b_f}{2}\frac{(h-\rho_t)}{h\rho_f} m_p$$

Energy stored in line 2/3

$$= m_p \frac{g}{2}\left(\frac{\delta_a}{\rho_f}\right) + m_p\rho_f\left(2\frac{\delta_a}{g}\right) = \left[\frac{g}{2}\frac{(h-\rho_t)}{h\rho_f} + 2\rho_f\frac{(h-\rho_t)}{gh}\right] m_p$$

Energy stored in line 2/4

$$= m_p c\left(\frac{\delta_a}{\rho_f} + \theta + \frac{\delta_a}{\rho_s} - \theta\right) = c\left(\frac{h-\rho_t}{h}\right)\left(\frac{1}{\rho_f} + \frac{1}{\rho_s}\right) m_p$$

Energy stored in line 3/4

$$= \frac{g}{2}\left(\frac{h-\rho_t}{h\rho_s}\right) m_p + 2\rho_s\left(\frac{h-\rho_t}{hg}\right) m_p$$

Energy stored in line 4/5

$$= m_p \frac{b_f}{2}\left(\frac{\delta_a}{\rho_s}\right) = m_p \frac{b_f}{2}\left(\frac{h-\rho_t}{h\rho_s}\right)$$

Energy stored in line 5/6

$$= m_p \frac{b_f}{2}\left(\frac{\delta_b}{\rho_s}\right) = \frac{b_f}{2}\left(\frac{h-\rho_t-\rho_b}{h\rho_s}\right) m_p$$

Energy stored in line 6/7

$$= m_p \frac{g}{2}\left(\frac{\delta_b}{\rho_s}\right) + m_p \rho_s \left(\frac{2\delta_b}{g}\right) = \left[\frac{g}{2}\frac{(h-\rho_t-\rho_b)}{h\rho_s} + \frac{2\rho_s(h-\rho_t-\rho_b)}{gh}\right] m_p$$

Energy stored in line 6/8

$$= m_p c\left(\frac{\delta_b}{\rho_s} + \theta + \frac{\delta_b}{s} - \theta\right) = c\left(\frac{h-\rho_t-\rho_b}{h}\right)\left(\frac{1}{\rho_s} + \frac{1}{s}\right) m_p$$

Energy stored in line 7/8

$$= \frac{g}{2}\left(\frac{h-\rho_t-\rho_b}{hs}\right) m_p + 2s\left(\frac{h-\rho_t-\rho_b}{sh}\right)$$

Energy stored in line 8/9

$$= \frac{b_f}{2}\left(\frac{\delta_b}{s}\right) m_p = \frac{b_f}{2}\left(\frac{h-\rho_t-\rho_b}{hs}\right) m_p$$

Energy stored along web (3)

$$= (\rho_f + \rho_s)\left(\frac{2\delta_a}{g}\right) m_p = 2(\rho_f + \rho_s)\left(\frac{h-\rho_t}{gh}\right) m_p$$

Energy stored along web (7)

$$= (\rho_s + s)\left(\frac{2\delta_b}{g}\right) m_p = 2(\rho_s + s)\left(\frac{h-\rho_t-\rho_b}{gh}\right) m_p$$

Total Energy

$$= 2M_p\left[\frac{b_f}{2}\left(\frac{h-\rho_t}{h}\right)\left(\frac{1}{\rho_f}+\frac{1}{\rho_f}+\frac{1}{\rho_s}+\frac{1}{\rho_s}\right)+2\rho_f\left(\frac{h-\rho_t}{h}\right)\left(\frac{1}{g}+\frac{1}{g}\right)\right.$$
$$+2\rho_s\left(\frac{h-\rho_t}{h}\right)\left(\frac{1}{g}+\frac{1}{g}\right)+\frac{b_f}{2}\left(\frac{h-\rho_t-\rho_b}{h}\right)\left(\frac{1}{\rho_s}+\frac{1}{\rho_s}+\frac{1}{s}+\frac{1}{s}\right)$$
$$\left.+2\rho_s\left(\frac{h-\rho_t-\rho_b}{h}\right)\left(\frac{1}{g}+\frac{1}{g}\right)+2s\left(\frac{h-\rho_t-\rho_b}{h}\right)\left(\frac{1}{g}+\frac{1}{g}\right)\right]$$

$$\omega_i = 4M_p\left\{\left[\frac{b_f}{2}\left(\frac{1}{\rho_f}+\frac{1}{\rho_s}\right)+(\rho_f+\rho_s)\left(\frac{2}{g}\right)\right]\left(\frac{h-\rho_t}{h}\right)\right.$$
$$\left.+\left[\frac{b_f}{2}\left(\frac{1}{\rho_s}+\frac{1}{s}\right)+(\rho_s+s)\left(\frac{2}{g}\right)\right]\left(\frac{h-\rho_t-\rho_b}{h}\right)\right\}$$

$$M_u\,\theta = 4\left(\frac{1}{4}t_p^{\,2}F_{py}\right)\{\quad''\quad\}$$

$$M_u = F_{py}\,t_p^{\,2}\left\{\left[\frac{b_f}{2}\left(\frac{1}{\rho_f}+\frac{1}{\rho_s}\right)+(\rho_f+\rho_s)\left(\frac{2}{g}\right)\right](h-\rho_t)+\right.$$
$$\left.\left[\frac{b_f}{2}\left(\frac{1}{\rho_s}+\frac{1}{s}\right)+(\rho_s+s)\left(\frac{2}{g}\right)\right](h-\rho_t-\rho_b)\right\}$$

$$0=\frac{d\omega_i}{ds}=\frac{b_f}{2}\left(\frac{-1}{s^2}\right)+\frac{2}{g}\quad\Rightarrow\quad s=\frac{1}{2}\sqrt{t_f g}$$

$$\therefore\ t_p=\left[\frac{M_u/F_{py}}{\left[\frac{b_f}{2}\left(\frac{1}{\rho_f}+\frac{1}{\rho_s}\right)+(\rho_f+\rho_s)\left(\frac{2}{g}\right)\right](h-\rho_t)+\left[\frac{b_f}{2}\left(\frac{1}{\rho_s}+\frac{1}{s}\right)+(\rho_s+s)\left(\frac{2}{g}\right)\right](h-\rho_t-\rho_b)}\right]^{1/2}$$

Four Bolt with Stiffener Outside the Bolt Holes

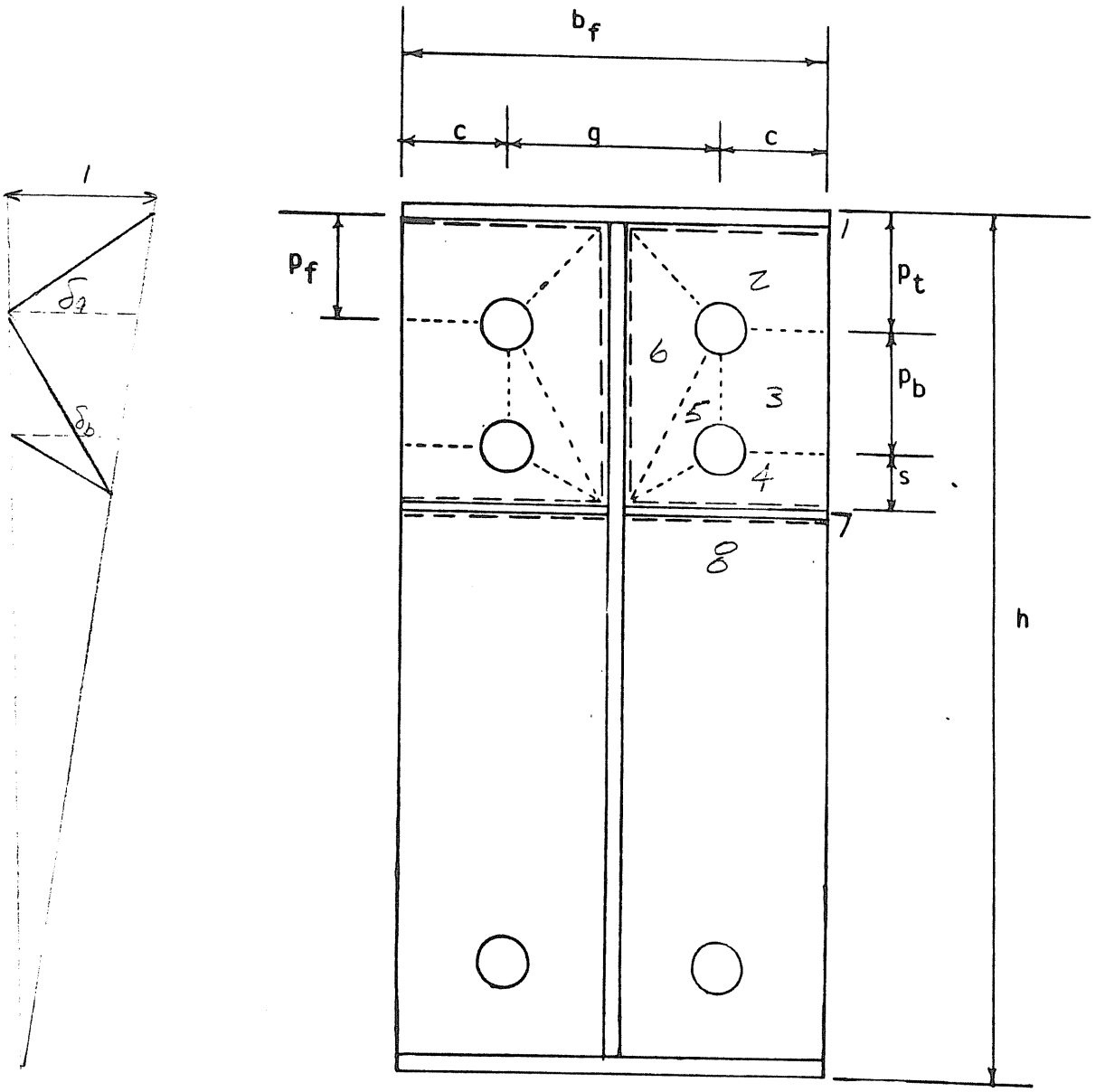

$$t_p = \left[\frac{M_u/F_{py}}{\frac{b_f}{2}\left(\frac{h-p_t}{p_f} + \frac{h-p_{t2}}{s} + \frac{1}{2}\right) + ?(p_f+p_b+s)\left(\frac{h-p_t}{g}\right) + \frac{2p_b}{g}(h-p_t-p_b)} \right]^{1/2}$$

where $p_{t2} = p_t + p_b$

Mechanism II Stiffener Outsider Collapse Lines

m_p = plastic moment capacity of the plate per unit length

line i/j denotes the line of intersection between the rigid segments i and j

Slopes in Panels in Mechanism-II

Panel	Slope Normal to X-axis	Slope Normal to y-axis
1	$\theta = 1/h$	0
2	$(\delta_a + \rho_f\theta)/\rho_f$	0
3	0	0
4	$-(\delta_b - s\theta)/s$	0
5	0	$2(\delta_b - s\theta)/g$
6	θ	$2\delta_a/g$
7	θ	0
8	θ	0

$$\delta_a = \frac{h-\rho_t}{h} \quad ; \quad \delta_b = \frac{h-\rho_t-\rho_b}{h}$$

Energy stored in line 1/2

$$= m_p \frac{b_f}{2}\left((\delta_a + \rho_f\theta)/\rho_f - \theta\right)$$

Energy stored in line 2/3

$$= m_p\, C\left[(\delta_a + \rho_f\theta)/\rho_f\right]$$

Energy stored in line 2/6

$$= m_p \frac{g}{2}\left[(\delta_a + \rho_f\theta)/\rho_f - \theta\right] + m_p\rho_f\left(2\frac{\delta_a}{g}\right)$$

Energy stored in line 3/4

$$= m_p\, C\left[(\delta_b - s\theta)/s\right]$$

Energy stored in line 3/5

$= m_p \rho_b \left[2(\delta_b - s\theta)/3 \right]$

Energy stored in line 4/5

$= m_p \, {}^{3}/_{2} \left[(\delta_b - s\theta)/3 \right] + m_p s \left[2(\delta_b - s\theta)/3 \right]$

Energy stored in line 4/7

$= m_p \, {}^{b_f}/_{2} \left[{}^{\delta_b}/_{s} \right]$

Energy stored in line 5/6

$= m_p \, {}^{3}/_{2}\theta + m_p(\rho_b + s)\left[2\frac{\delta_a}{3} - \frac{2(\delta_b - s\theta)}{3} \right]$

Energy stored in line 7/8

$= m_p \, {}^{b_f}/_{2} (\theta)$

Energy stored along web (6)

$= m_p (\rho_f + \rho_t + s) \, {}^{2\delta_a}/_{3}$

$s = u$

Total Energy

$$= 2m_p \Big[\left(\tfrac{b_f}{2}\right)\left(\tfrac{\delta_a}{\rho_f}\right) + c\left(\tfrac{\delta_a}{\rho_f} + \theta\right) + \tfrac{3}{2}\left(\tfrac{\delta_a}{\rho_f}\right) + \rho_f\left(\tfrac{2\delta_a}{3}\right) + \rho_b\left(\tfrac{2\delta_b}{3} - \tfrac{2s\theta}{3}\right)$$
$$+ c\left(\tfrac{\delta_b}{s} - \theta\right) + \tfrac{3}{2}\left(\tfrac{\delta_b}{s} - \theta\right) + s\left(\tfrac{2\delta_b}{3} - \tfrac{2s\theta}{3}\right) + \tfrac{b_f}{2}\left(\tfrac{\delta_b}{s}\right)$$
$$+ \tfrac{3}{2}\theta + (\rho_b + s)\left[2\tfrac{\delta_a}{3} - 2\tfrac{\delta_b}{3} + \tfrac{2s\theta}{3} \right] + \tfrac{b_f}{2}\theta$$
$$+ (\rho_f + \rho_t + s)\,2\tfrac{\delta_a}{3} \Big]$$

$$w_i = 4M_p \left[\frac{b_f}{2h}\left(\frac{h - \rho_t}{\rho_f} + \frac{h - \rho_t - \rho_b}{s} + \frac{1}{2} \right) + \frac{2(h - \rho_t)}{3h}(\rho_f + \rho_b + s) \right.$$
$$\left. + \frac{2\rho_b}{3}\left(\frac{h - \rho_t - \rho_b}{h} \right) \right]$$

$$M_u\theta = 4\left(\tfrac{1}{4} t\rho^2 F_{py}\right)\left[\quad " \quad \right]$$

$$M_u = F_{py} t_p^2 \left[\frac{b_f}{2} \left(\frac{h - \rho_t}{\rho_f} + \frac{h - \rho_t - \rho_b}{5} + \frac{1}{2} \right) + \frac{2(h-\rho_t)}{5} (\rho_f + \rho_b + 5) + \frac{2\rho_b}{5} (h - \rho_t - \rho_b) \right]$$

$$\therefore \quad t_p = \left[\frac{M_u / F_{py}}{\frac{b_f}{2} \left(\frac{h - \rho_t}{\rho_f} + \frac{h - \rho_t - \rho_b}{5} + \frac{1}{2} \right) + \frac{2(h-\rho_t)}{5} (\rho_f + \rho_b + 5) + \frac{2\rho_b}{5} (h - \rho_t - \rho_b)} \right]^{1/2}$$

APPENDIX C

FB2-3/4-3/8-16 TEST RESULTS

MBMA TEST SUMMARY

Project: MBMA/Conn.

Test No.: FB2-3/4-3/8-16

Test Date: 2/10/84

Purpose: Load to failure - Full pretension

Rows of Bolts in Tension: 2 **Bolts/Row:** 2

Bolt Diameter: 3/4" **Plate Thickness:** 3/8" (.375)

Beam Depth: 16" **Flange Width:** 6"

Web Thickness: 1/4" **Flange Thickness:** 1/4"

Moment of Inertia: 263.64 $in.^4$

Pretension Force: 28 kips

Failure Load: 23.8 kips vertical load; 92.8 ft - kips moment at end plate

Failure Mode: Yielding of end plate

Predicted Failure Loads:

Method: Yield-line Theory **Load:** 24.6 kips (96.0 ft - kips)

Method: **Load:**

Maximum Displacements:

Vertical: 2.474 in.

Horizontal top flange: 0.114 in.

Horizontal bottom flange: 0.351 in.

Maximum plate separation: **East:** 0.0 **Centerline:** .049 **West:** .025

Discussion:

-Instrumented bolts were used in the test. Pretension force was obtained by using the data acquisition system to monitor the bolt tension as torque was applied.

-Failure load was approximately 3% less than predicted by yield line analysis.

-Maximum applied load was 23.8 kips corresponding to a moment at the end plate of 92.8 ft - kips.

-Bolt force in interior bolt was approximately 7% more than the exterior bolt.

-Vertical displacement was close to prediction up to a moment of 80 ft - kips at which time the curve began to lean over.

-Plate separation was approximately one half as much as predicted up to 60 ft - kips.

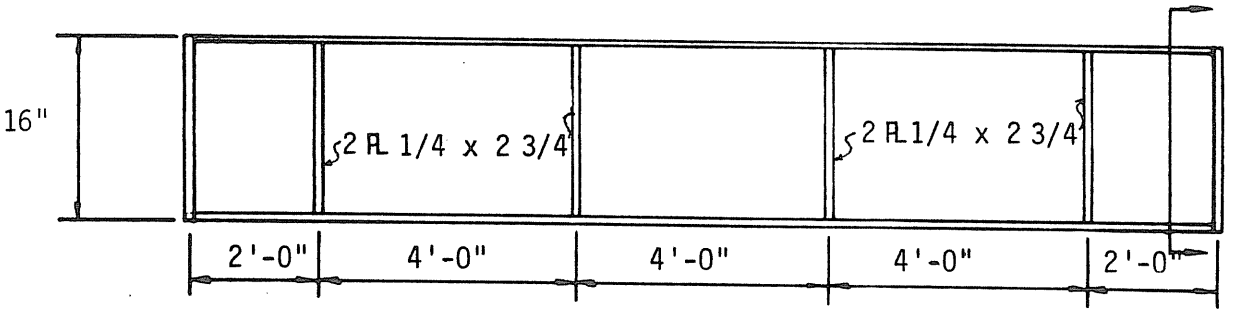

a) Elevation

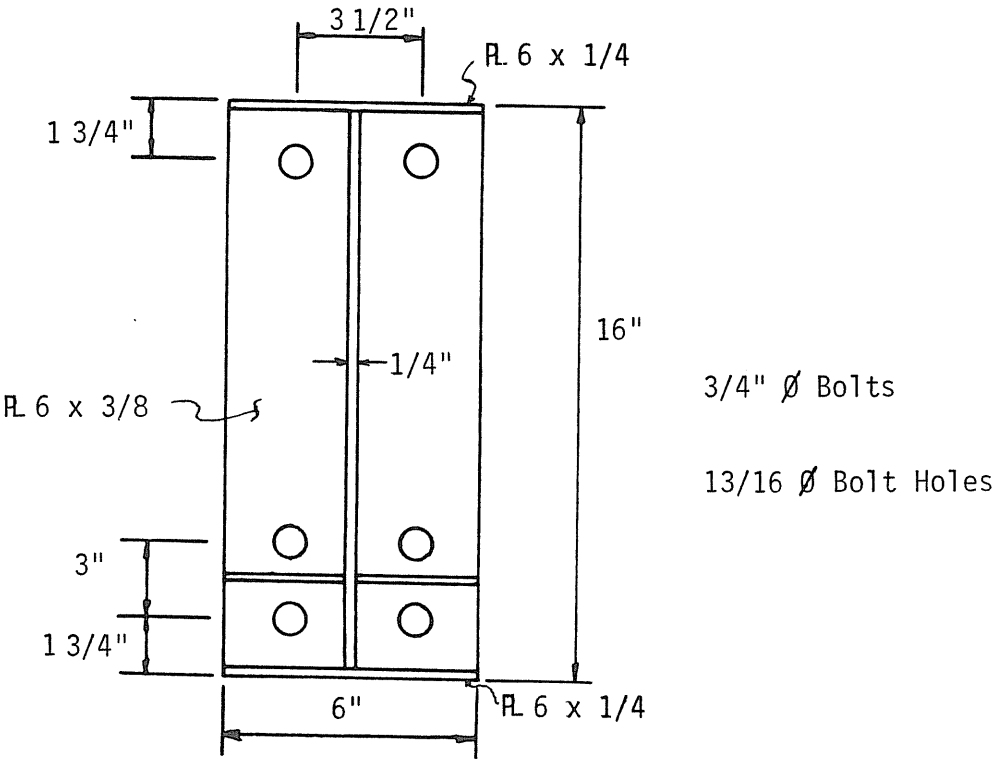

b) End-Plate

Figure C.1 Specimen Details, Test FB2-3/4-3/8-16

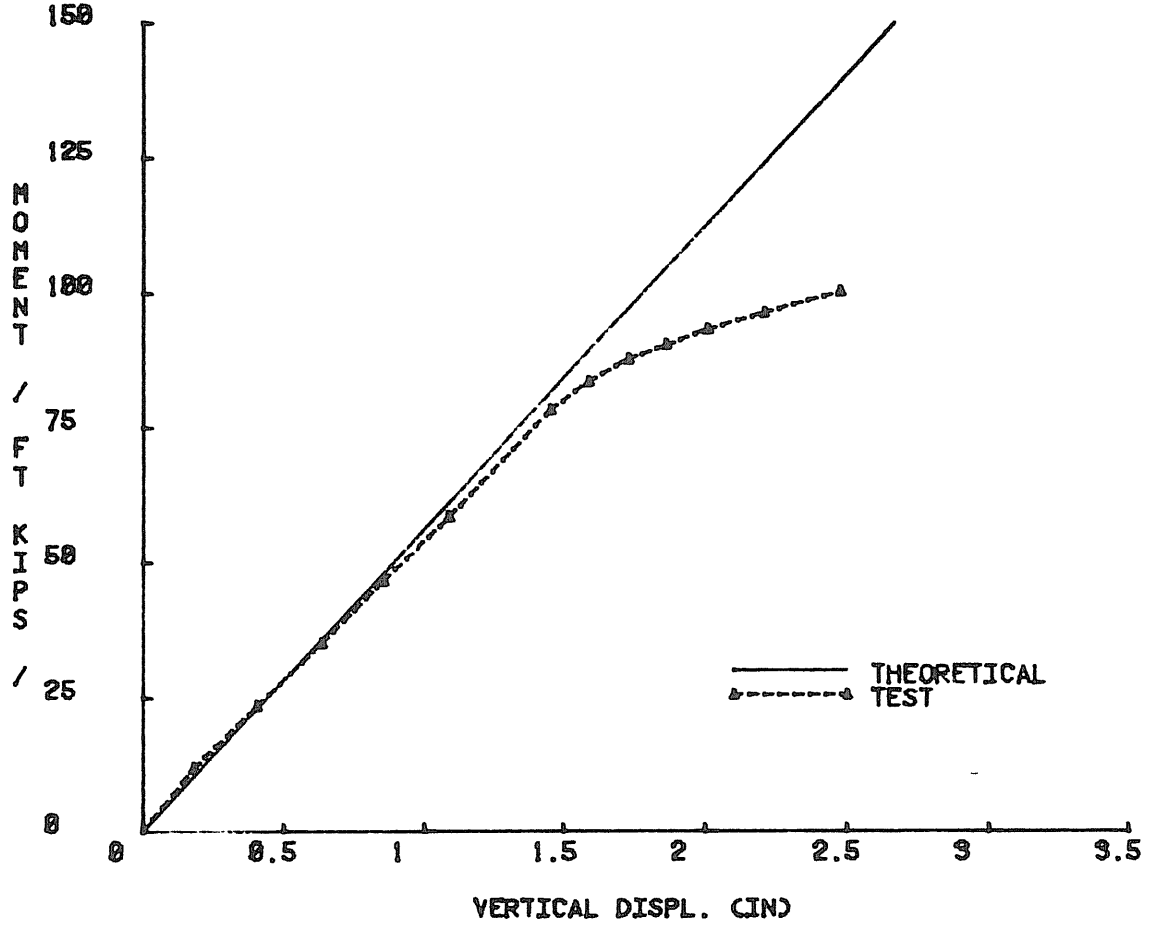

Figure C.2 MOMENT VS VERTICAL DISPL., FB2-3/4-3/8-16

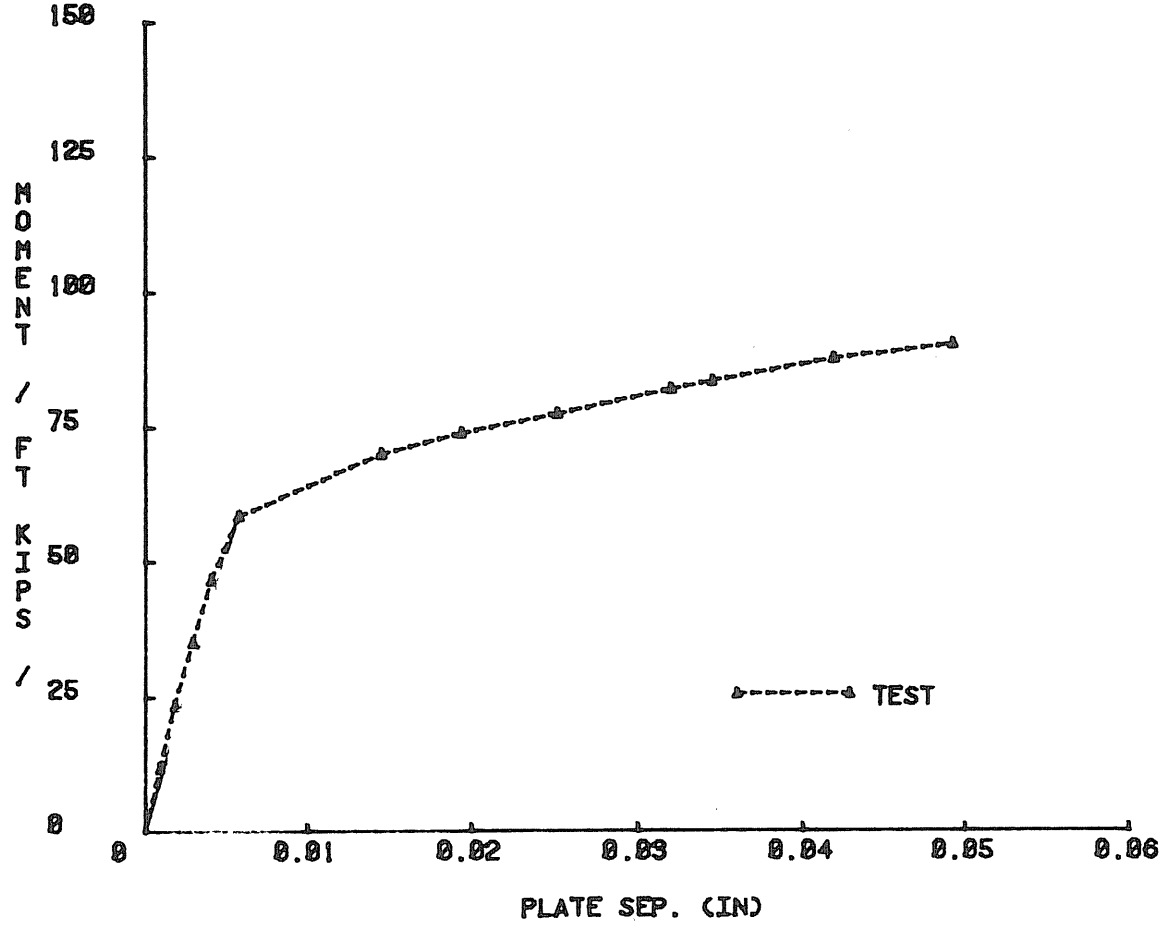

Figure C.3 **MOMENT VS PLATE SEPARATION, FB2-3/4-3/8-16**

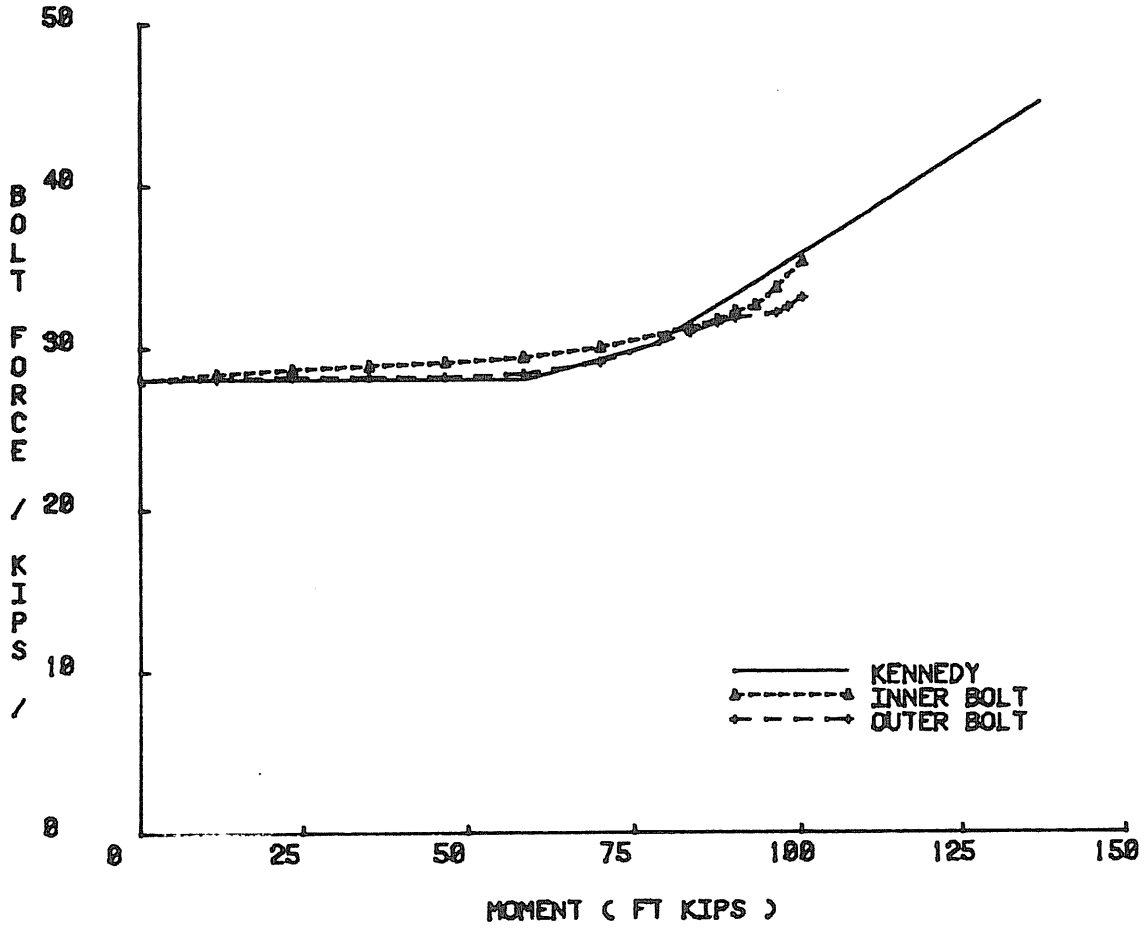

Figure C.4 BOLT FORCE VS MOMENT, FB2-3/4-3/8-16

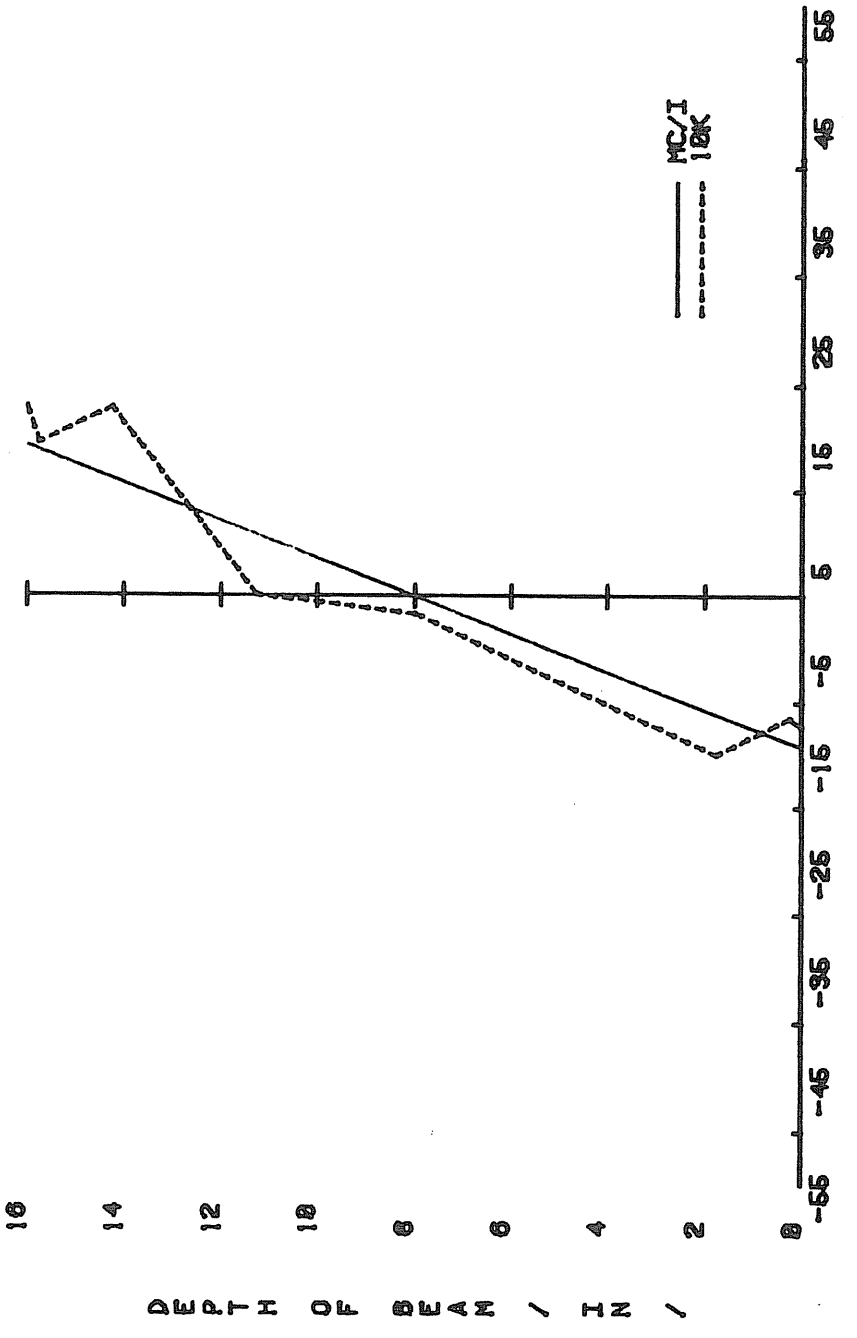

Figure C.5 LOAD VS STRESS. FB2-3/4-3/8-18

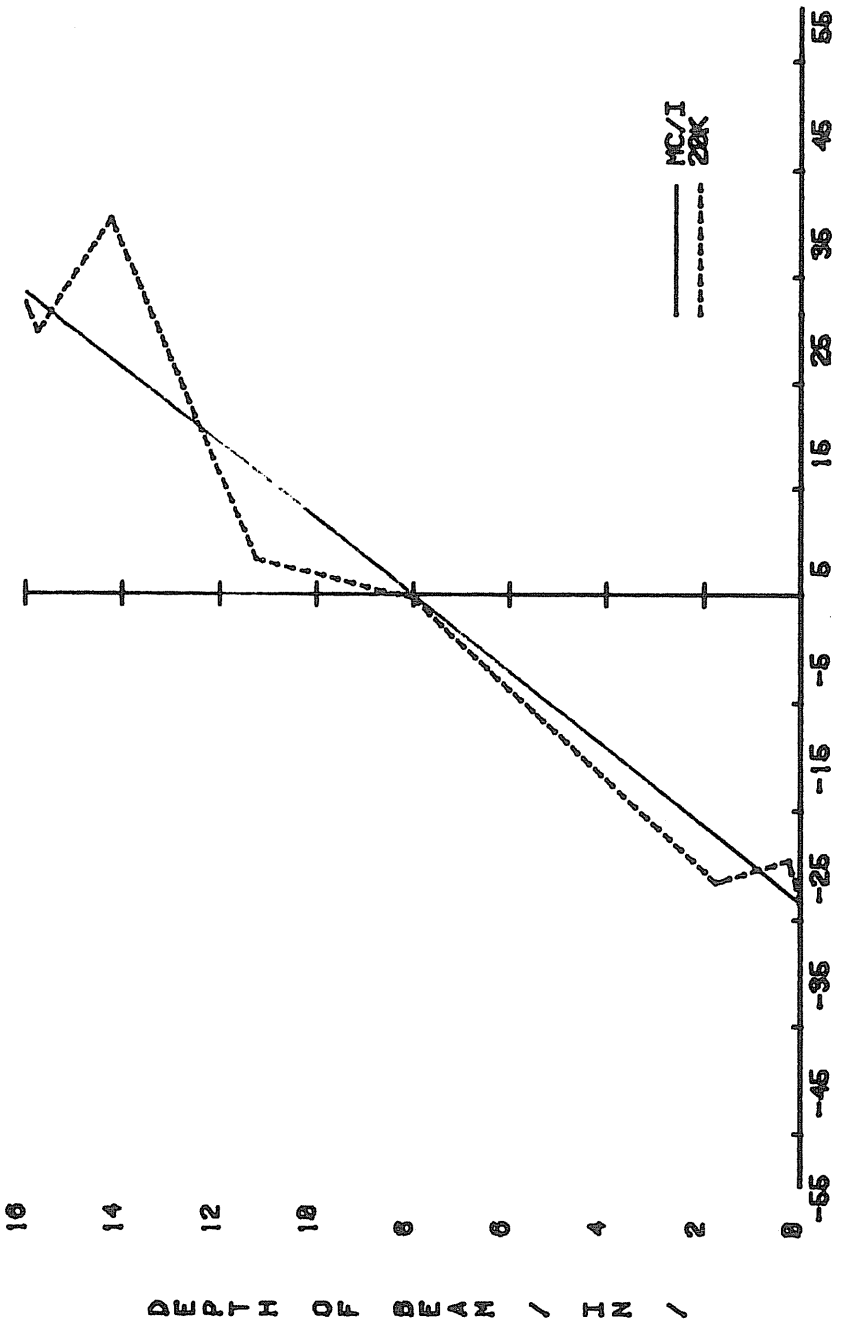

Figure C.6 LOAD VS STRESS, FB2-3/4-3/8-16

APPENDIX D

FO2-3/4-3/8-16 TEST RESULTS

MBMA TEST SUMMARY

Project: MBMA/Conn.

Test No.: F02-3/4-3/8-16

Test Date: 2-16-84

Purpose: Load to failure - Full pretension

Rows of Bolts in Tension: 2 **Bolts/Row:** 2

Bolt Diameter: 3/4" **Plate Thickness:** 3/8"

Beam Depth: 16" **Flange Width:** 6"

Web Thickness: 1/4" **Flange Thickness:** 1/4"

Moment of Inertia: 263.64 $in.^4$

Pretension Force: 28 kips

Failure Load: 18.6 kips vertical load; 74.4 ft-kips moment at end plate

Failure Mode: Yielding of end plate causing excessive plate separation

Predicted Failure Loads:

Method: Yield Line Theory **Load:** 79.1 ft-kips (19.8 kips)

Method: **Load:**

Maximum Displacements:

Vertical: 3.972 (2.053" at 18.6 kips)

Horizontal top flange: .363" (.033" at 18.6 kips)

Horizontal bottom flange: .626" (.220" at 18.6 kips)

Maximum plate separation: East: 0.0 Centerline: .0543" West: .0339"

Discussion:

-Instrumented bolts were used in the test. Pretension force was obtained by using the data acquisition system to monitor the bolt tension as torque was applied.

-Failure load was approximately 6% less than predicted by yield line analysis.

-Failure load of end plate was 18.6 kips corresponding to a moment at the end plate of 74.4 ft-kips. However, the test was continued until a load of 24.4 kips (97.5 ft-kips) was attained.

-The bolt force in the exterior bolt was approximately 6% more than the interior bolt force.

-Vertical displacement was close to predicted up to 25 ft-kips at which time the curve began to lean over.

-Plate separation was approximately one half as much as predicted up to 25 ft-kips.

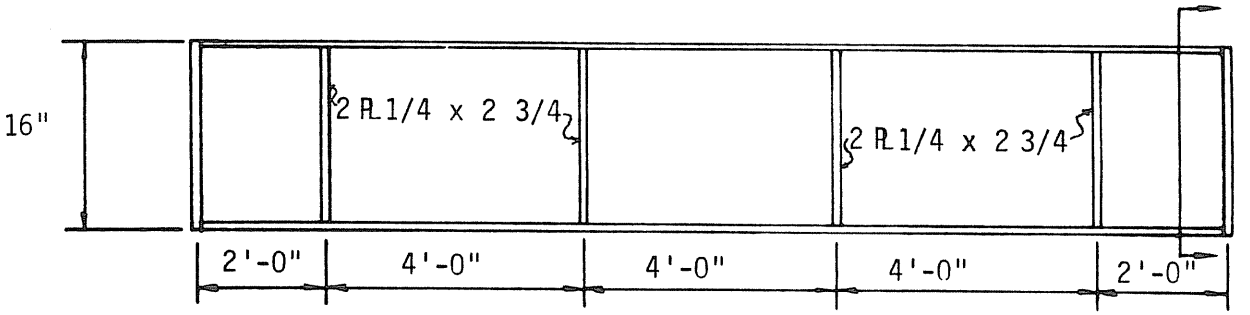

a) Elevation

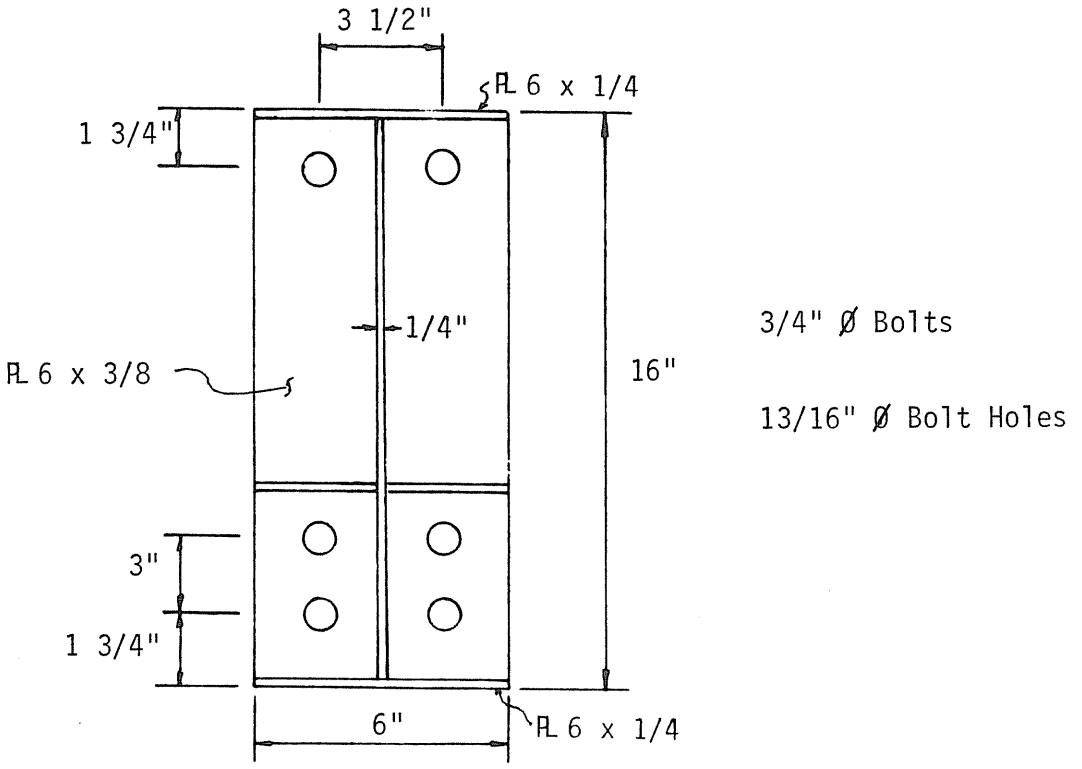

b) End Plate

Figure D.1 Specimen Details, Test F02-3/4-3/8-16

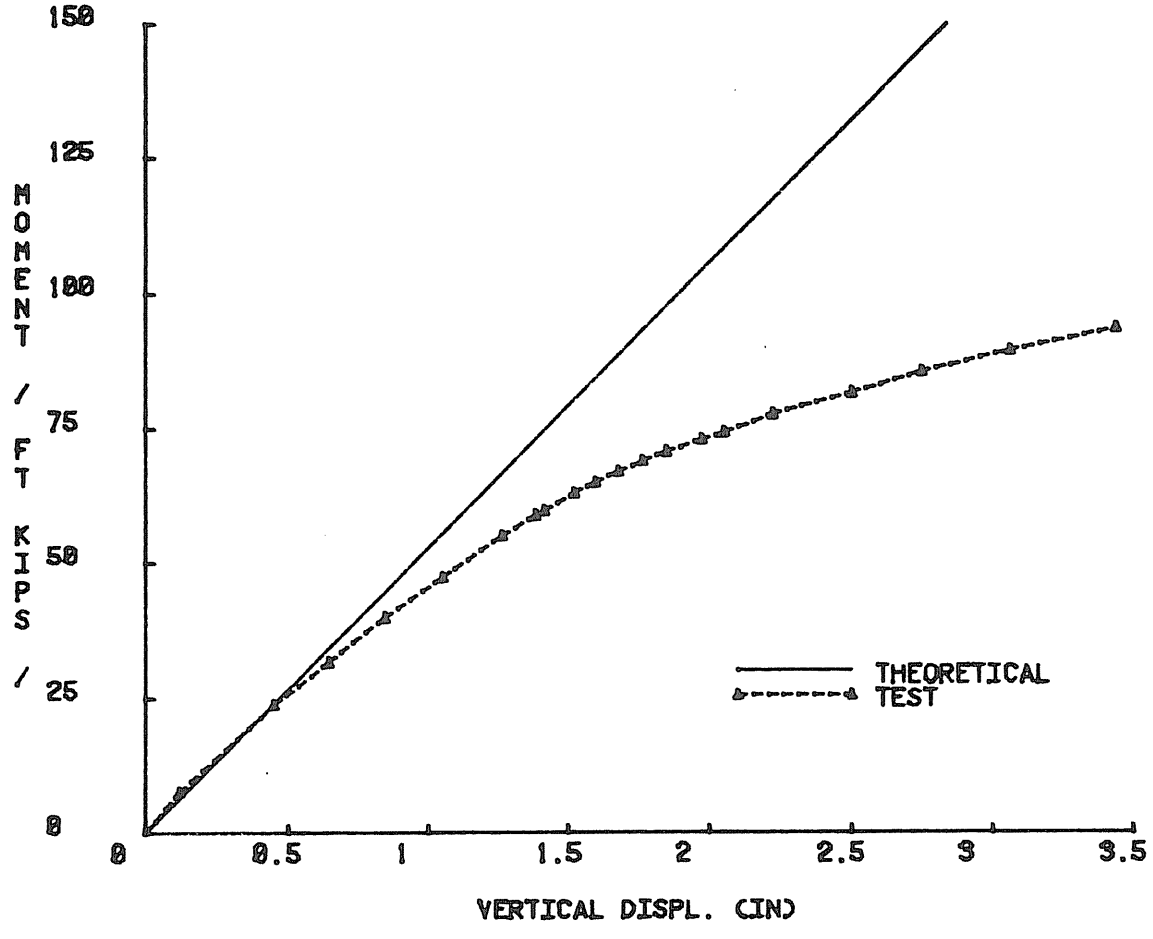

Figure D.2 MOMENT VS VERTICAL DISPLACEMENT, F02-3/4-3/8-16

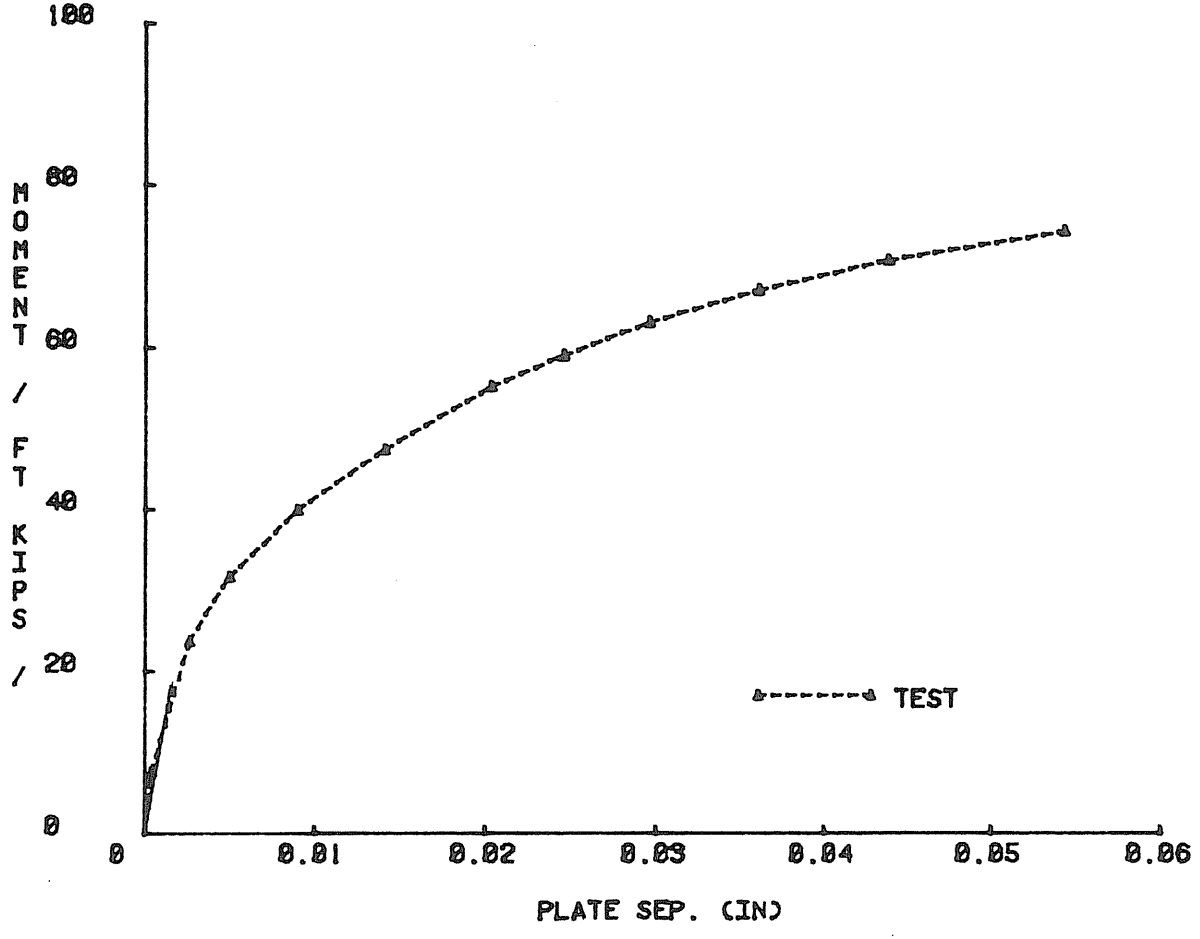

Figure D.3 **MOMENT VS PLATE SEPARATION, FO2-3/4-3/8-16**

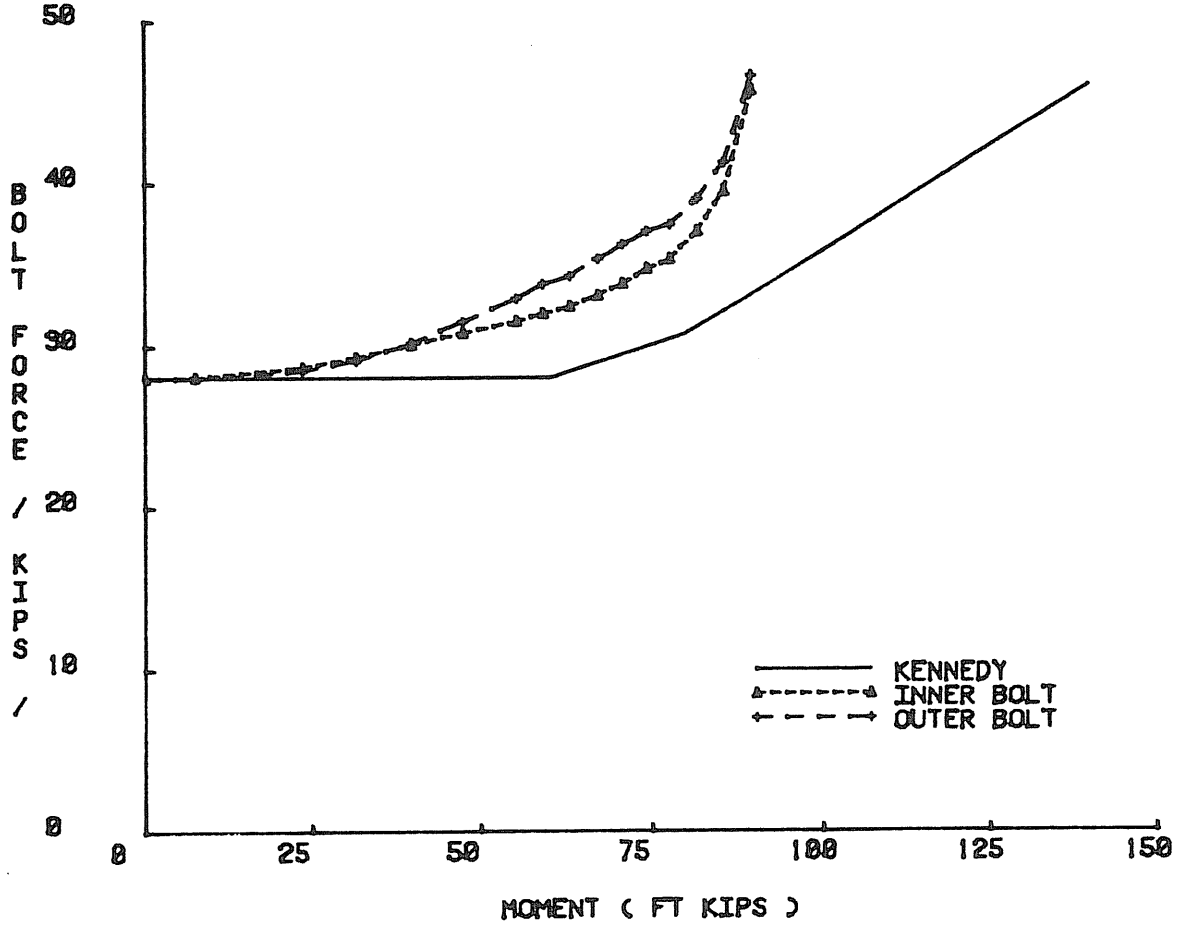

Figure D.4 BOLT FORCE VS MOMENT, F02-3/4-3/8-16

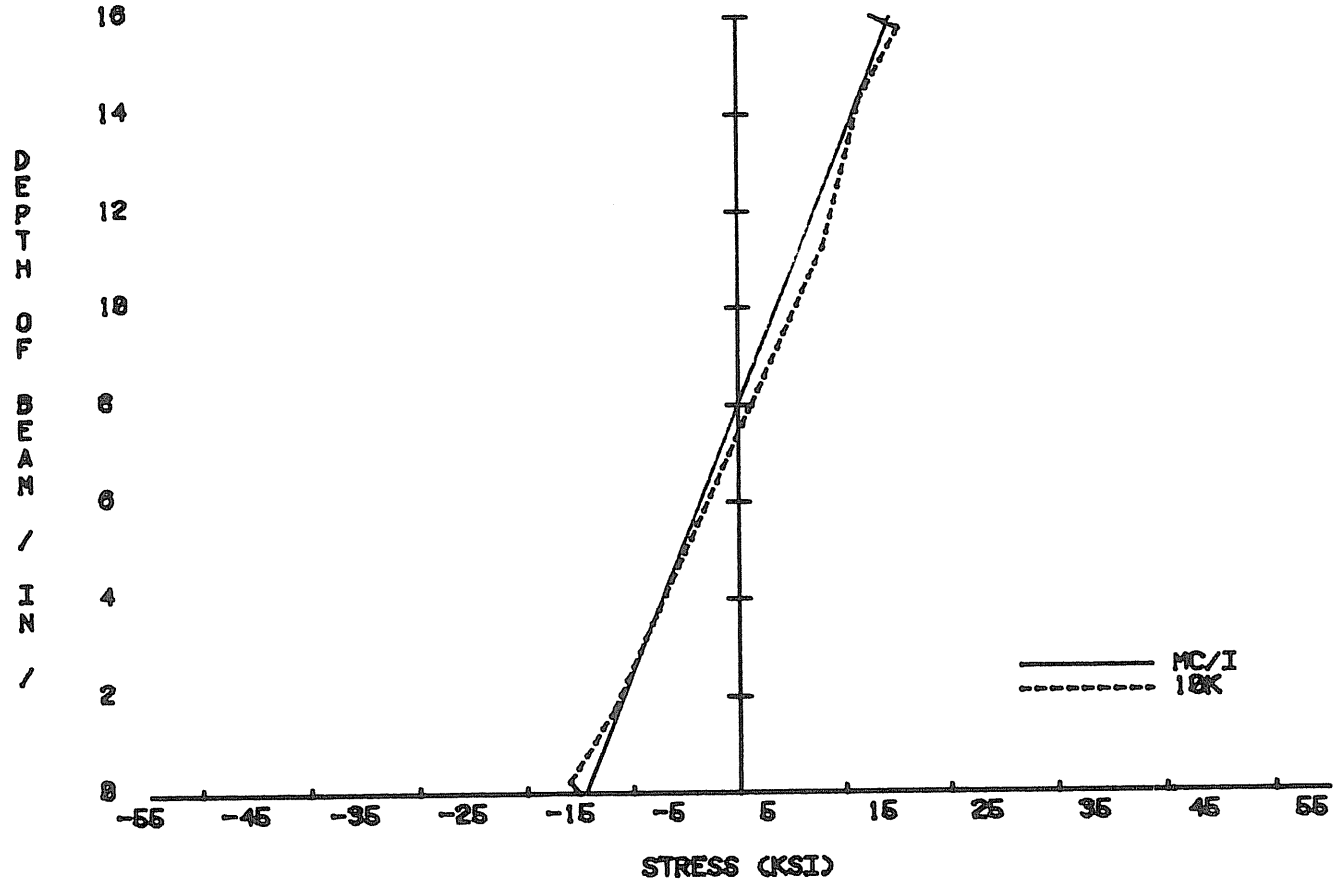

Figure D.5 LOAD VS STRESS, F02-3/4-3/8-18

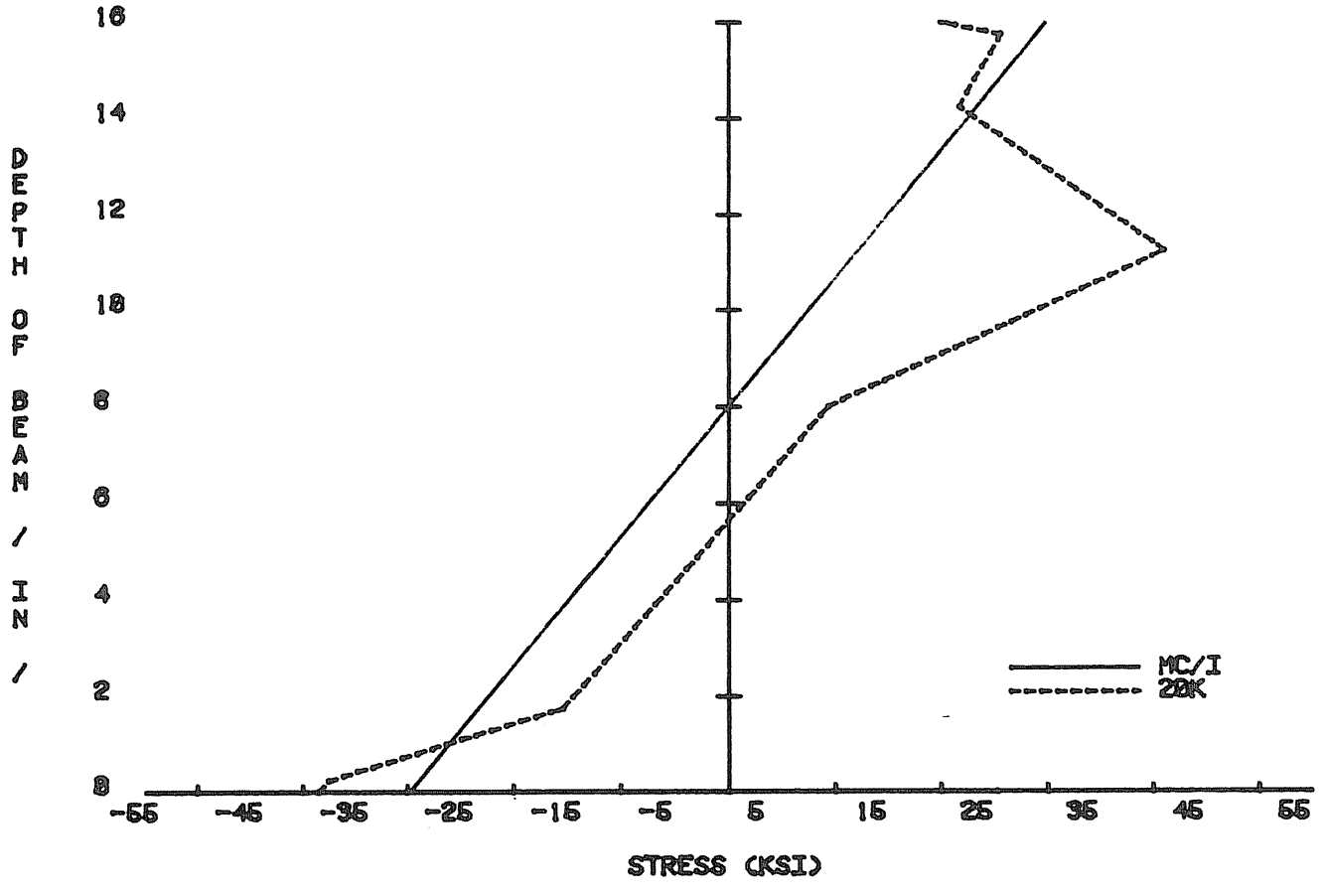

Figure D.6 LOAD VS STRESS, F02-3/4-3/8-16

APPENDIX E

FB2-3/4-3/8-24 TEST RESULTS

MBMA TEST SUMMARY

Project: MBMA/Conn.

Test No.: FB2-3/4-3/8-24

Test Date: 3-26-84

Purpose: Load to failure

Rows of Bolts in Tension: 2 **Bolts/Row:** 2

Bolt Diameter: 3/4" **Plate Thickness:** 3/8"

Beam Depth: 16" **Flange Width:** 6"

Web Thickness: 1/4" **Flange Thickness:** 1/4"

Moment of Inertia: 693.4 $in.^4$

Pretension Force: 28.0 kips

Failure Load: 35.1 kips vertical load; 146.2 ft-kips moment at end plate

Failure Mode: Yielding of end plate

Predicted Failure Loads:

Method: Yield Line Theory **Load:** 37.1 kips or 154.6 ft-kips

Method: **Load:**

Maximum Displacements:

Vertical: 1.93 in.

Horizontal top flange: 0.216

Horizontal bottom flange: -0.032

Maximum plate separation: East: 0.0 Centerline: 0.0933 West: 0.0432

Discussion:

-Instrumented bolts were used in the test. Pretension force was obtained by using the data acquisition system to monitor the bolt tension as torque was applied.

-Failure load was approximately 5% less than predicted by yield line analysis.

-Failure load of end plate was 37.1 kips corresponding to a moment at the end plate of 154.6 ft-kips. The test was further continued until a load of 43.0 kips (179.2 ft-kips) was attained.

-The bolt force in the outer bolt was approximately 15% more than the bolt force in the inner bolt at failure load.

-Vertical displacement was close to predicted up to a vertical load of 7.2 kips at which point the curve began to lean over.

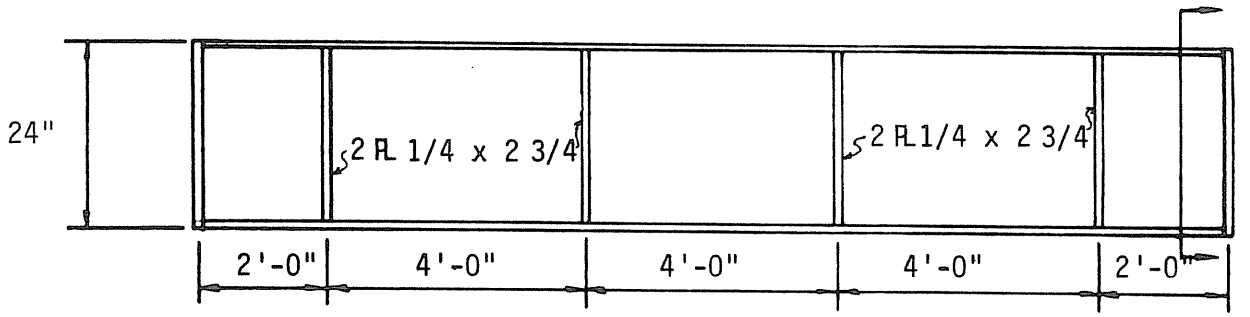

a) Elevation

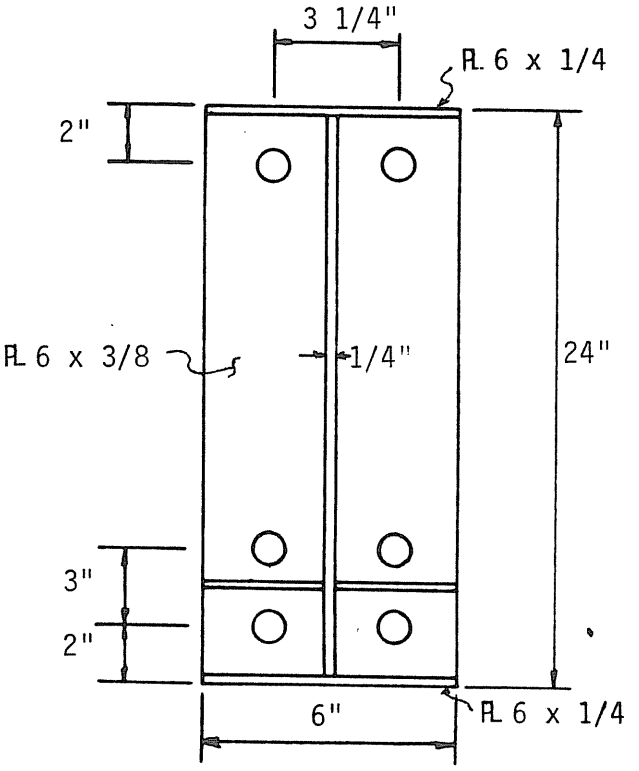

3/4 " Ø Bolts

13/16" Ø Bolt Holes

b) End-Plate

Figure E.1 Specimen Details, Test FB2-3/4-3/8-24

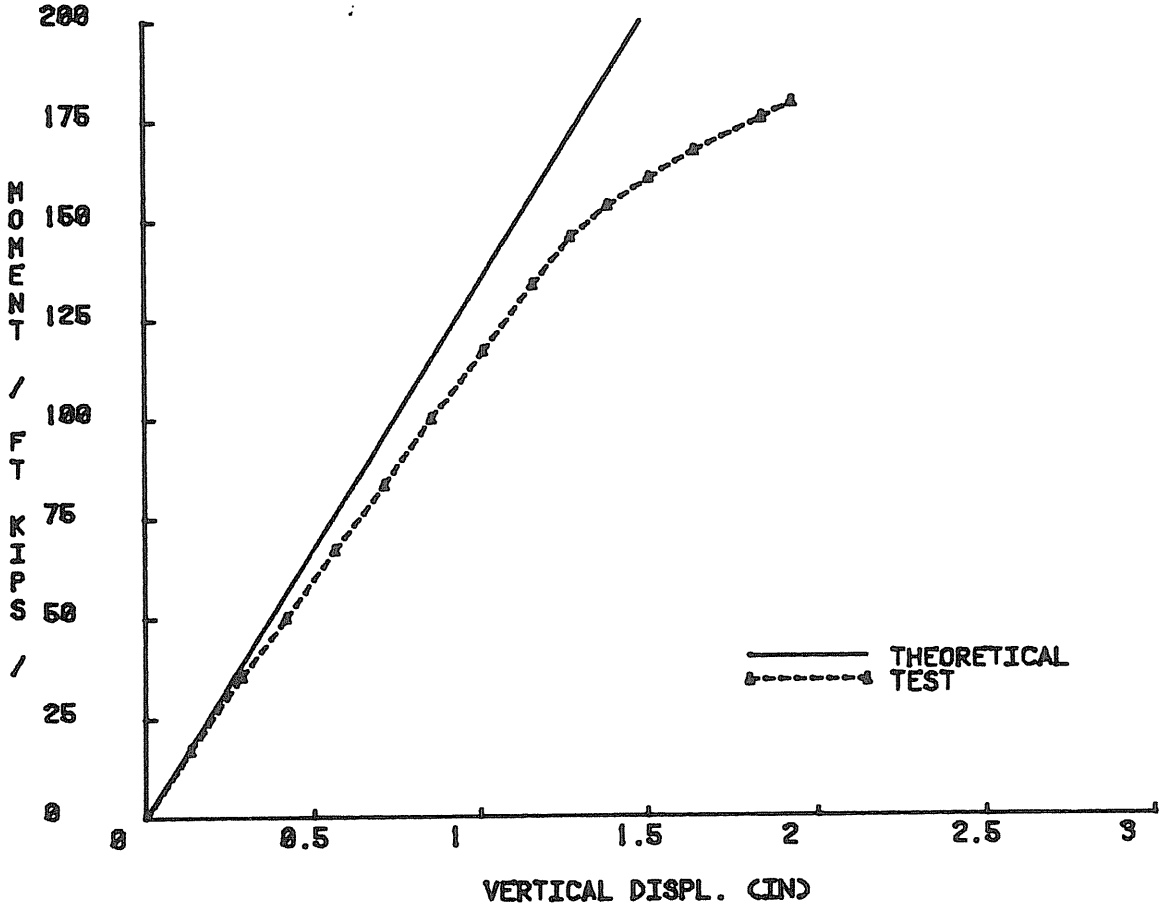

Figure E.2 MOMENT VS VERTICAL DISPL., FB2-3/4-3/8-24

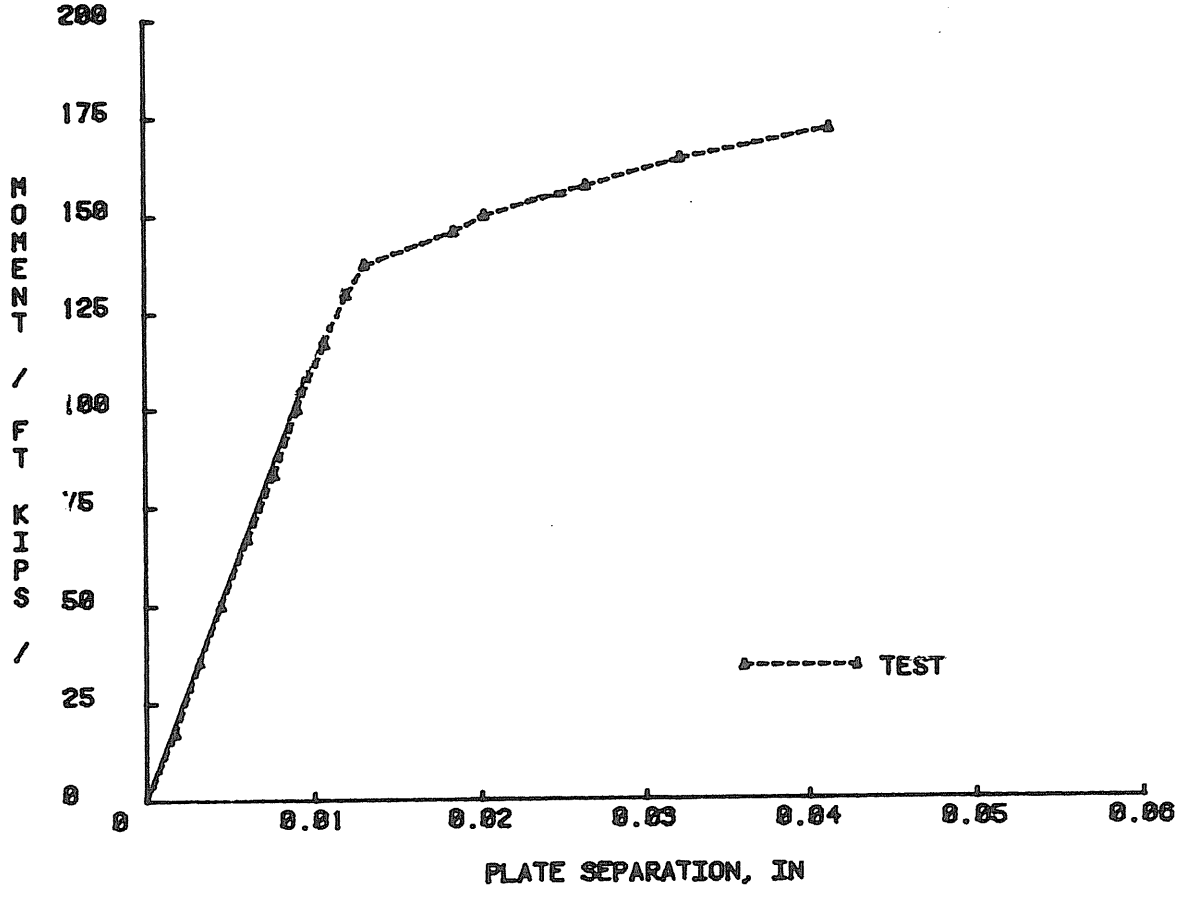

Figure E.3 **MOMENT VS PLATE SEPARATION**, FB2-3/4-3/8-24

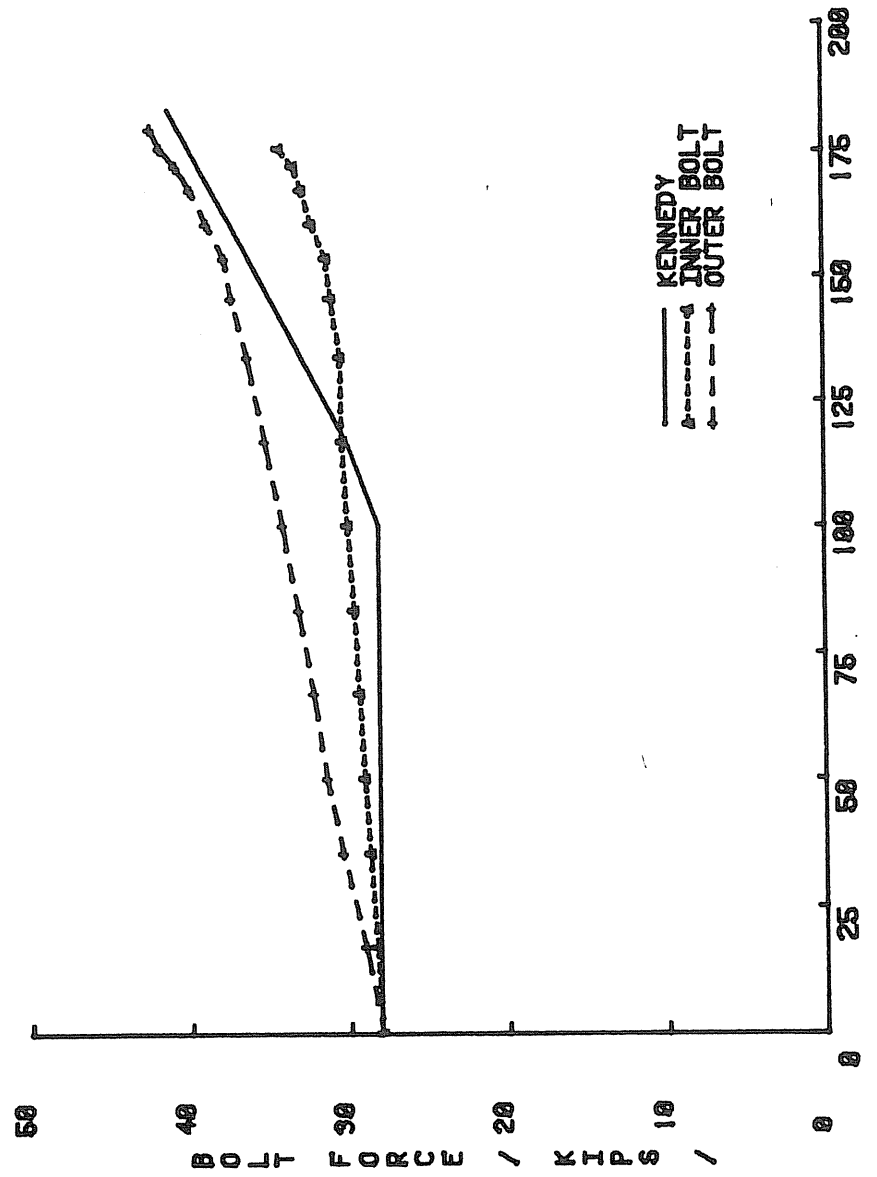

Figure E.4 BOLT FORCE VS MOMENT, FB2-3/4-3/8-24

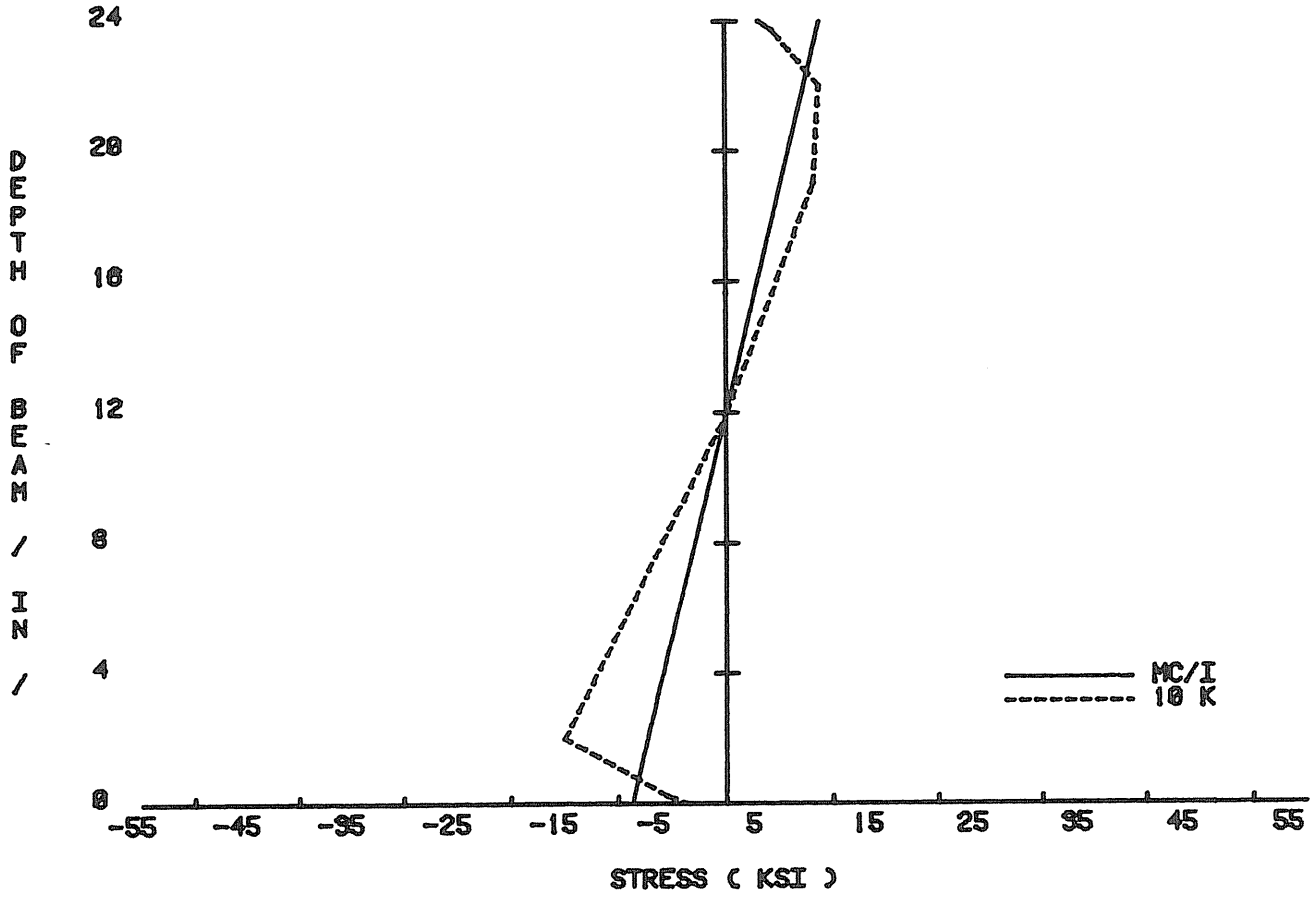

Figure E.5 **LOAD VS STRESS, FB2-3/4-3/8-24**

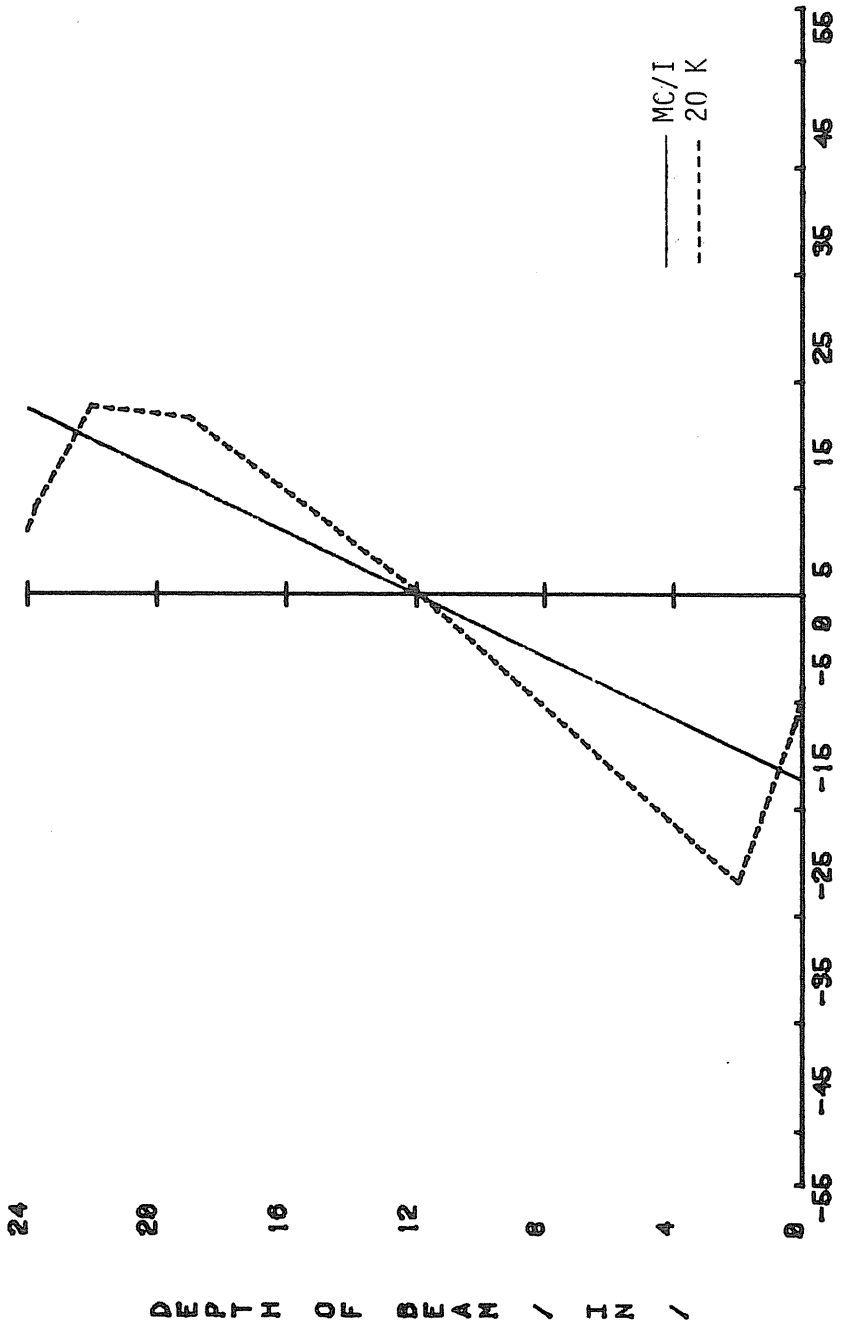

Figure E.6 LOAD VS STRESS, FB2-3/4-3/8-24

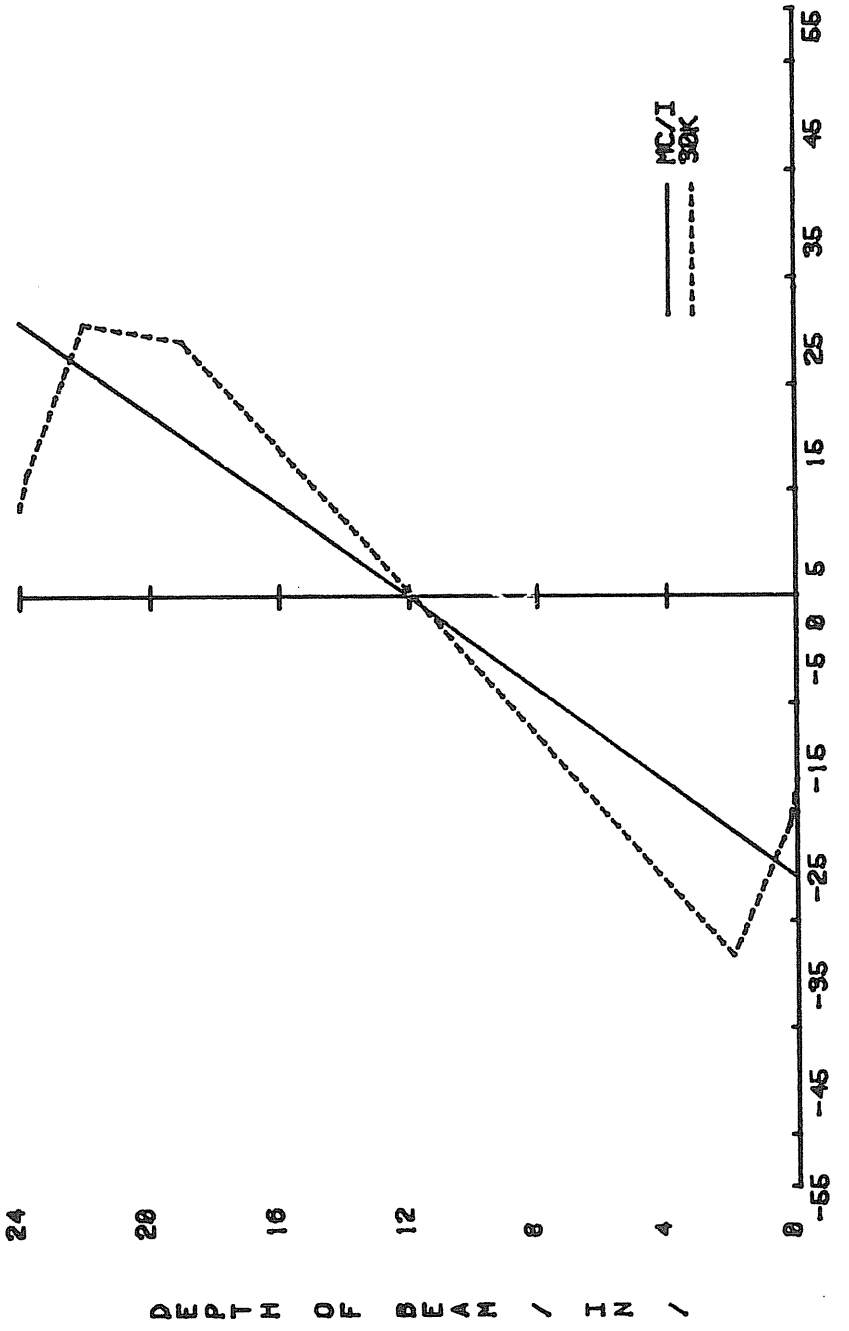

Figure E.7 LOAD VS STRESS, FB2-3/4-3/8-24

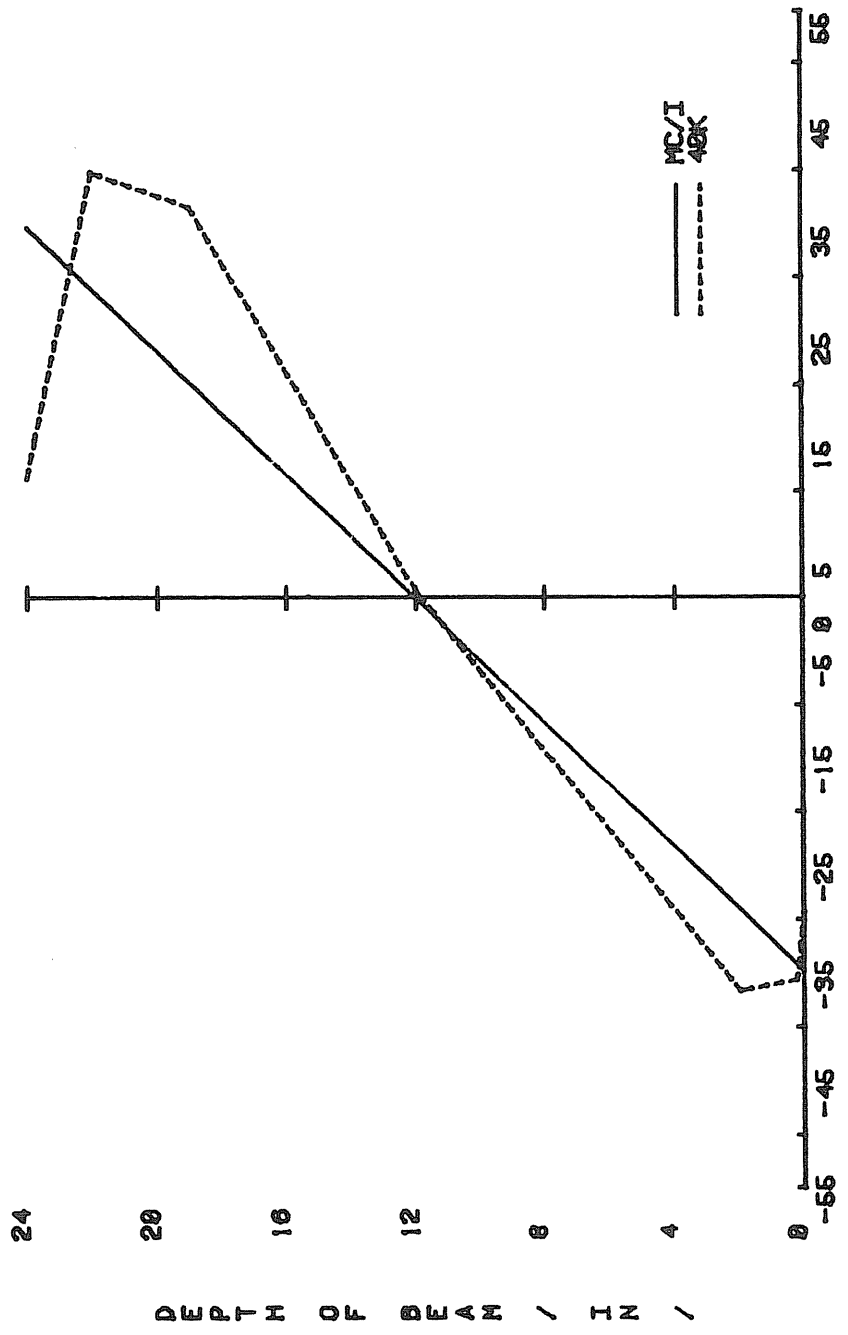

Figure E.8 LOAD VS STRESS, FB2-3/4-3/8-24

APPENDIX F

F02-3/4-3/8-24 TEST RESULTS

MBMA TEST SUMMARY

Project: MBMA/Conn.

Test No.: F02-3/4-3/8-24

Test Date: 3/15/84

Purpose: Load to failure - Full pretension

Rows of Bolts in Tension: 2 **Bolts/Row:** 2

Bolt Diameter: .75" **Plate Thickness:** .375"

Beam Depth: 24" **Flange Width:** 6"

Web Thickness: .25" **Flange Thickness:** .25"

Moment of Inertia: 693.4 $in.^4$

Pretension Force: 28 kips

Failure Load: 29 kip vertical load; 120.2 ft-kips at end plate

Failure Mode: Yielding of end plate

Predicted Failure Loads:

Method: Yield-line Theory **Load:** 30.2 kips (125.1 ft-kips)

Method: **Load:**

Maximum Displacements:

Vertical: 1.842 in.

Horizontal top flange: .138 in.

Horizontal bottom flange: .223 in.

Maximum plate separation: East: .0433 Centerline: .0265 West: 0.0

Discussion:

-Instrumented bolts were used in the test. Pretension force was obtained by using the data acquisition system to monitor the bolt tension as torque was applied.

-Failure load was approximately 4% less than predicted by yield line analysis.

-Failure load of end plate was 29 kips corresponding to a moment at the end plate of 125 ft-kips. The test was continued until a load of 34.6 kips (143 ft-kips) was attained.

-The bolt force in the interior bolt was 35 kips at failure load (29 kips) and 47 kips at a load at 34.6 kips. The strain gage in the outer bolt did not operate properly.

-Vertical displacement was close to theoretical up to 35 ft-kips at which time the curve began to lean over.

-Plate separation followed theoretical up to 40 ft-kips

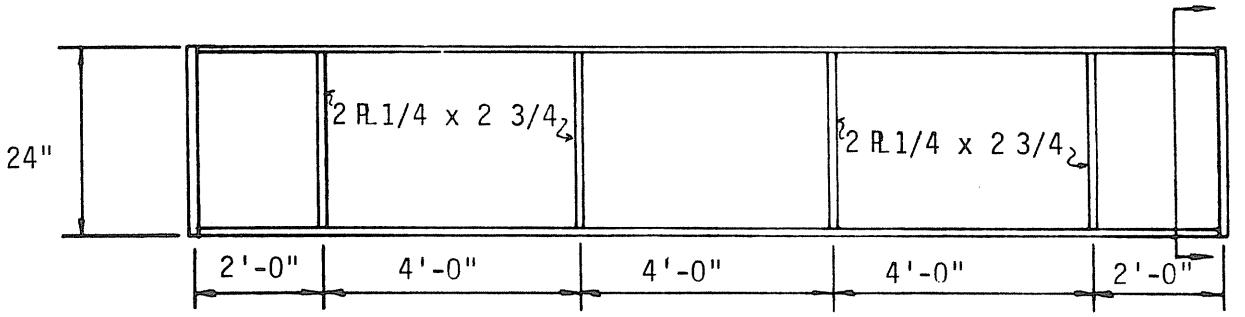

a) Elevation

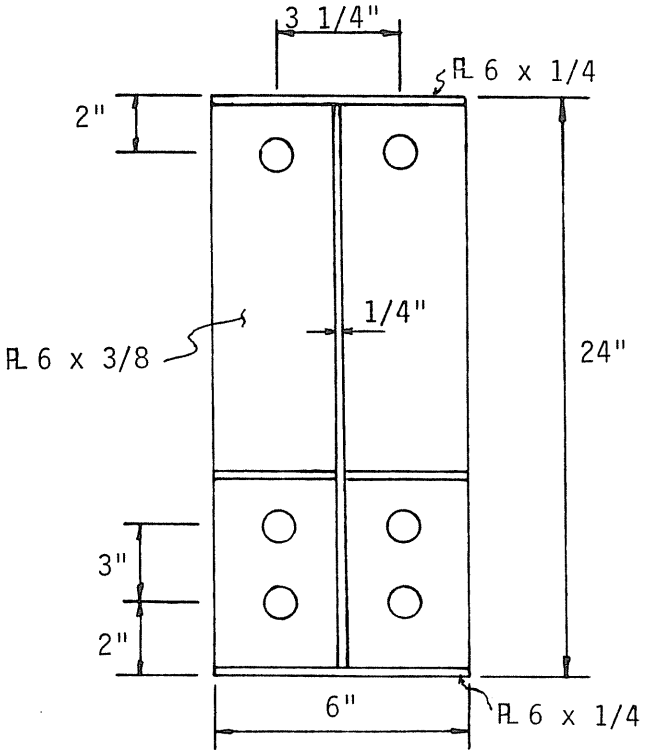

3/4" Ø Bolts

13/16" Ø Bolt Holes

b) End Plate

Figure F.1 Specimen Details, Test F02-3/4-3/8-24

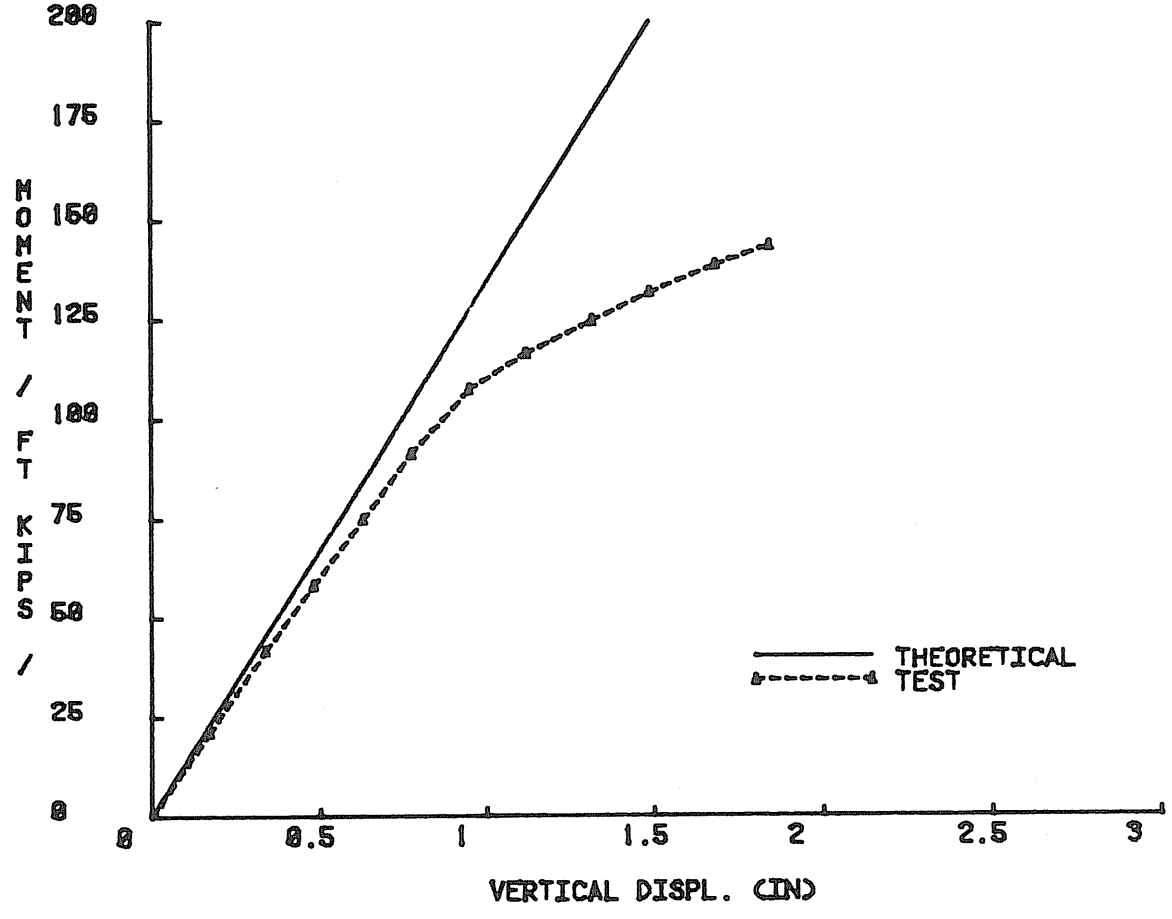

Figure F.2 MOMENT VS VERTICAL DISPL., FD2-3/4-3/8-24

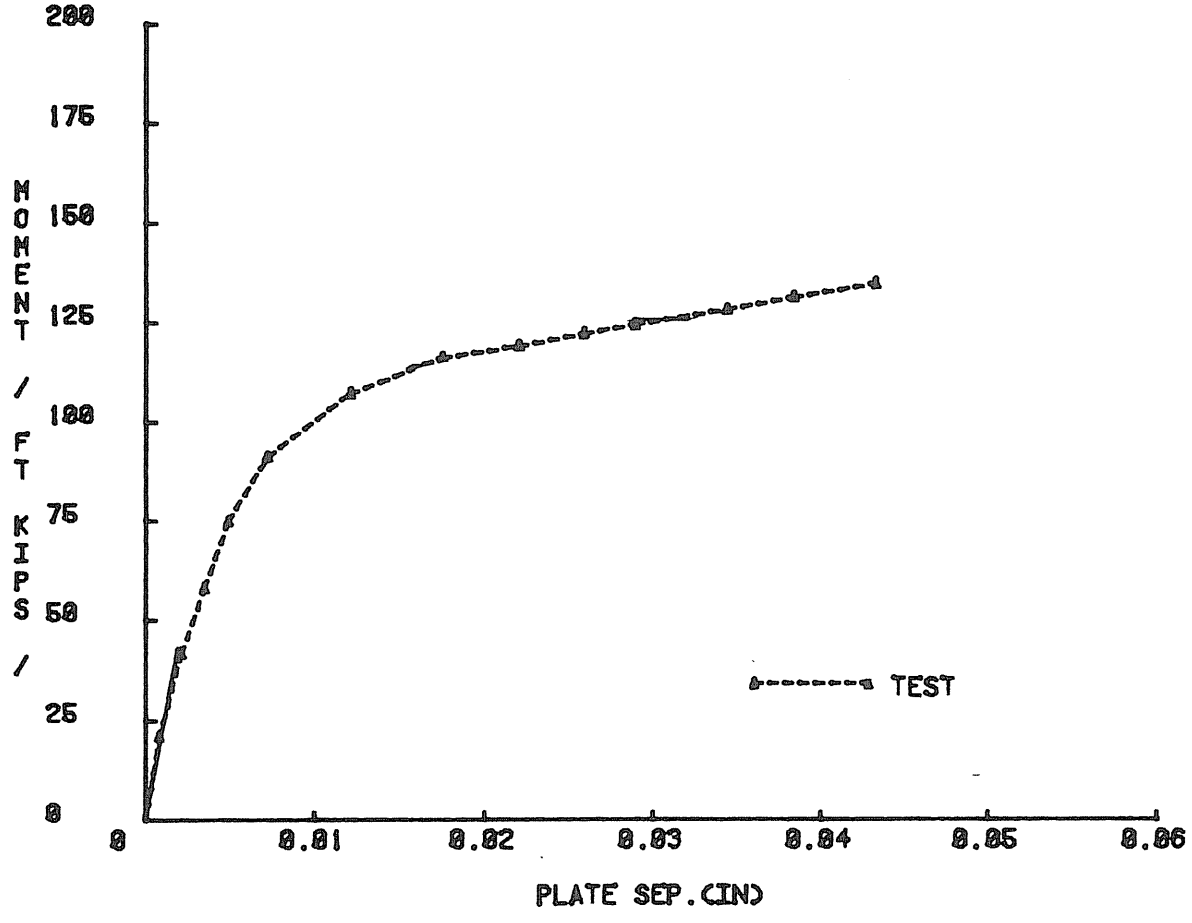

Figure F.3 MOMENT VS PLATE SEPARATION, F02-3/4-3/8-24

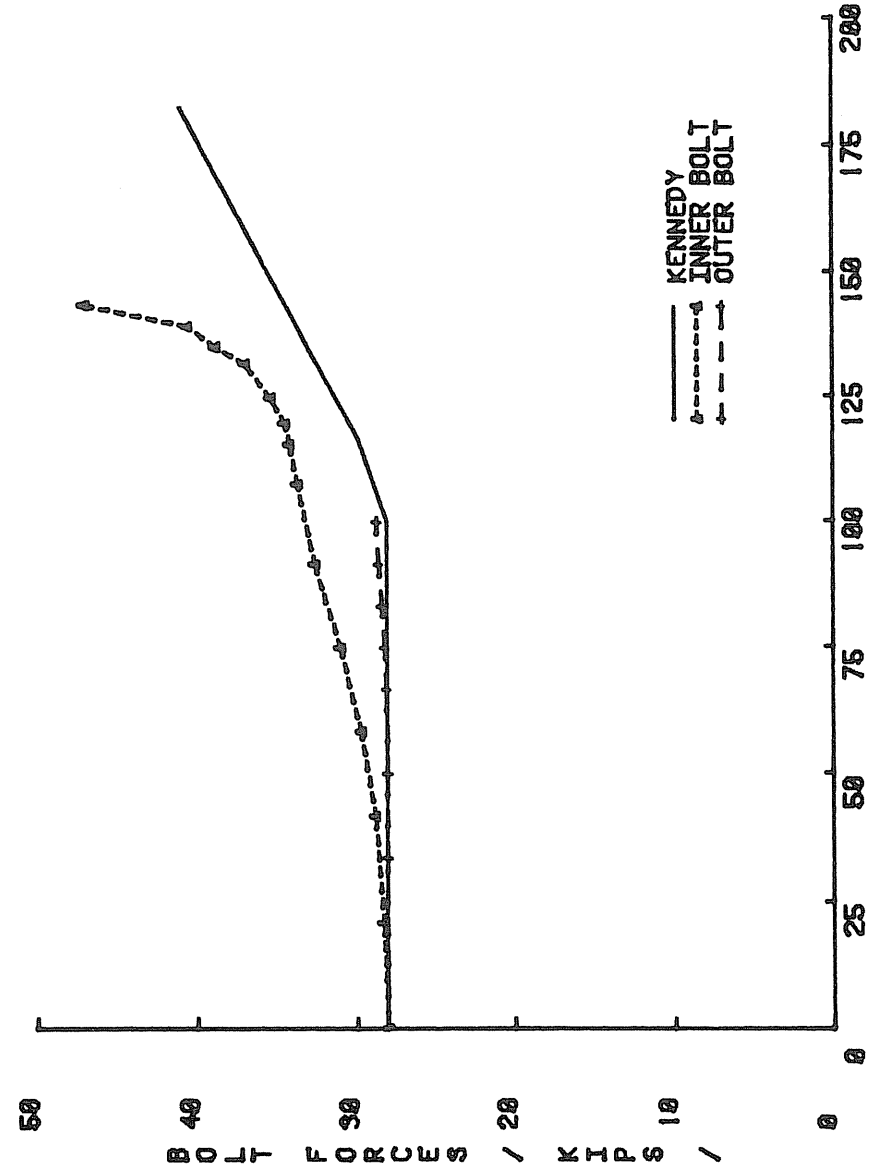

Figure F.4 BOLT FORCES VS MOMENT, F02-3/4-3/8-24

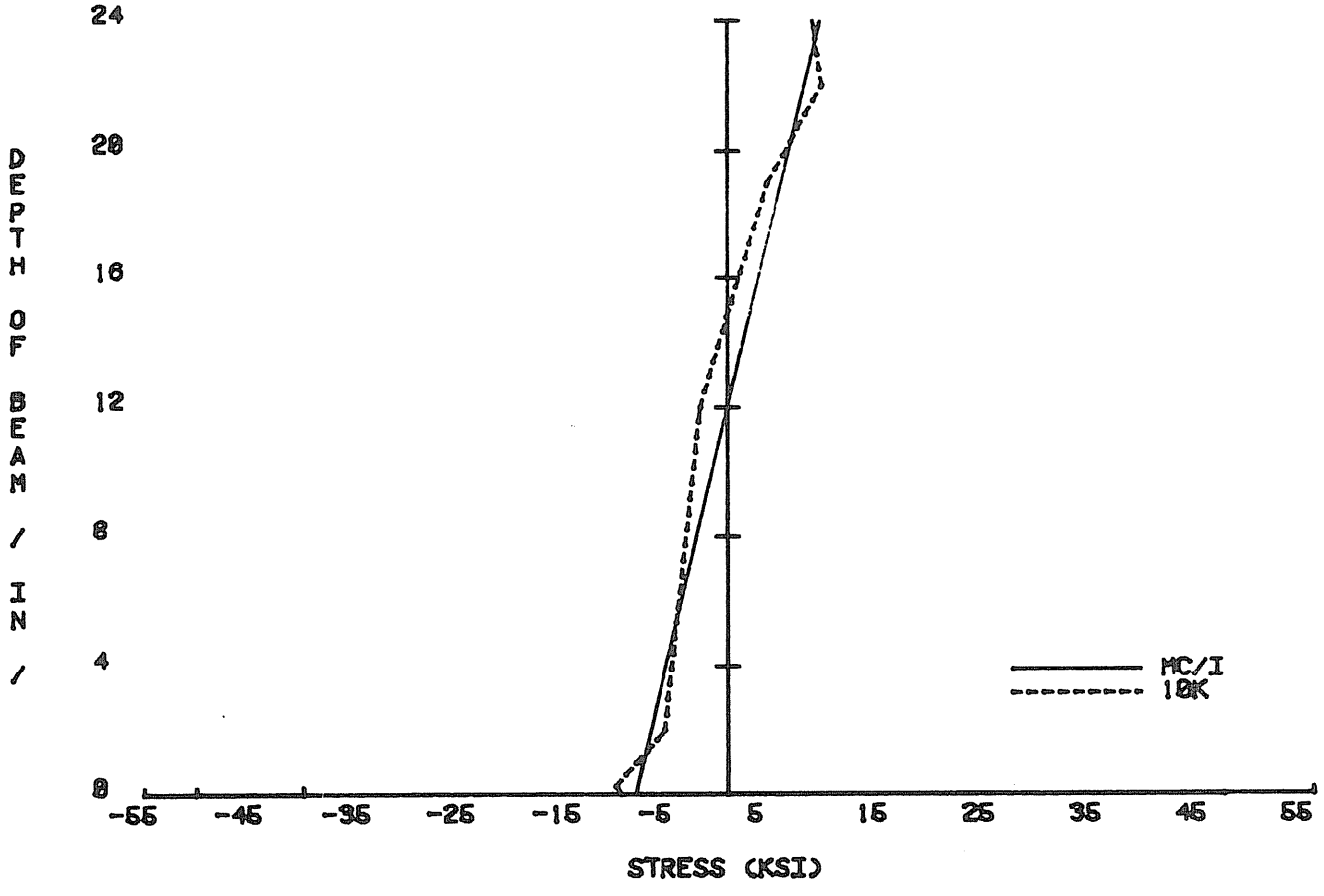

Figure F.5 LOAS VS STRESS, F02-3/4-3/8-24

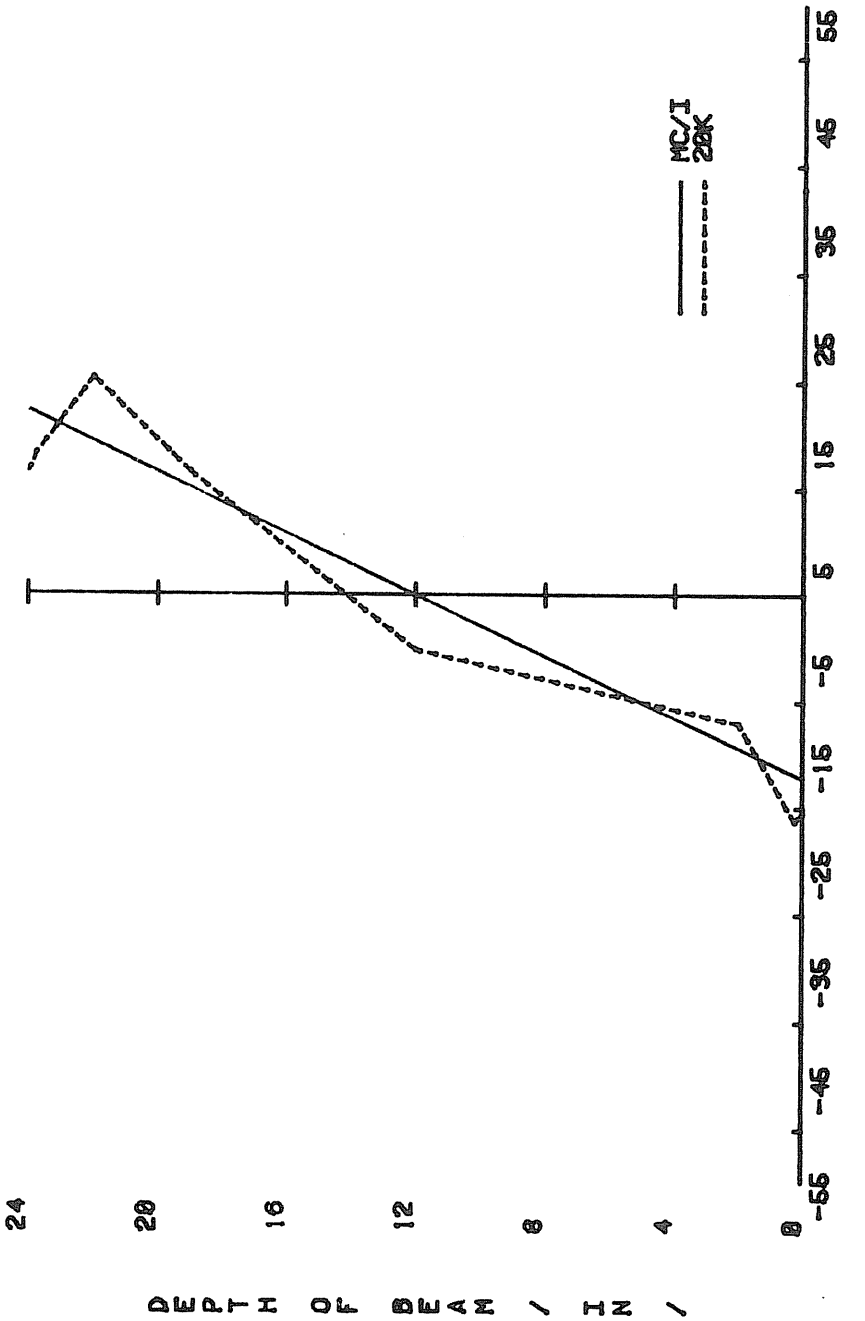

Figure F.6 LOAD VS STRESS, F02-3/4-3/8-24

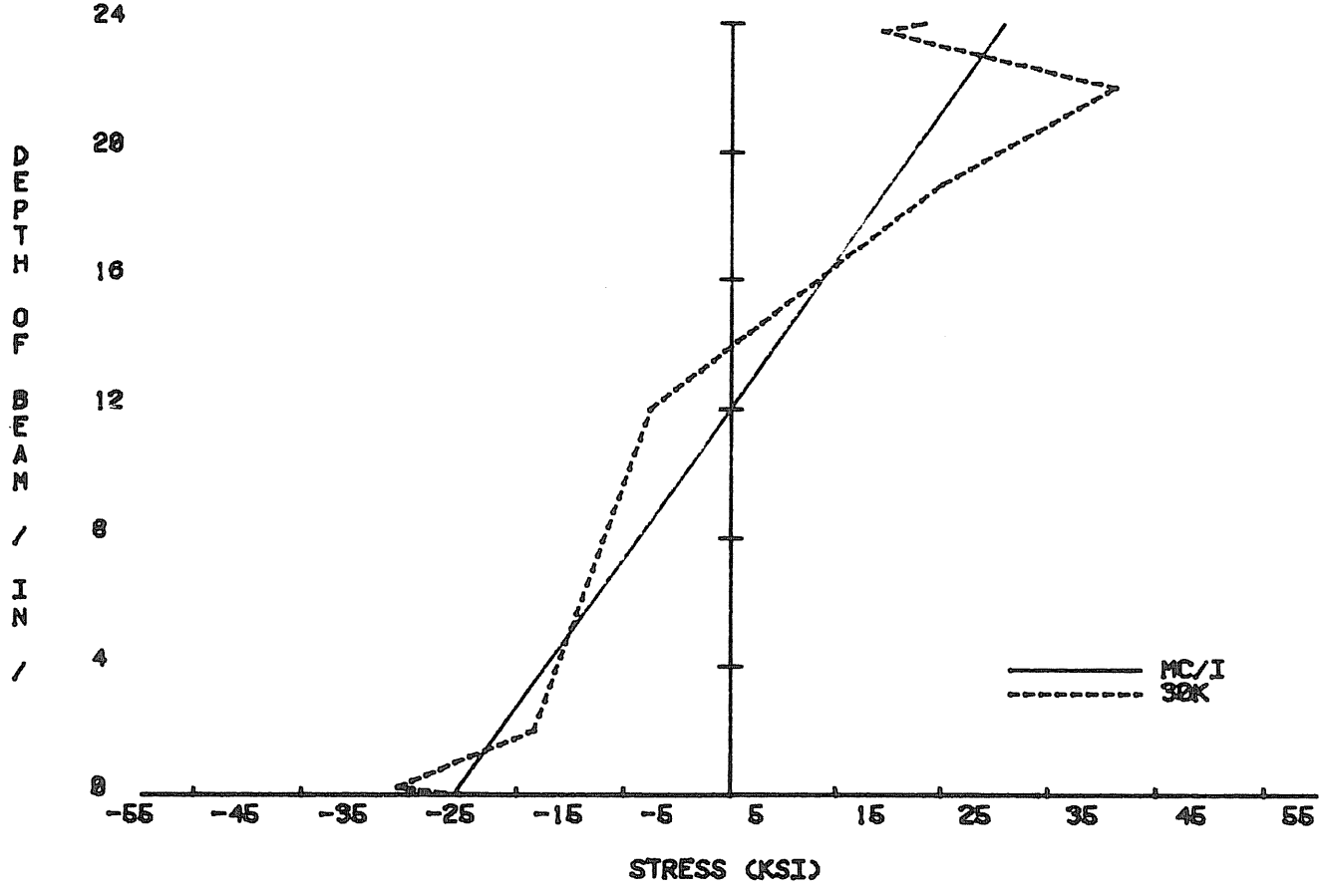

Figure F.7 LOAD VS STRESS, F02-3/4-3/8-24

APPENDIX G

FB2-5/8-3/8-16 TEST RESULTS

MBMA TEST SUMMARY

Project: MBMA Conn.

Test No.: FB2-5/8-3/8-16

Test Date: 5/30/84

Purpose: Load to Failure - Full Pretension

Rows of Bolts in Tension: 2 **Bolts/Row:** 2

Bolt Diameter: 5/8 in. **Plate Thickness:** 3/8 in. (.383 in.)

Beam Depth: 16 in. **Flange Width:** 6 in.

Web Thickness: .25 in. **Flange Thickness:** .25 in.

Moment of Inertia: 263 $in.^4$

Pretension Force: 19 kips

Failure Load: 27.1 kips vertical load; 108.4 ft.-kips at end plate

Failure Mode: Yield of end plate

Predicted Failure Loads:

Method: Yield line theory **Load:** 28.9 kips or 115.8 ft.-kips

Method: **Load:**

Maximum Displacements:

Vertical: 2.80 in.

Horizontal top flange: .124 in.

Horizontal bottom flange: .112 in.

Maximum plate separation: East: .033 in. Centerline: .048 in. West: —

Discussion:

-Instrumented bolts were used in the test. Pretension force was obtained by using the data acquisition system to monitor the bolt tension as torque was applied.

-Failure of end plate occurred at 27.1 kips (108.4 ft.-kips) which was 6% less than predicted by yield line analysis.

-Vertical deflection followed theoretical up to 50 ft.-kips at which point it began to lean over.

-Plate separation followed theoretical up to 70 ft.-kips.

-Bolt forces reached proof load (27 kips) in the outer bolt at 83 ft.-kips, while the inner bolt reached proof load at 100 ft.-kips.

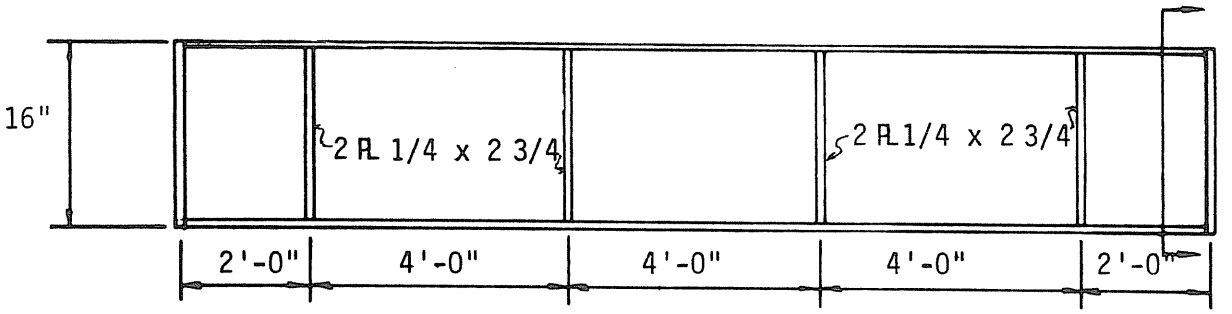

a) Elevation

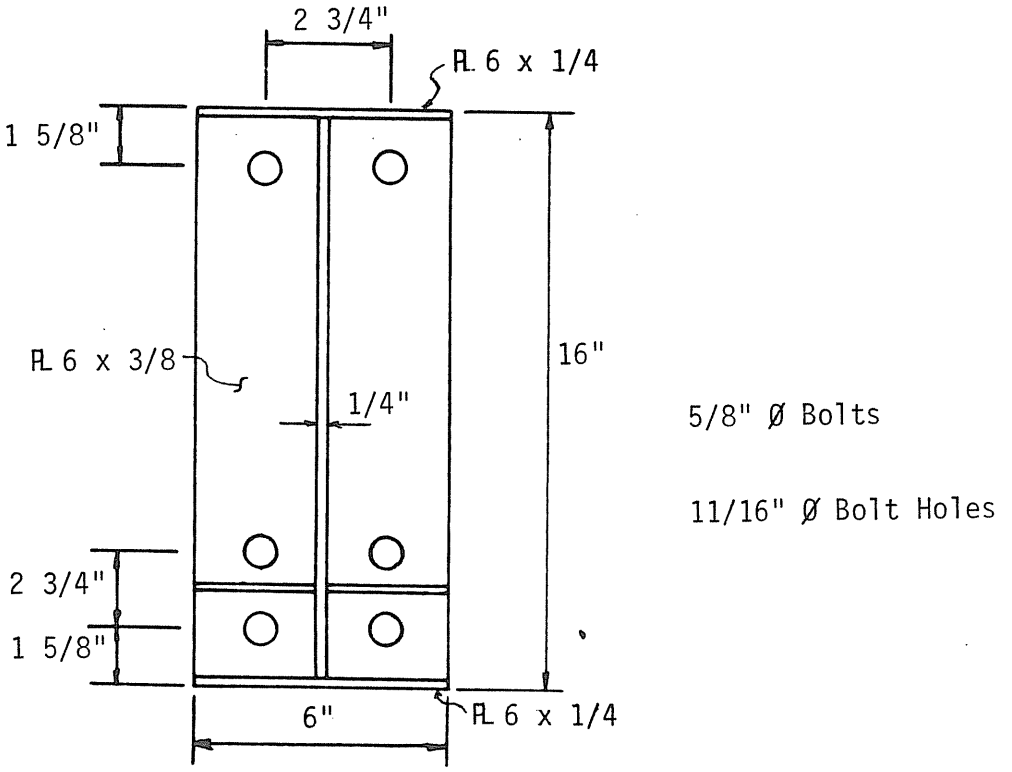

b) End-Plate

Figure G.1 Specimen Details, Test FB2-5/8-3/8-16

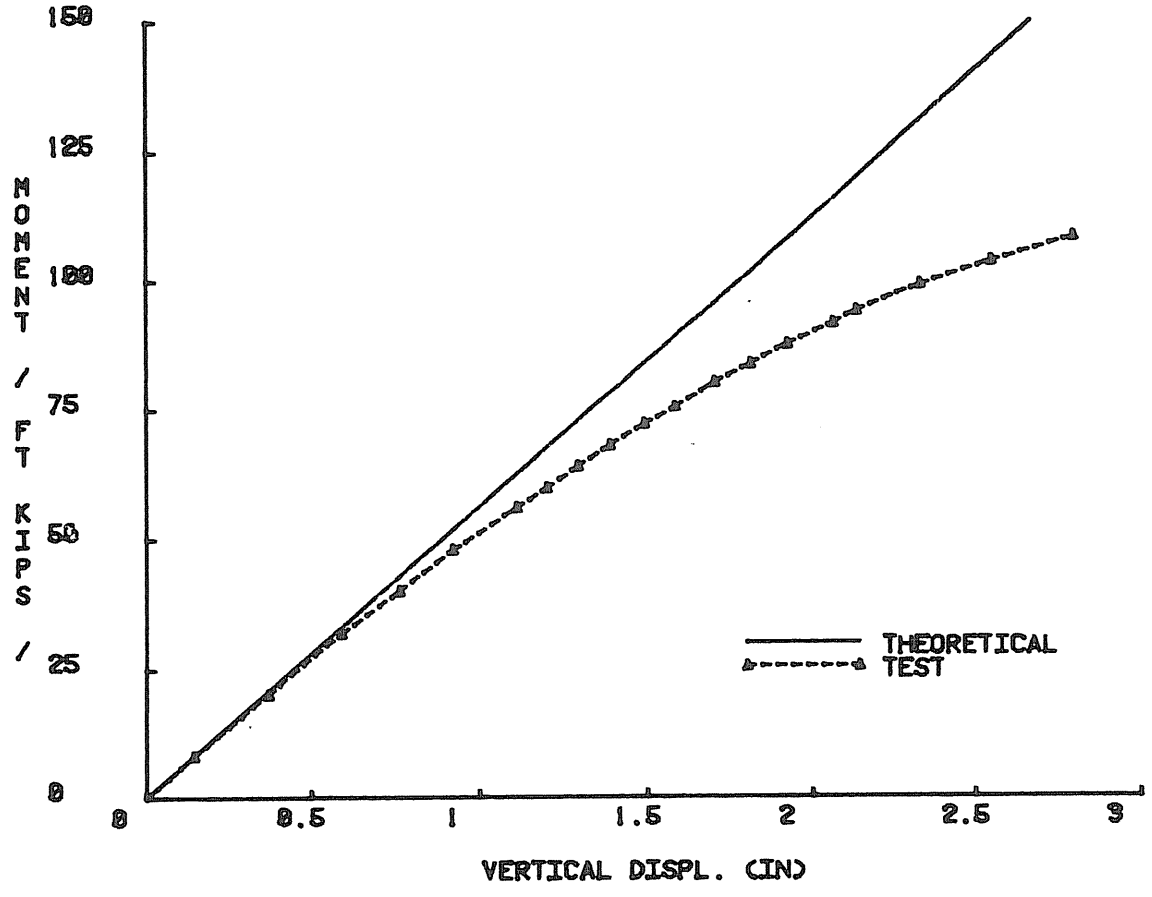

Figure G.2 **MOMENT VS VERTICAL DISPLACEMENT, FB2-5/8-3/8-16**

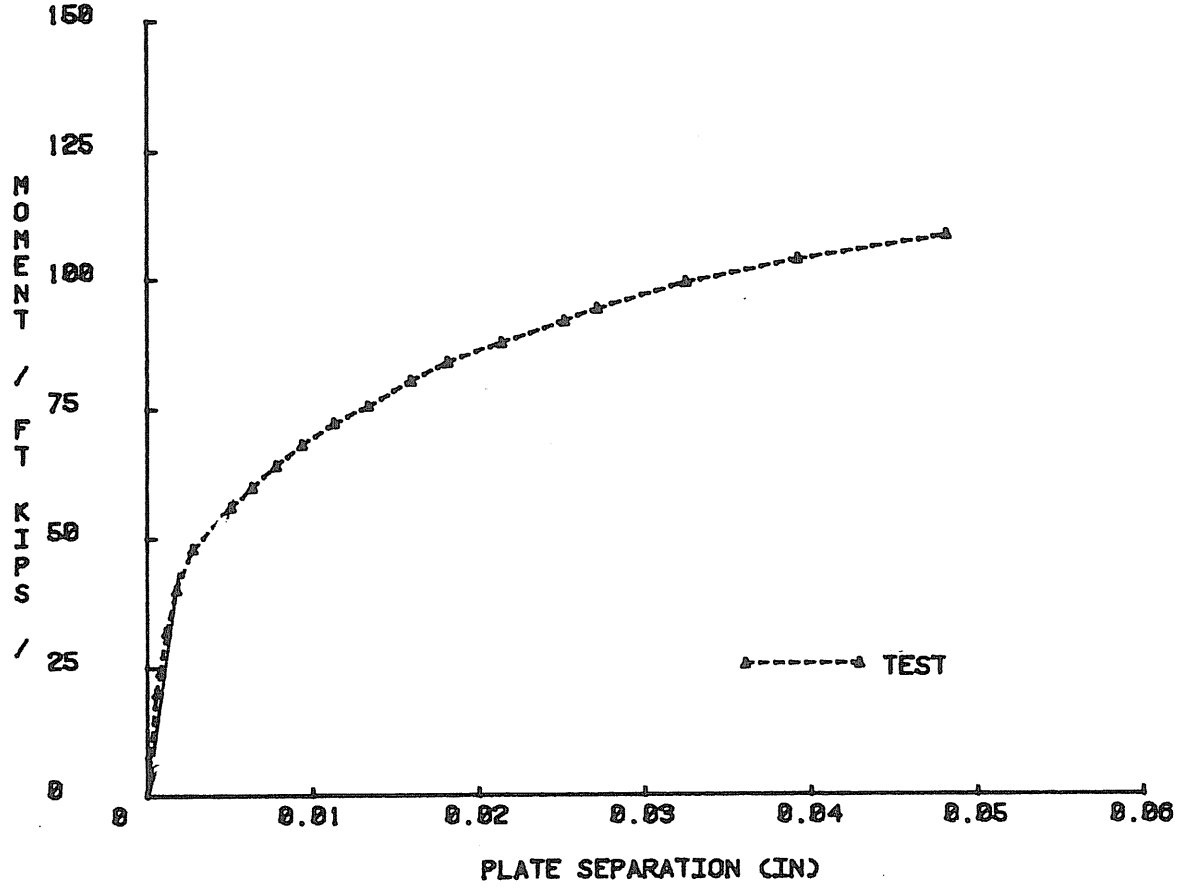

Figure G.3 MOMENT VS PLATE SEPARATION, FB2-5/8-3/8-16

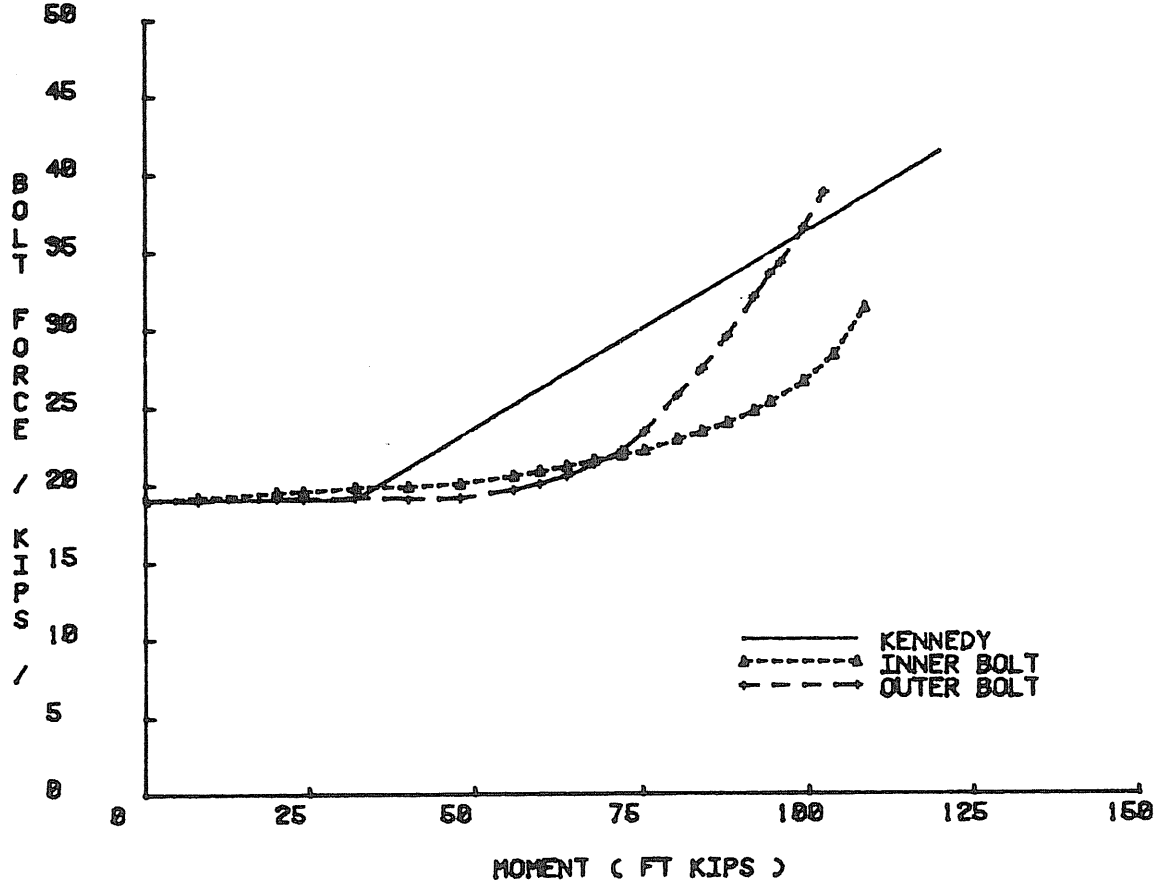

Figure G.4 BOLT FORCE VS MOMENT, FB2-5/8-3/8-16

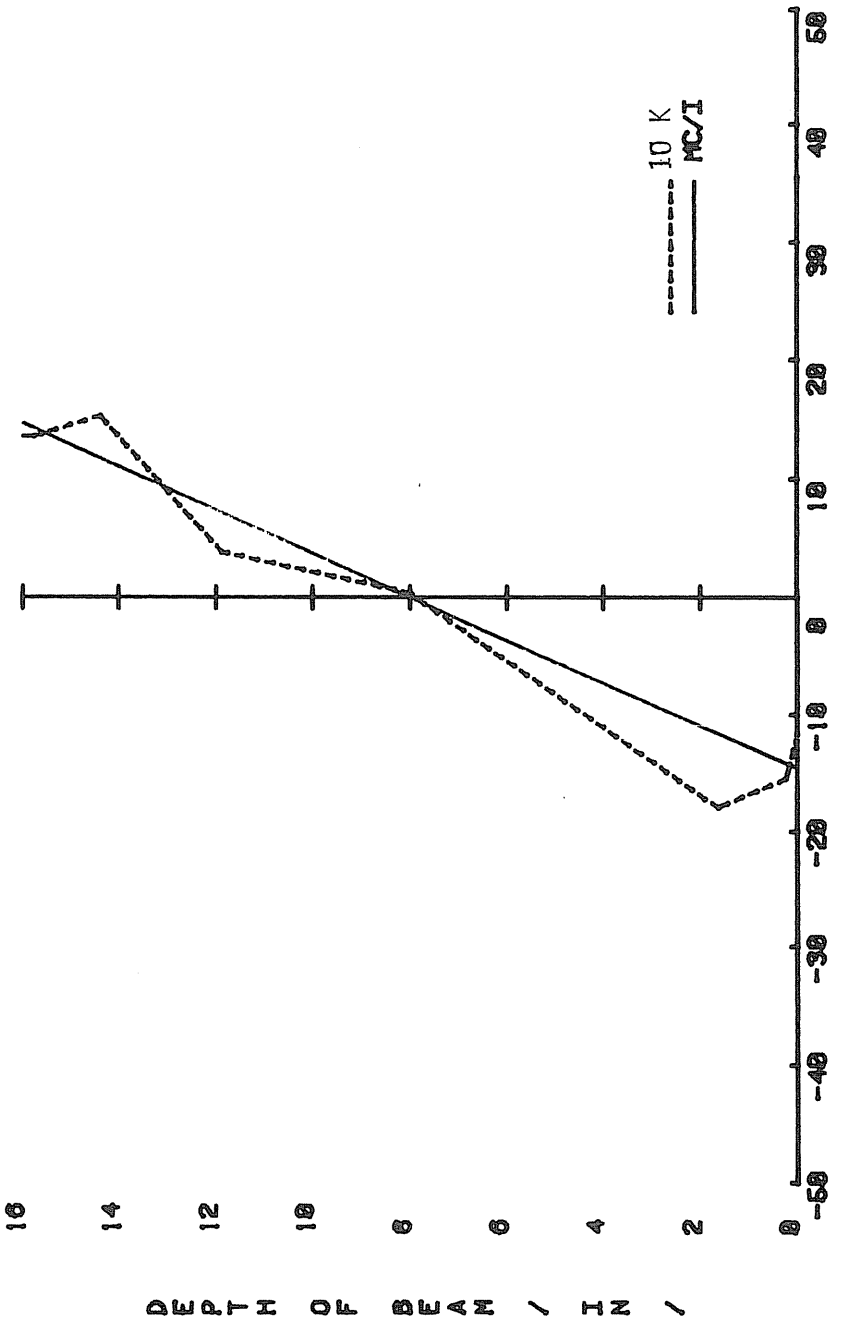

Figure G.5 **LOAD VS STRESS, FB2-5/8-3/8-16**

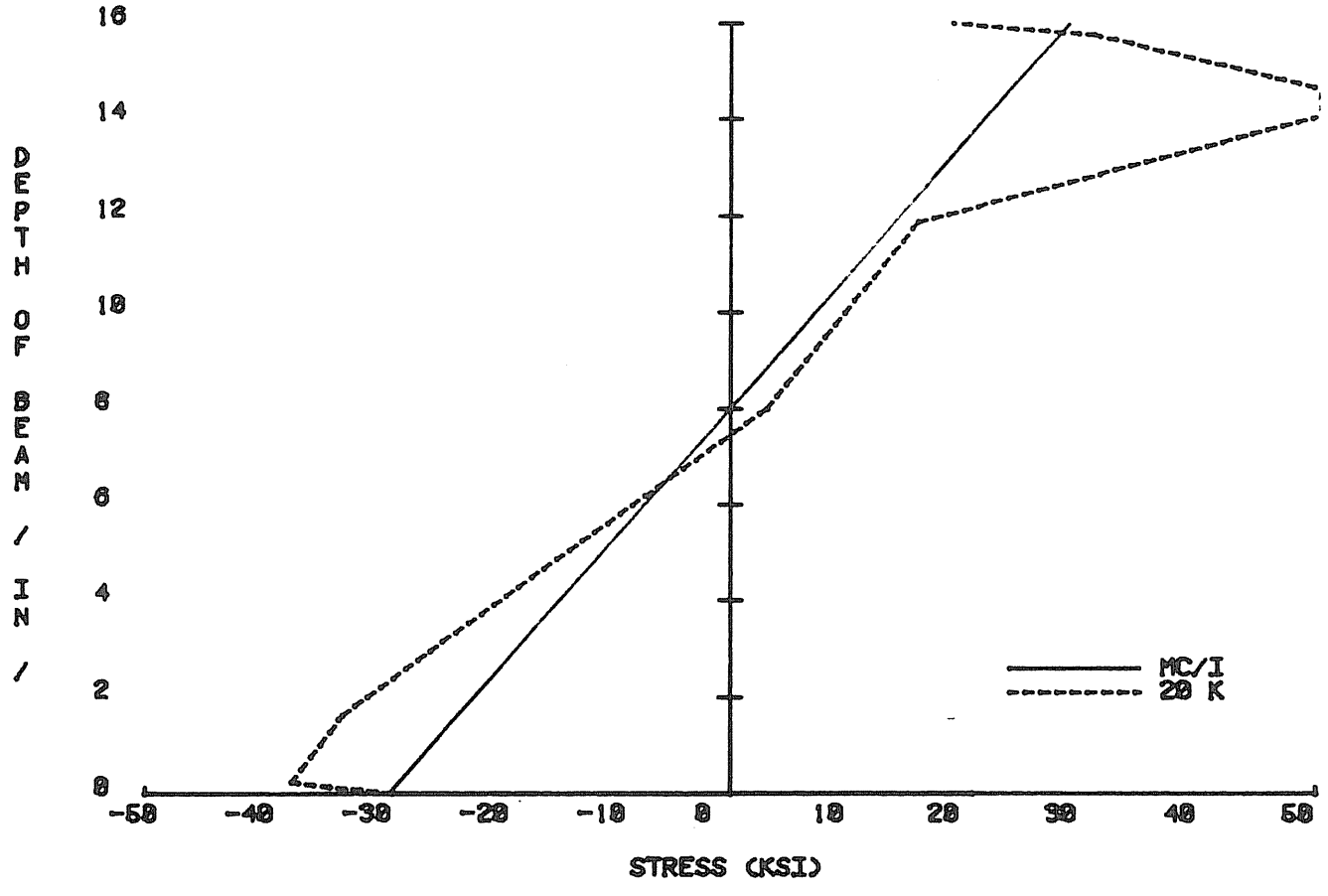

Figure G.6 LOAD VS STRESS, FB2-5/8-3/8-16

APPENDIX H

F02-5/8-3/8-16 TEST RESULTS

MBMA TEST SUMMARY

Project: MBMA Conn.

Test No.: F02-5/8-3/8-16

Test Date: 5/24/84

Purpose: Load to Failure - Full Pretension

Rows of Bolts in Tension: 2 Bolts/Row: 2

Bolt Diameter: 5/8 in. Plate Thickness: 3/8 in. (.383 in.)

Beam Depth: 16 in. Flange Width: 6 in.

Web Thickness: 1/4 in. Flange Thickness: 1/4 in.

Moment of Inertia: 263 $in.^4$

Pretension Force: 19 kips

Failure Load: 21.3 kips vertical load; 85.0 ft.-kips at end plate

Failure Mode: Yield of end plate

Predicted Failure Loads:

Method: Yield line analysis Load: 20.8 kips (83.1 ft.-kips)

Method: Load:

Maximum Displacements:

Vertical: 2.22 in.

Horizontal top flange: .033 in.

Horizontal bottom flange: .237 in.

Maximum plate separation: East: .0217 in. Centerline: .030 in. West: —

Discussion:

-Instrumented bolts were used in the test. Pretension force was obtained by using the data acquisition system to monitor the bolt tension as torque was applied.

-Failure of end plate occurred at 21.3 kips (85 ft.-kips) which was 2% more than predicted by yield line analysis.

-Vertical deflection followed theoretical up to 45 ft.-kips at which point it began to lean over.

-Plate separation followed theoretical up to 30 ft.-kips at which point it began to lean over.

-Bolt forces reached proof load (27 kips) in the outer bolt at 69 ft.-kips and in the inner bolt at 75 ft.-kips.

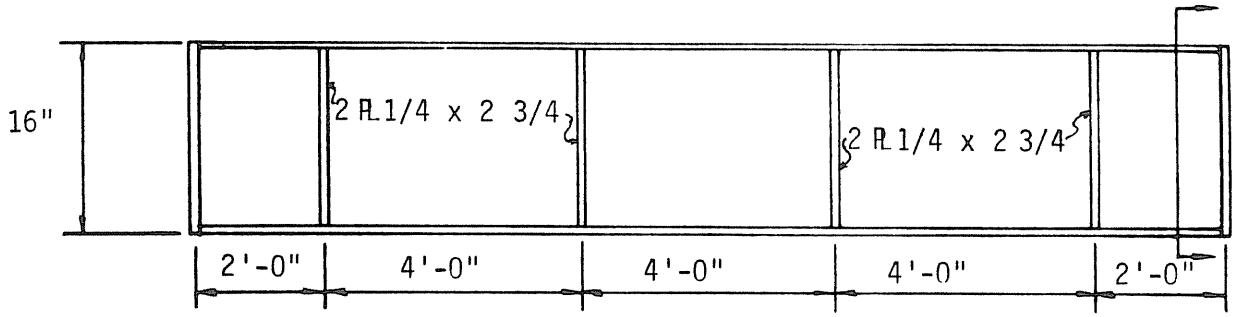

a) Elevation

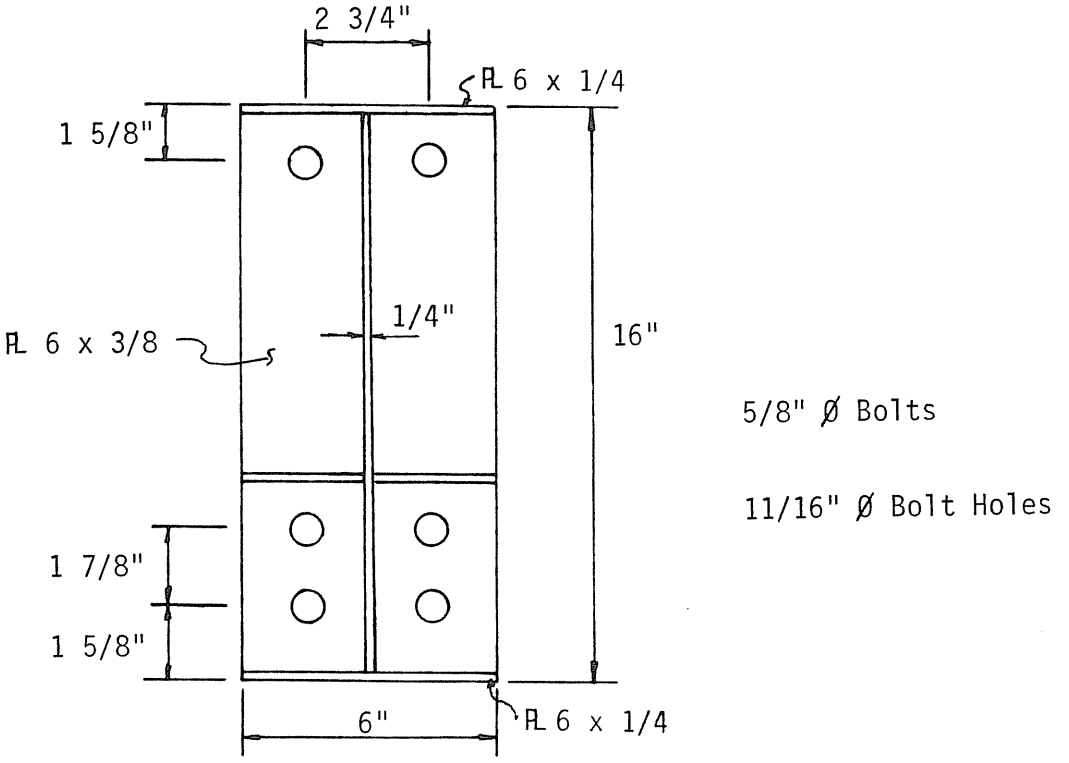

b) End Plate

Figure H.1 Specimen Details, Test F02-5/8-3/8-16

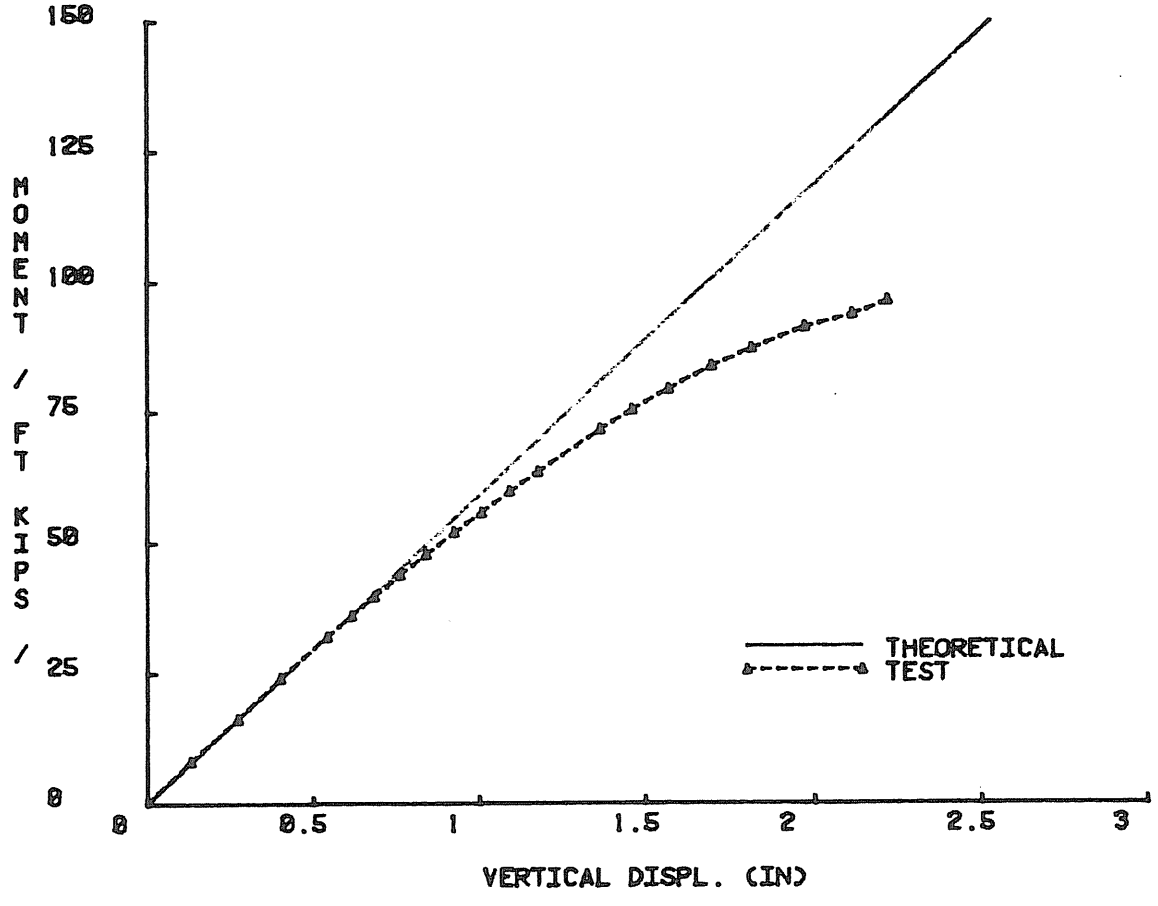

Figure H.2 **MOMENT VS VERTICAL DISPLACEMENT, F02-5/8-3/8-16**

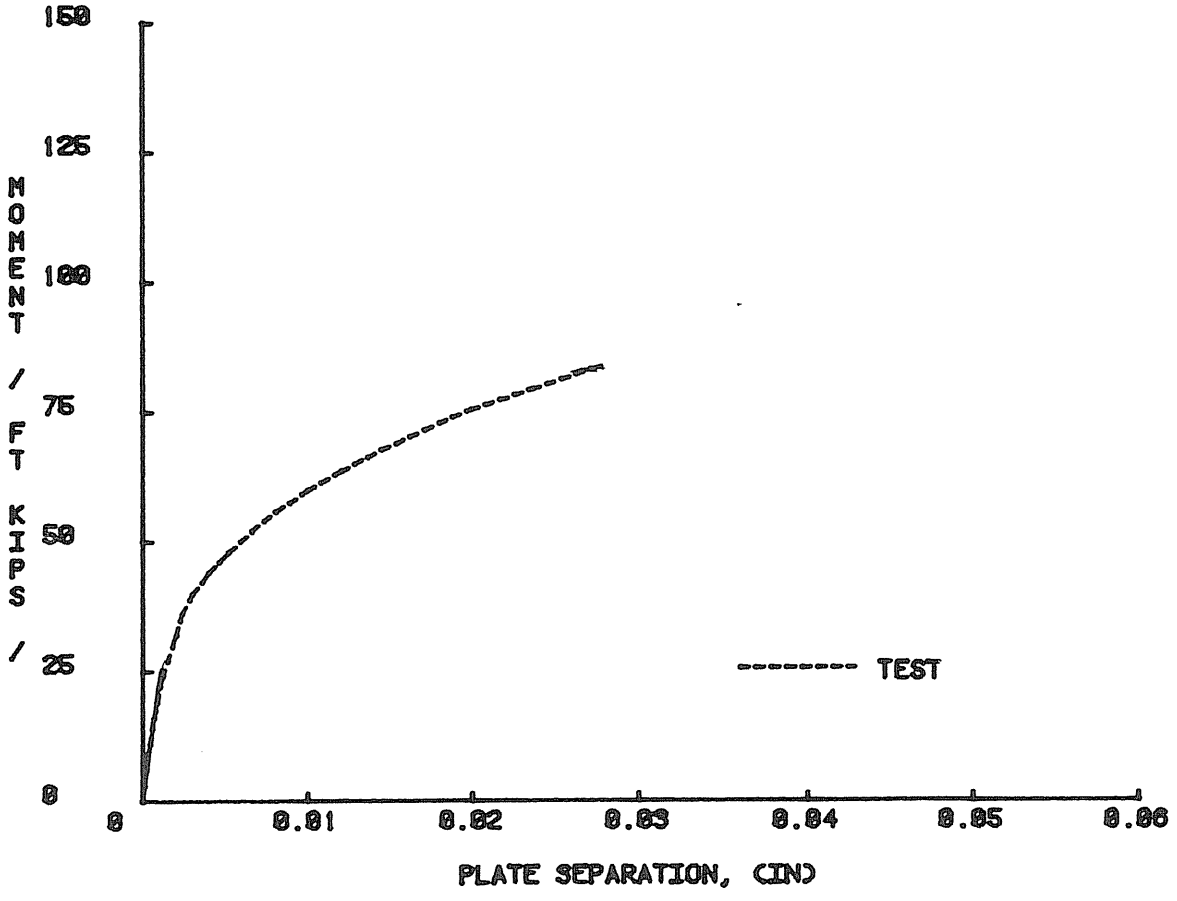

Figure H.3 MOMENT VS PLATE SEPARATION, F02-5/8-3/8-16

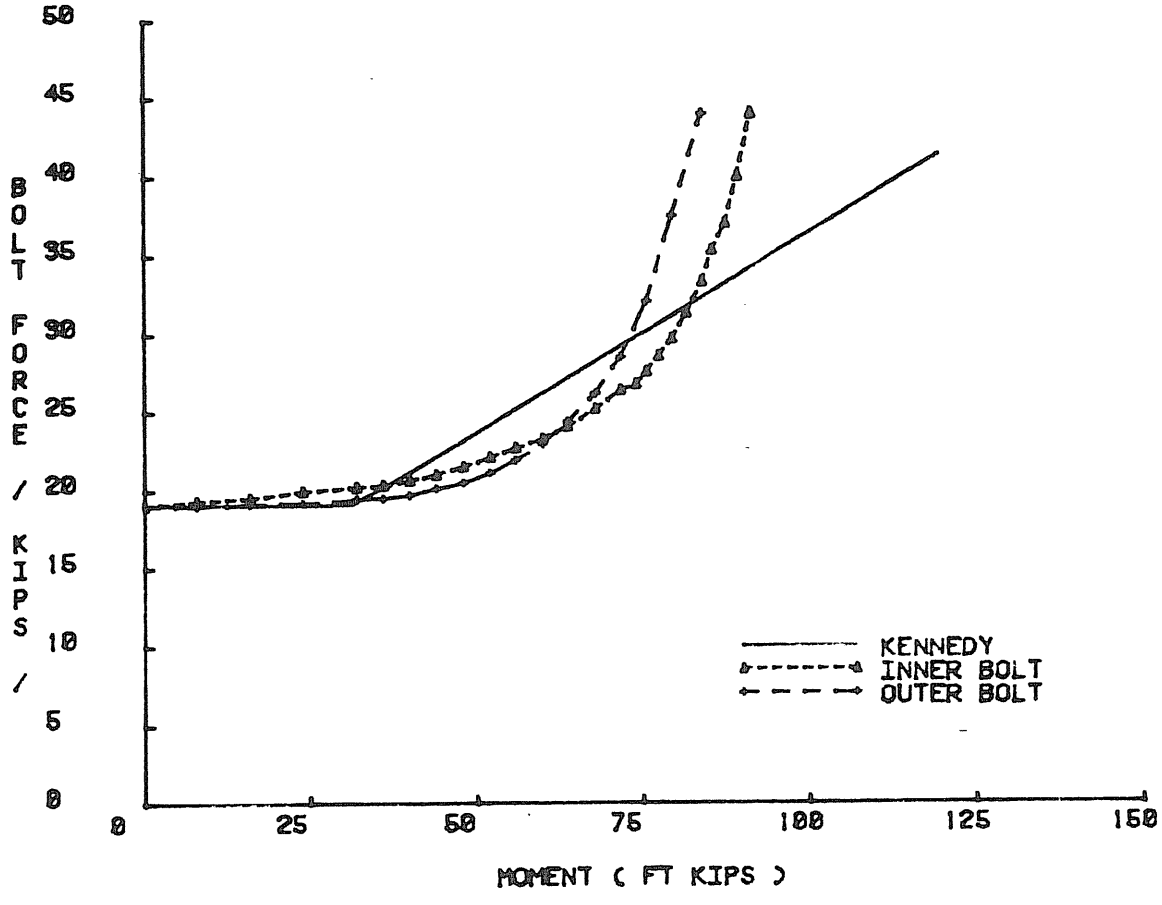

Figure H.4 BOLT FORCE VS MOMENT, F02-5/8-3/8-16

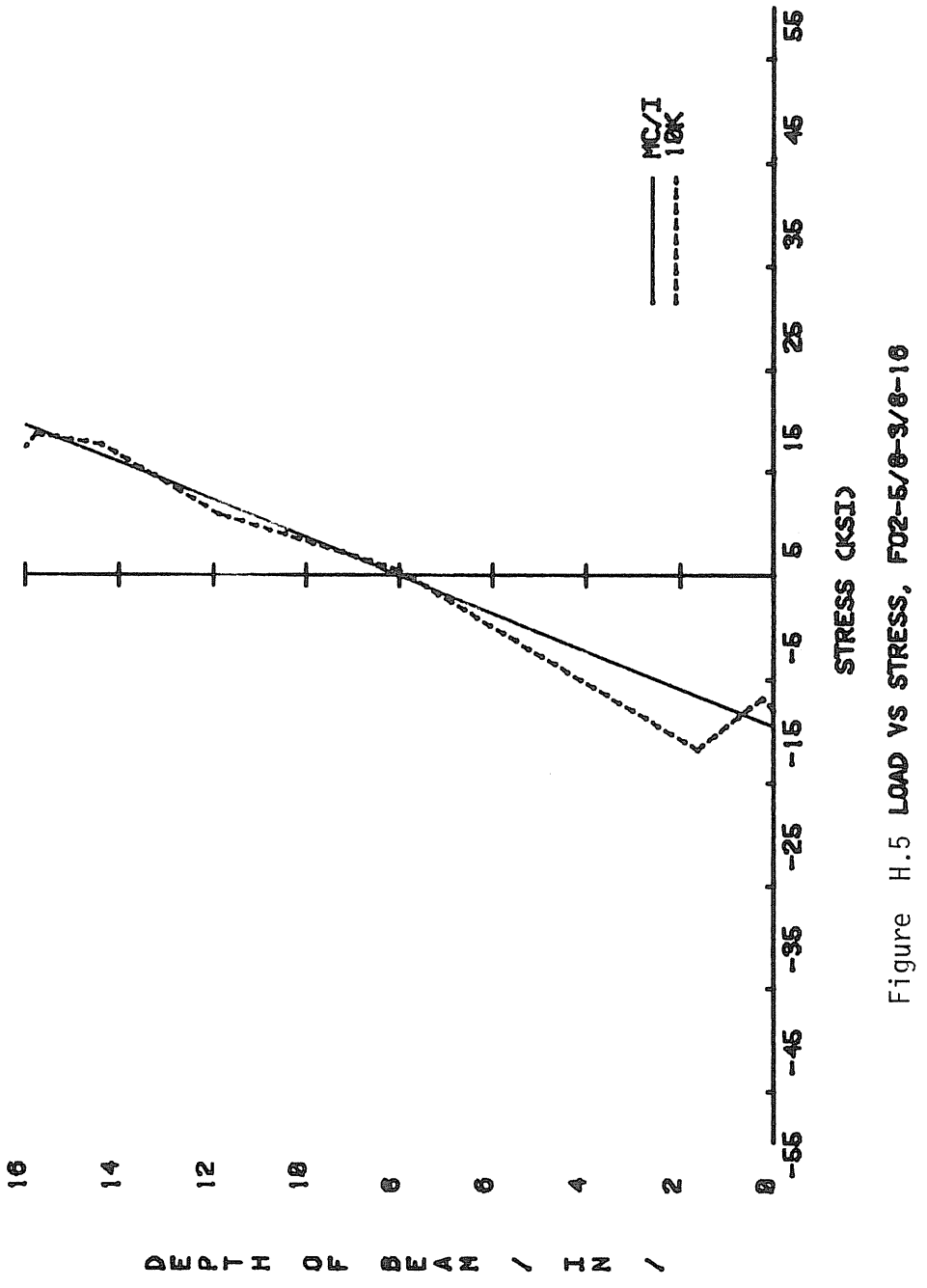

Figure H.5 LOAD VS STRESS, F02-5/8-3/8-16

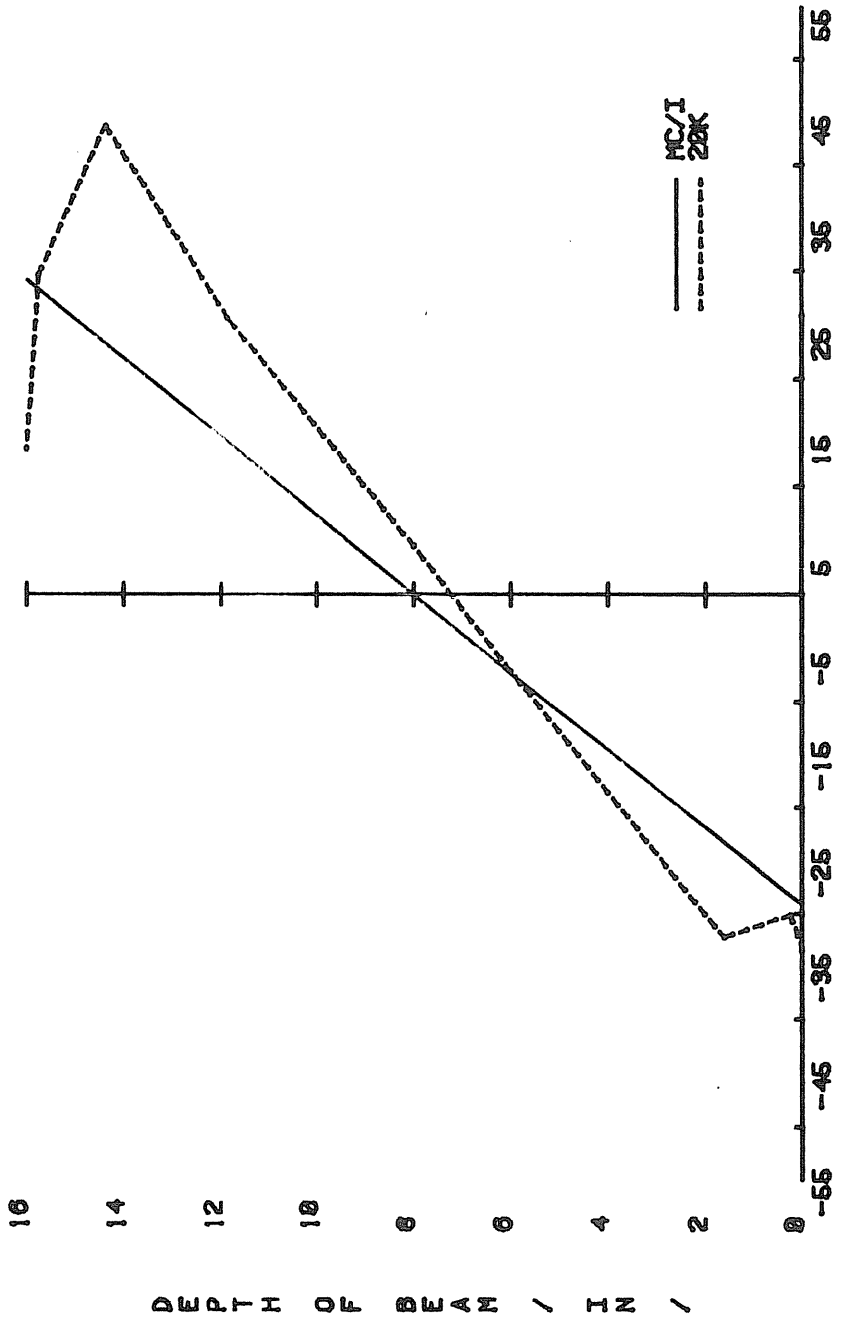

Figure H.6 **LOAD VS STRESS, F02-5/8-3/8-10**

APPENDIX I

FB2-3/4-1/2-23 TEST RESULTS

MBMA TEST SUMMARY

Project: MBMA Conn.

Test No.: FB2-3/4-1/2-23

Test Date: 7-2-84

Purpose: Load to failure - full pretension

Rows of Bolts in Tension: 2 Bolts/Row: 2

Bolt Diameter: .75 in. Plate Thickness: .50 in.

Beam Depth: 23 in. Flange Width: 6 in.

Web Thickness: .375 in. Flange Thickness: .375 in.

Moment of Inertia: 920 $in.^4$

Pretension Force: 28 kips

Failure Load: 41 kips vertical load; 254 ft.-kips at end plate

Failure Mode: Yielding of end plate

Predicted Failure Loads:

Method: Yield Line Theory Load: 41.9 kips or 260 ft.-kips

Method: Load:

Maximum Displacements:

Vertical: 3.20 in.

Horizontal top flange: .233 in.

Horizontal bottom flange: .240 in.

Maximum plate separation: East: .026 in. Centerline: .0405 in. West: —

Discussion:

- Instrumented bolts were used in the test. Pretension force was obtained by using the data acquisition system to monitor the bolt tension as torque was applied.
- Failure of end plate occurred at 41 kips (254 ft.-kips) which was 2% less than predicted by yield line analysis.
- Vertical deflection followed theoretical up to 60 ft.-kips at which point it began to lean over.
- Bolt forces reached proof load (38.8 kips) in the inner bolt at 29 kips (180 ft.-kips) and in the outer bolt at 35.5 kips (220 ft.-kips).

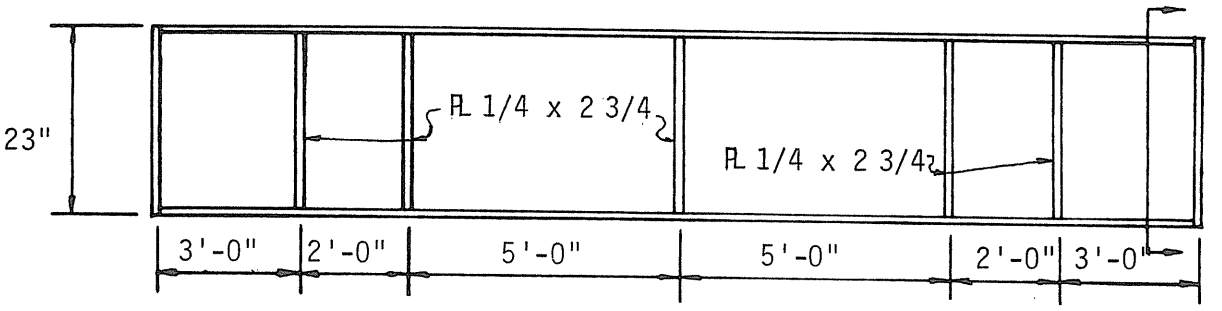

a) Elevation

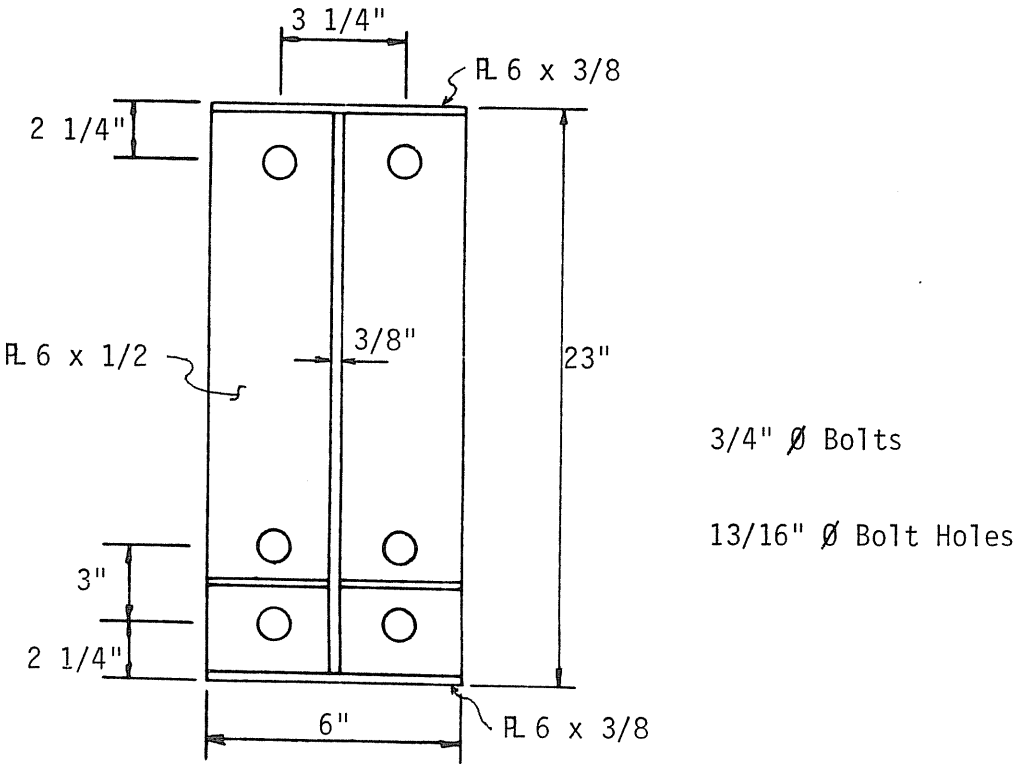

b) End Plate

Figure I.1 Specimen Details, Test FB2-3/4-1/2-23

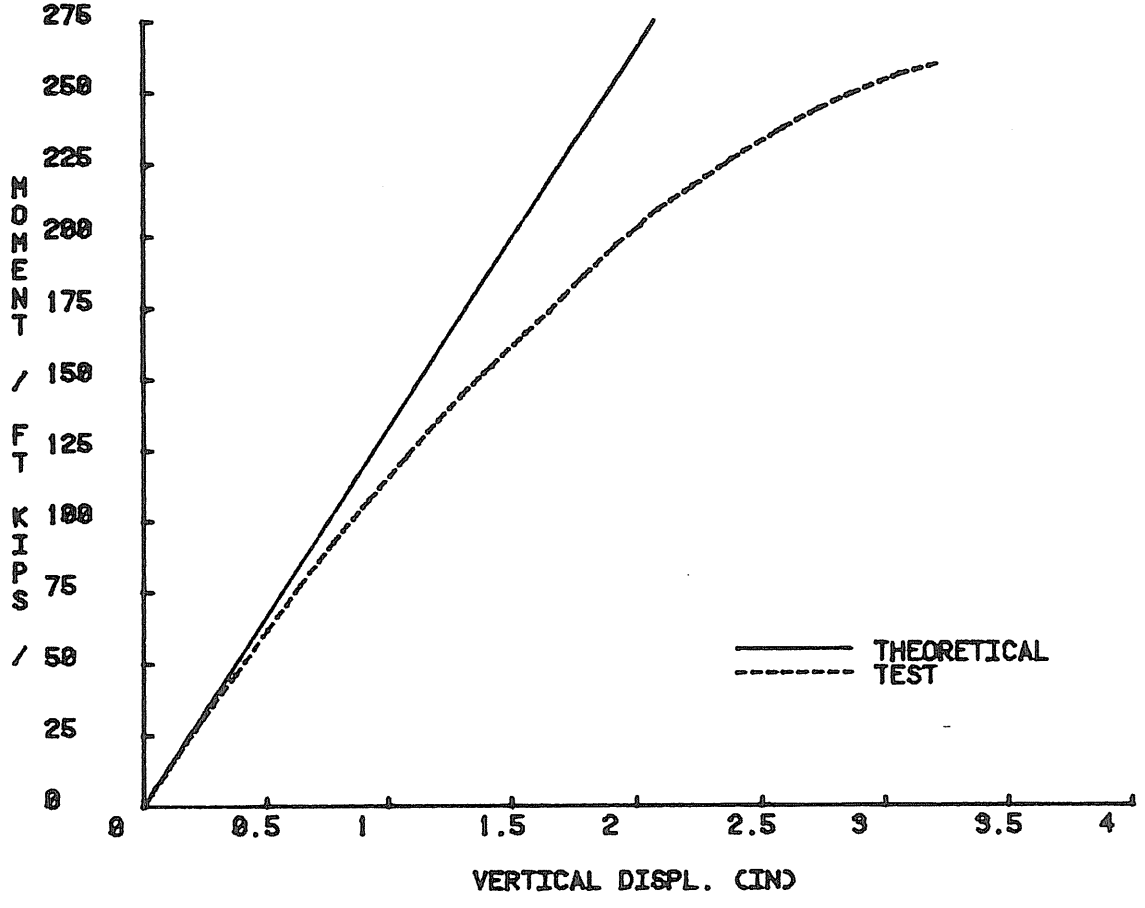

Figure I.2 **MOMENT VS VERTICAL DISPLACEMENT, FB2-3/4-1/2-23**

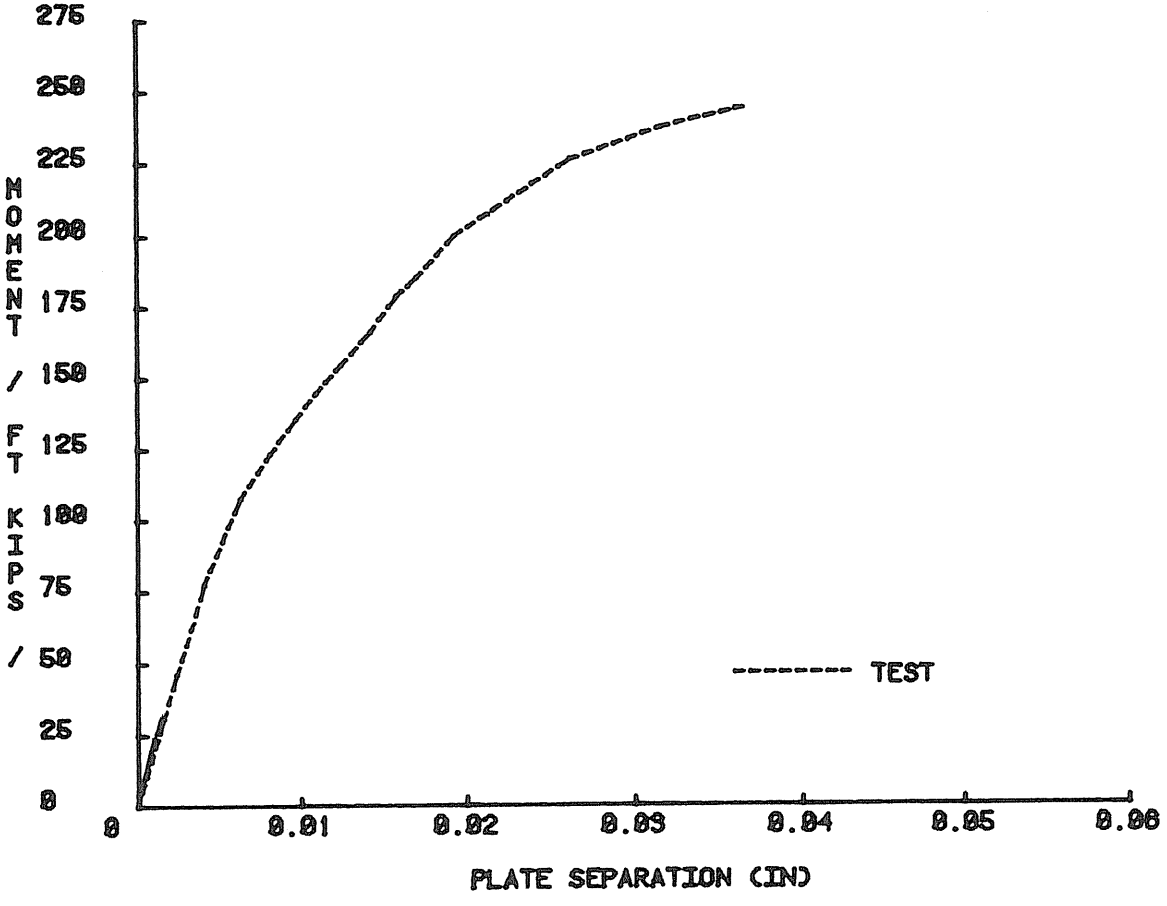

Figure I.3 MOMENT VS PLATE SEP., FB2-3/4-1/2-23

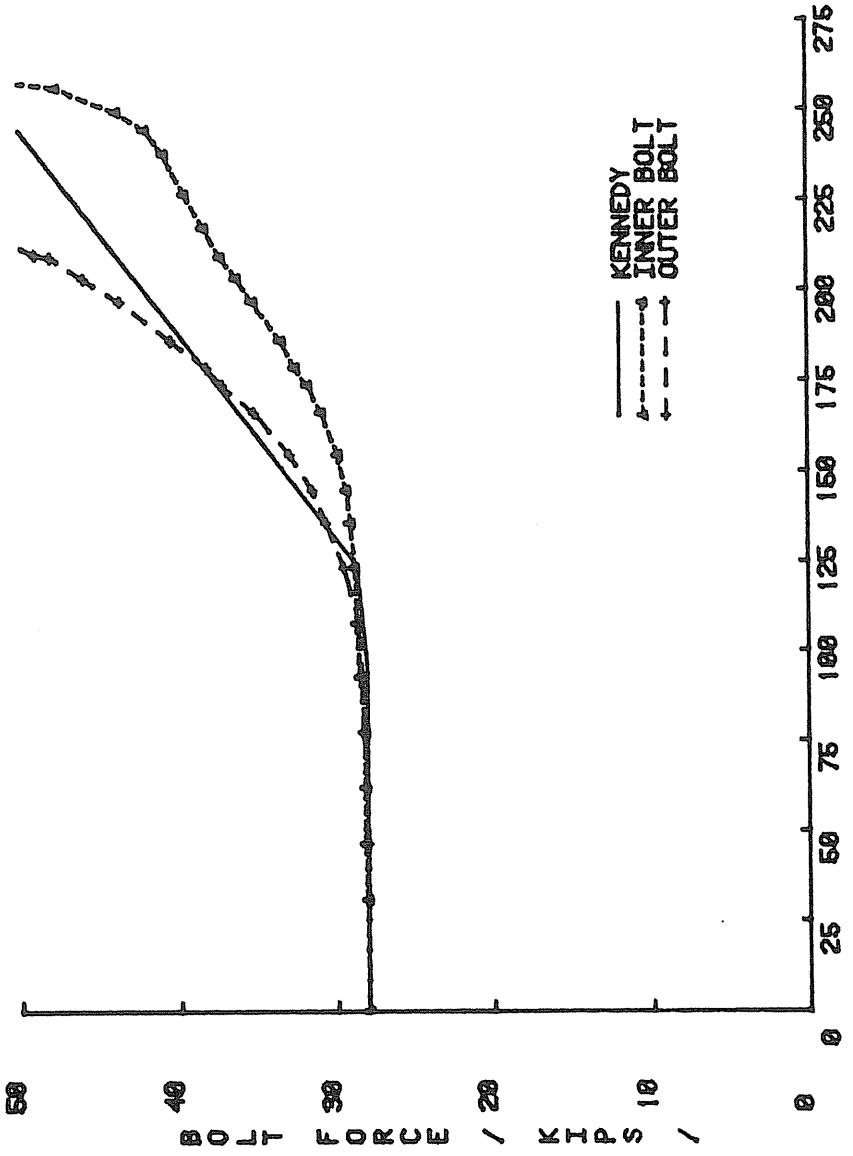

Figure I.4 MOMENT VS BOLT FORCE, FB2-3/4-1/2-23

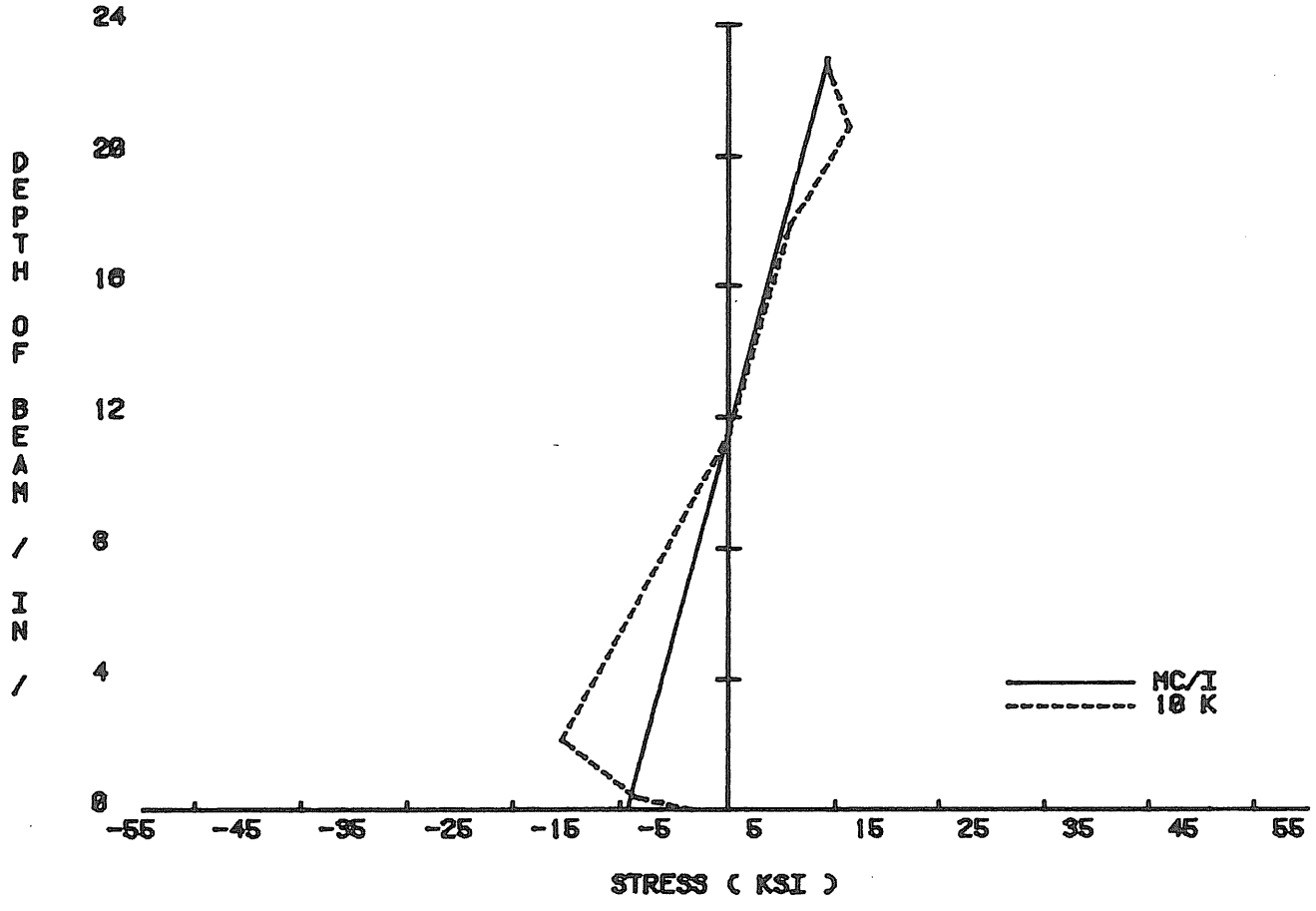

Figure I.5 **LOAD VS STRESS, FB2-3/4-1/2-23**

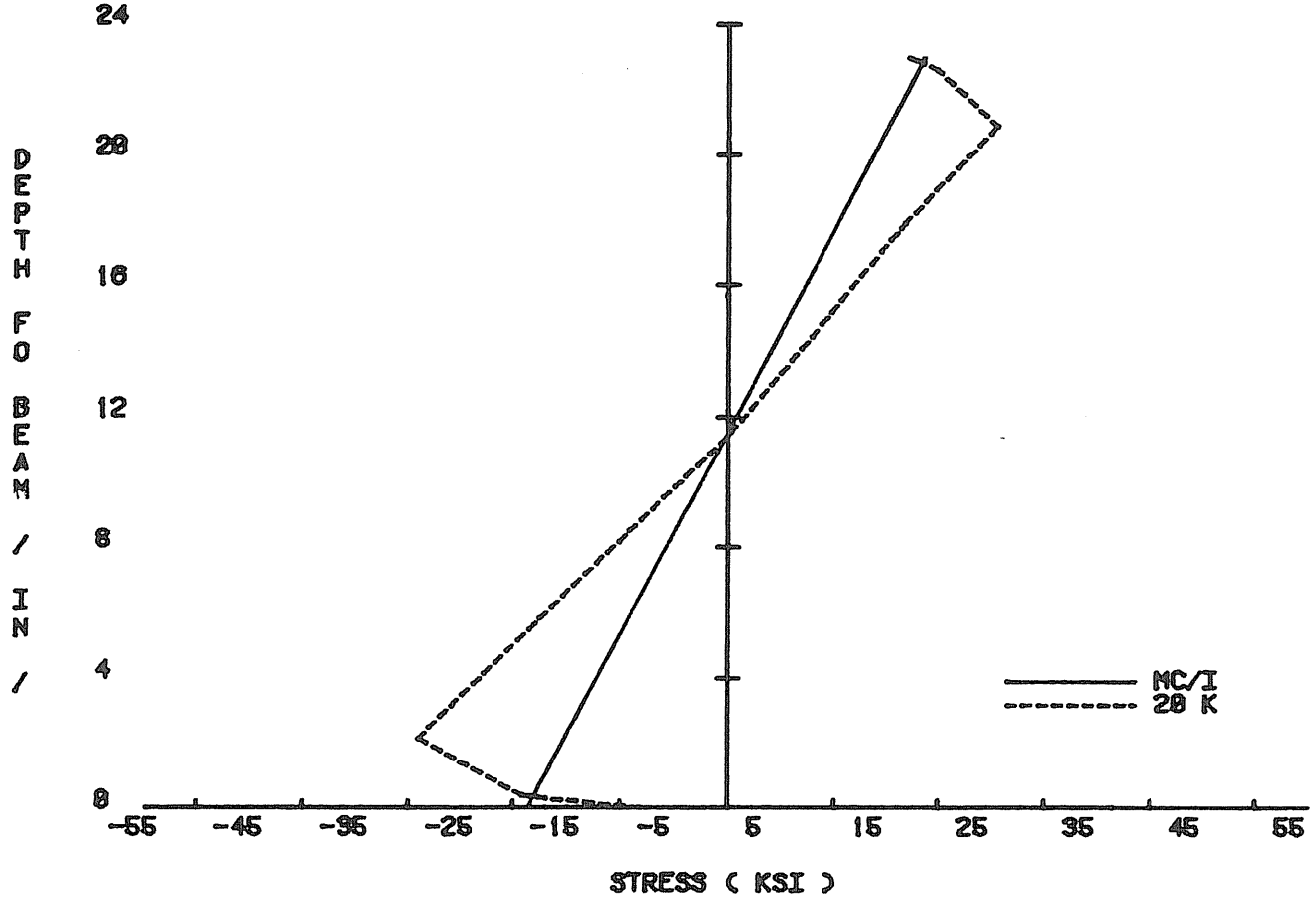

Figure I.6 **LOAD VS STRESS, FB2-3/4-1/2-23**

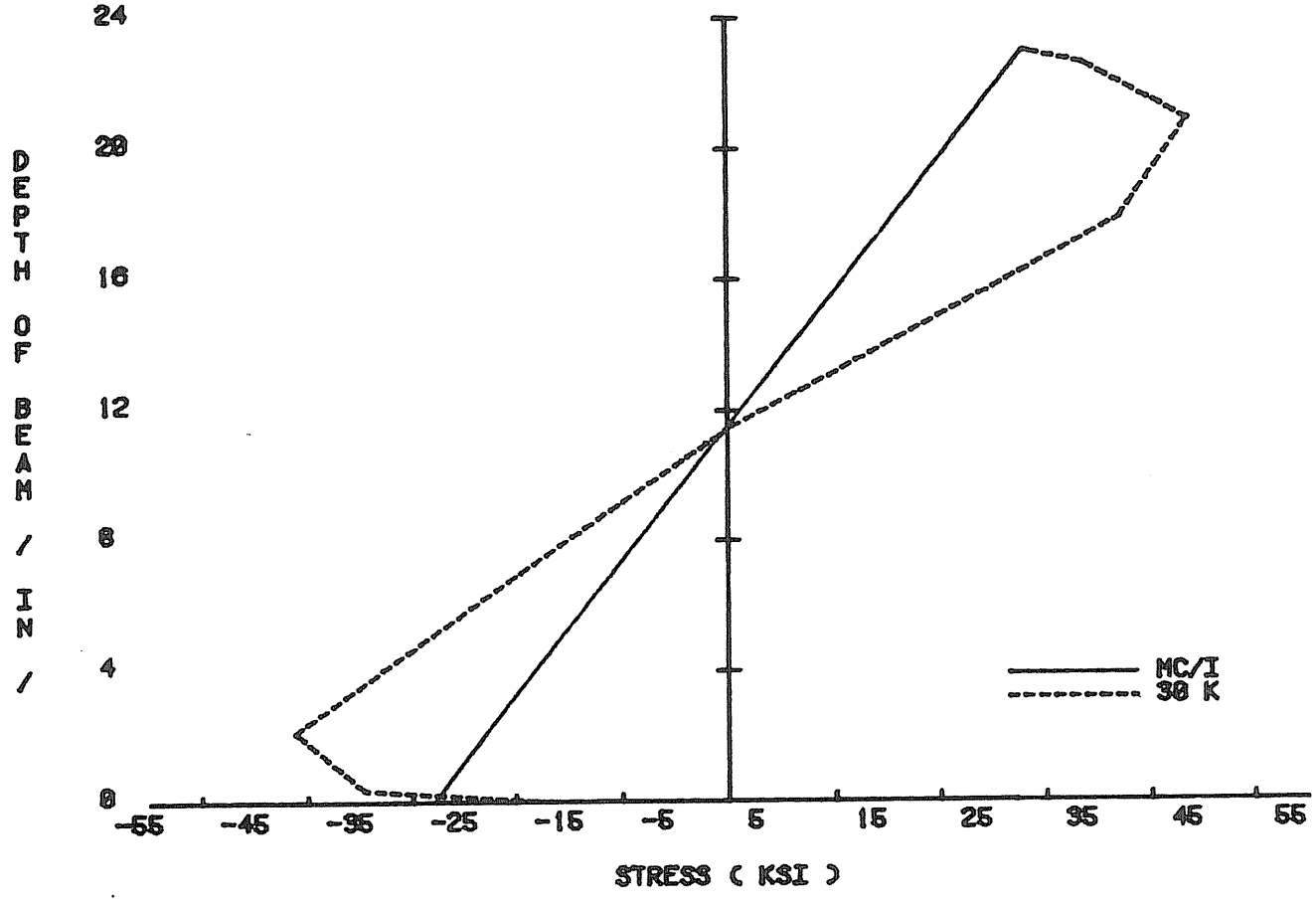

Figure I.7 LOAD VS STRESS, FB2-3/4-1/2-23

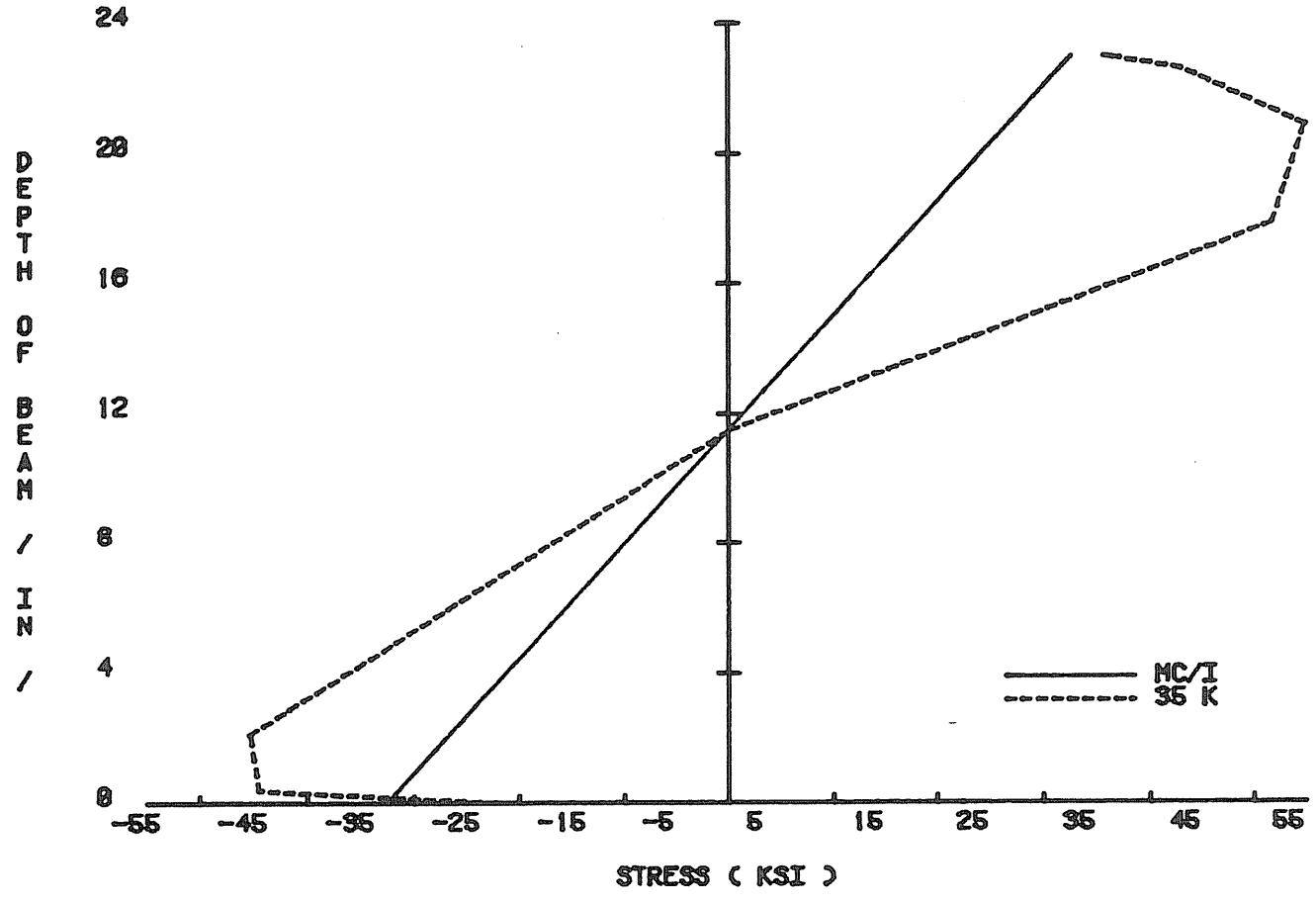

Figure I.8 **LOAD VS STRESS, FB2-3/4-1/2-23**

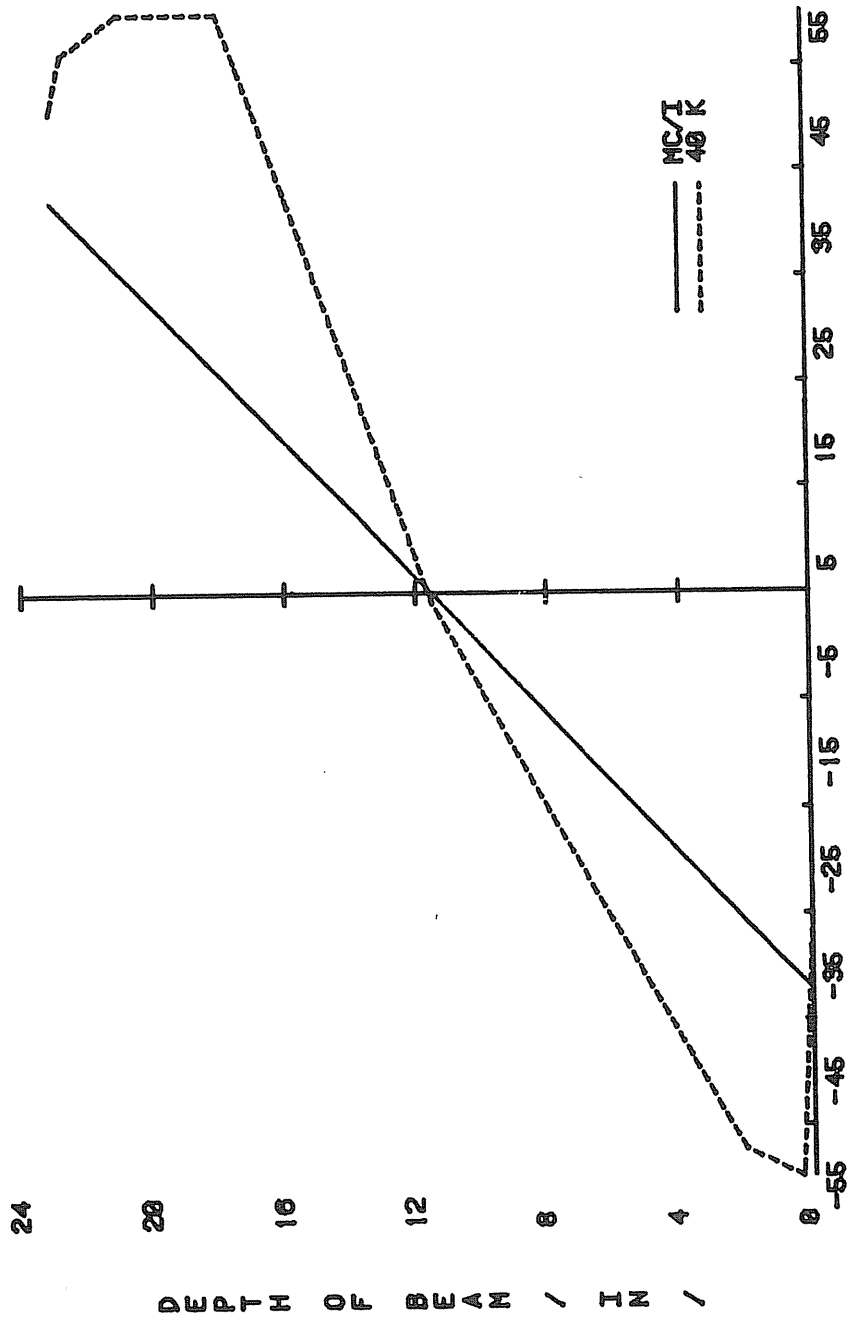

Figure I.9 LOAD VS STRESS, FB2-3/4-1/2-23

APPENDIX J

FO2-3/4-1/2-23 TEST RESULTS

MBMA TEST SUMMARY

Project: MBMA Conn.

Test No.: F02-3/4-1/2-23

Test Date: 7-6-84

Purpose: Load to failure - full pretension

Rows of Bolts in Tension: 2 Bolts/Row: 2

Bolt Diameter: .75 in. Plate Thickness: .5 in.

Beam Depth: 23 in. Flange Width: 6 in.

Web Thickness: .375 in. Flange Thickness: .375 in.

Moment of Inertia: 920 $in.^4$

Pretension Force: 28 kips

Failure Load: 34.5 kips vertical load; 207 ft.-kips at end plate

Failure Mode: Yielding of end plate

Predicted Failure Loads:

Method: Yield Line Theory Load: 36.3 kips or 218.0 ft.-kips

Method: Load:

Maximum Displacements:

Vertical: 1.862 in.

Horizontal top flange: .466 in.

Horizontal bottom flange: .128 in.

Maximum plate separation: East: .0166 in. Centerline: .046 in. West: —

Discussion:

- Instrumented bolts were used in the test. Pretension force was obtained by using the data acquisition system to monitor the bolt tension as torque was applied.
- Failure of end plate occurred at 34.5 kips (207 ft.-kips) which was 5% less than predicted by yield line analysis.
- Vertical deflection followed theoretical up to 70 ft.-kips at which point it began to lean over.
- Bolt forces reached proof load (38.8 kips) in the inner bolt at 27.6 kips (166 ft.-kips) and in the outer bolt at 28.4 kips (170 ft.-kips).

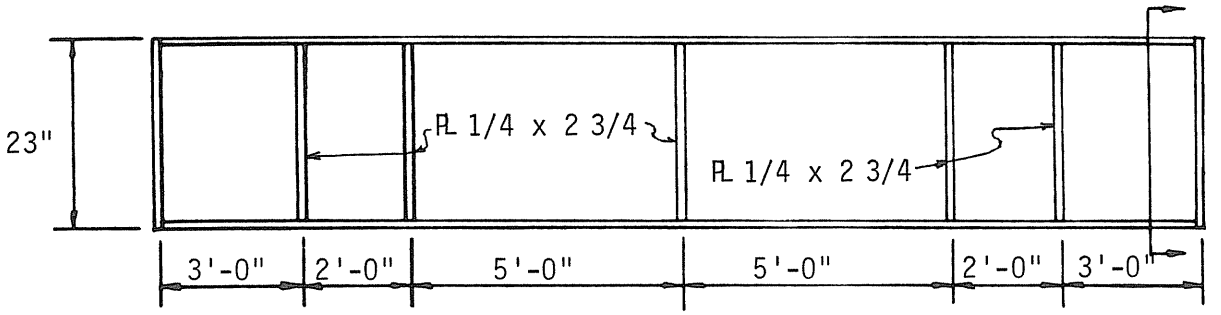

a) Elevation

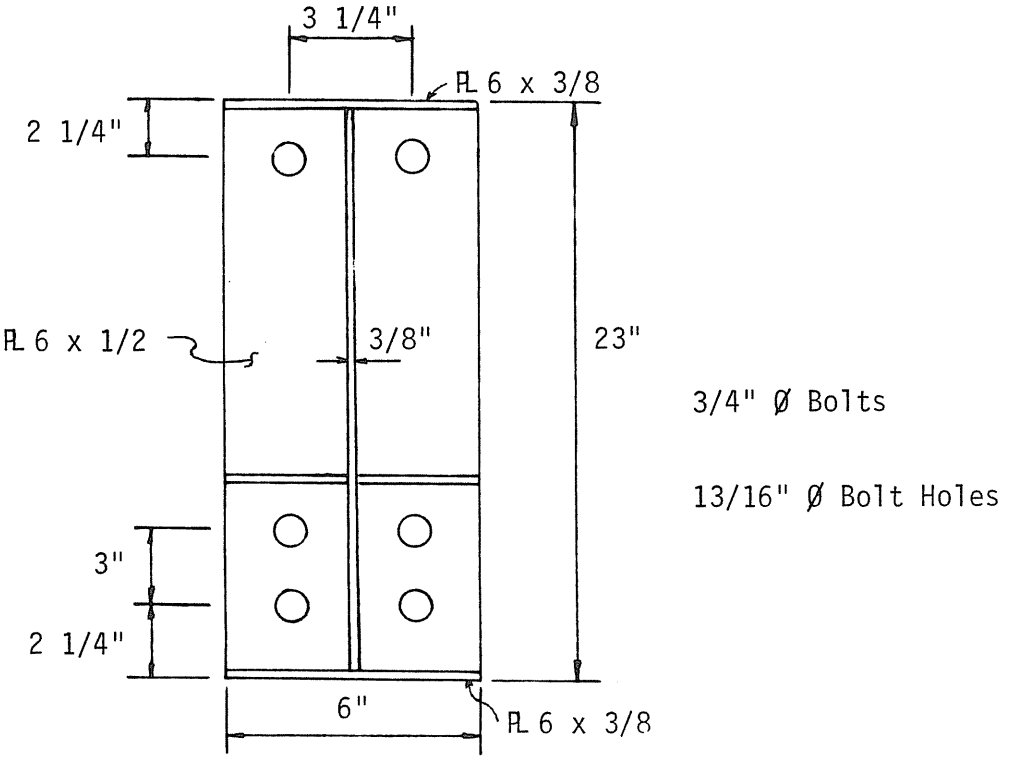

b) End Plate

Figure J.1 Specimen Details, Test F02-3/4-1/2-23

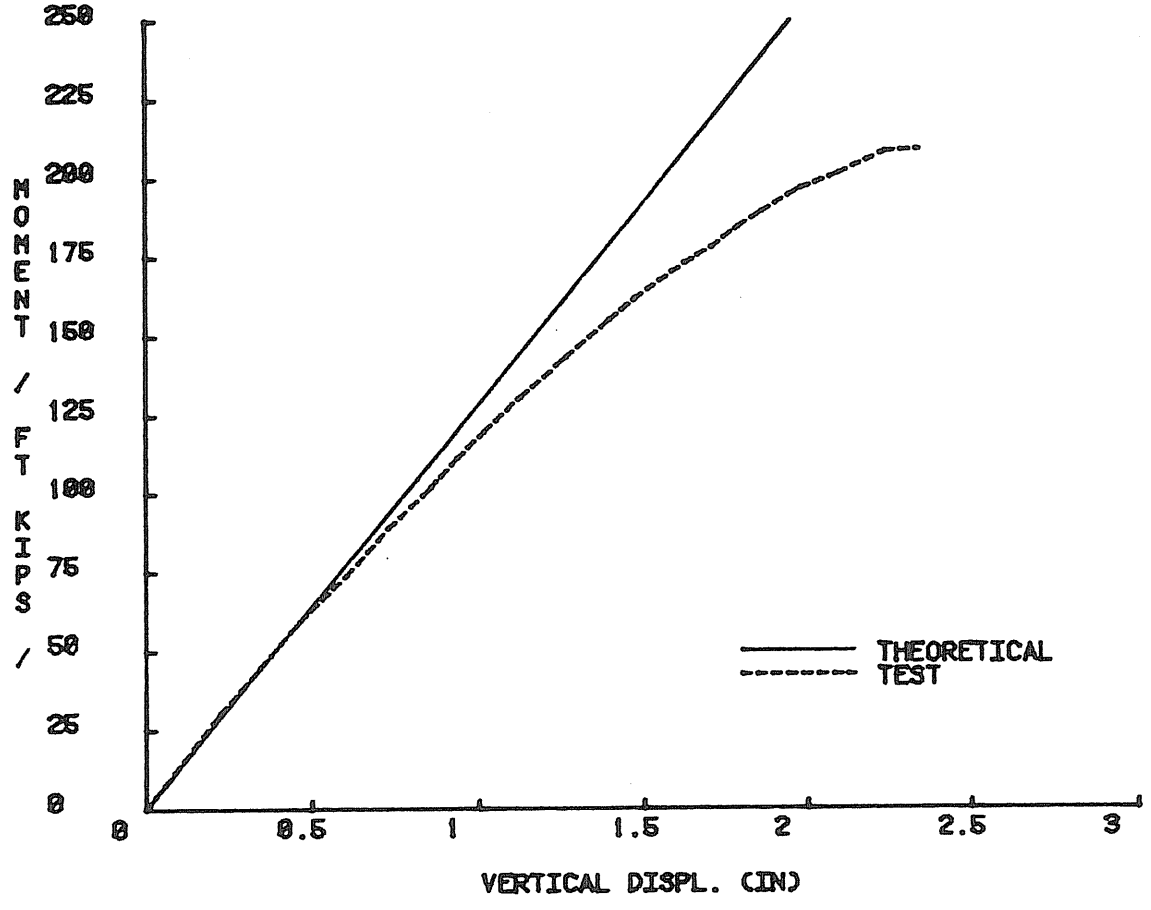

Figure J.2 **MOMENT VS VERTICAL DISPLACEMENT, F02-3/4-1/2-23**

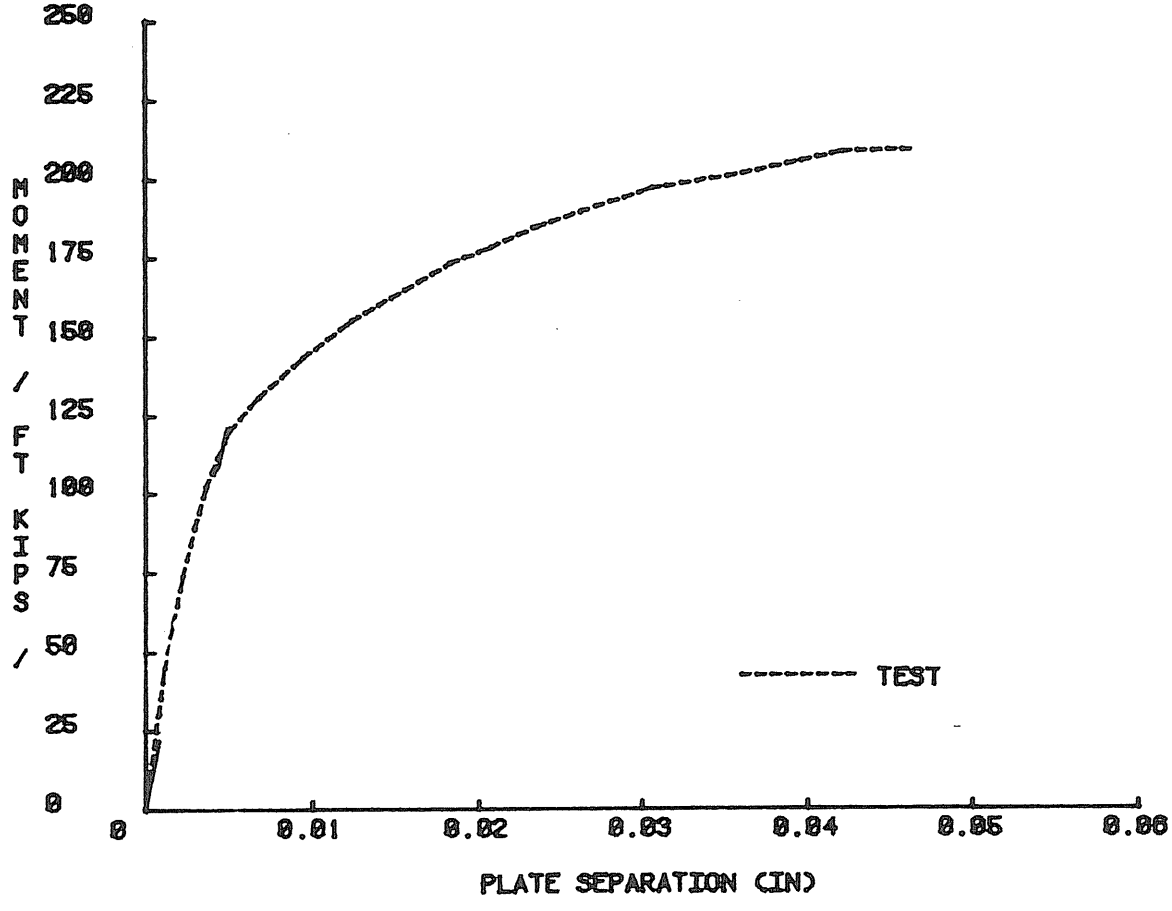

Figure J.3 MOMENT VS PLATE SEPARATION, F02-3/4-1/2-23

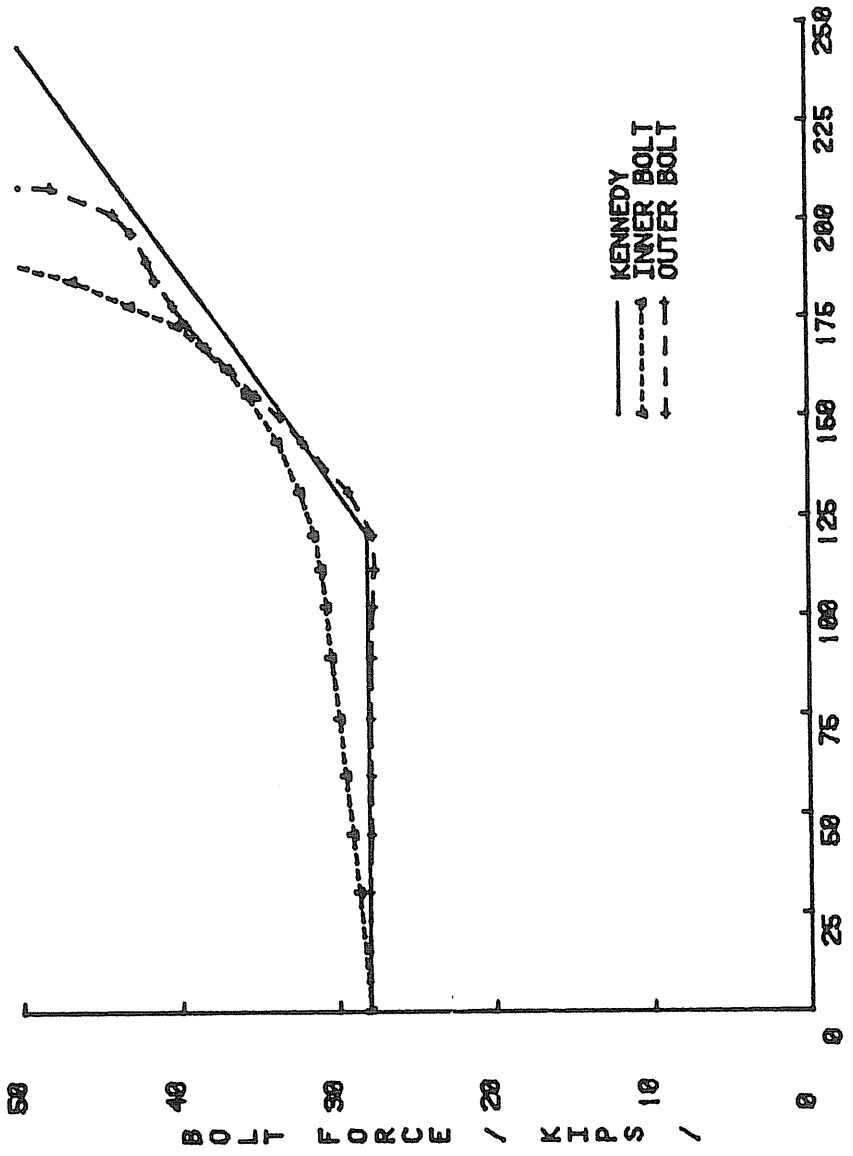

Figure J.4 BOLT FORCE VS MOMENT, F02-3/4-1/2-23

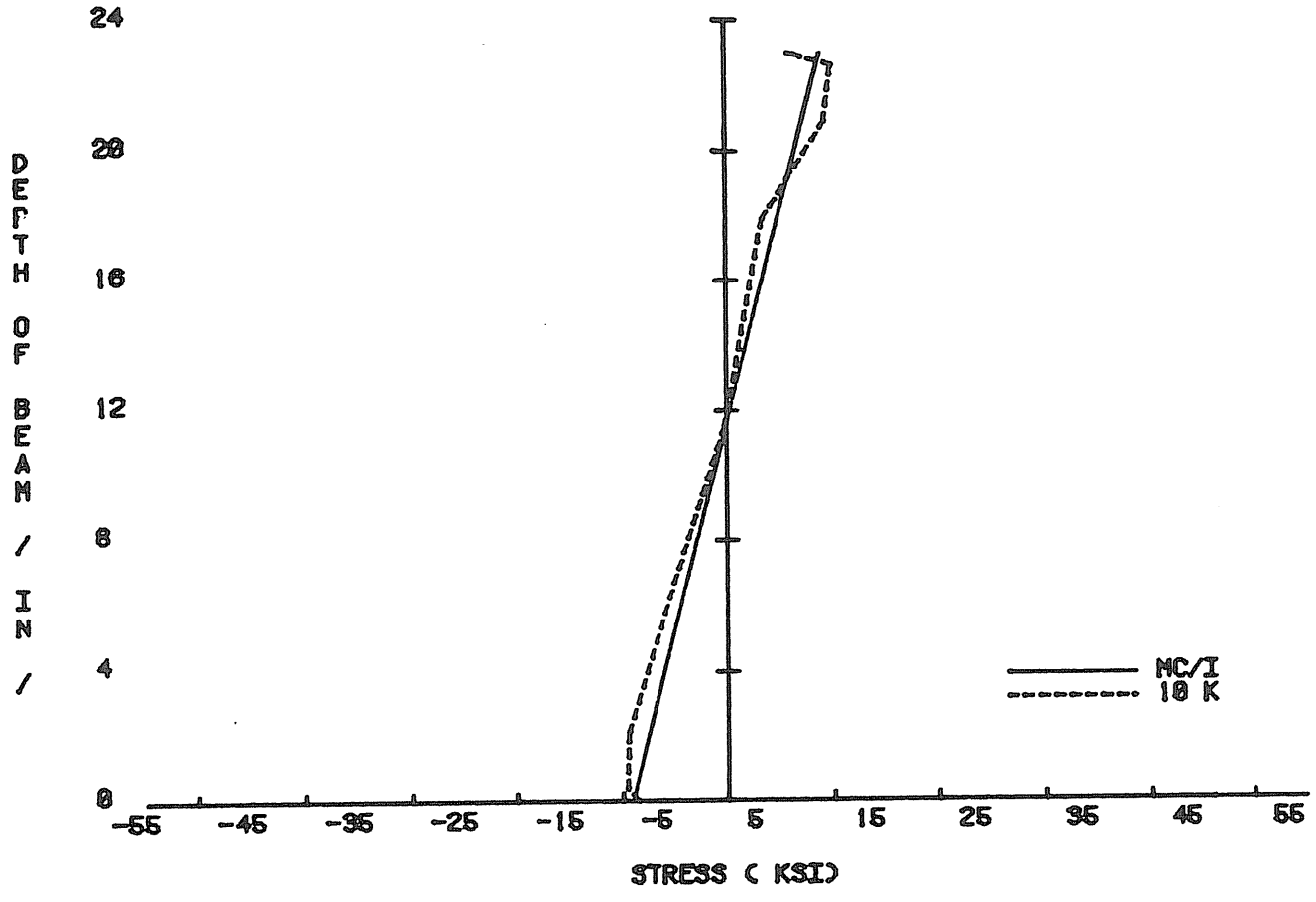

Figure J.5 **LOAD VS STRESS, F02-3/4-1/2-23**

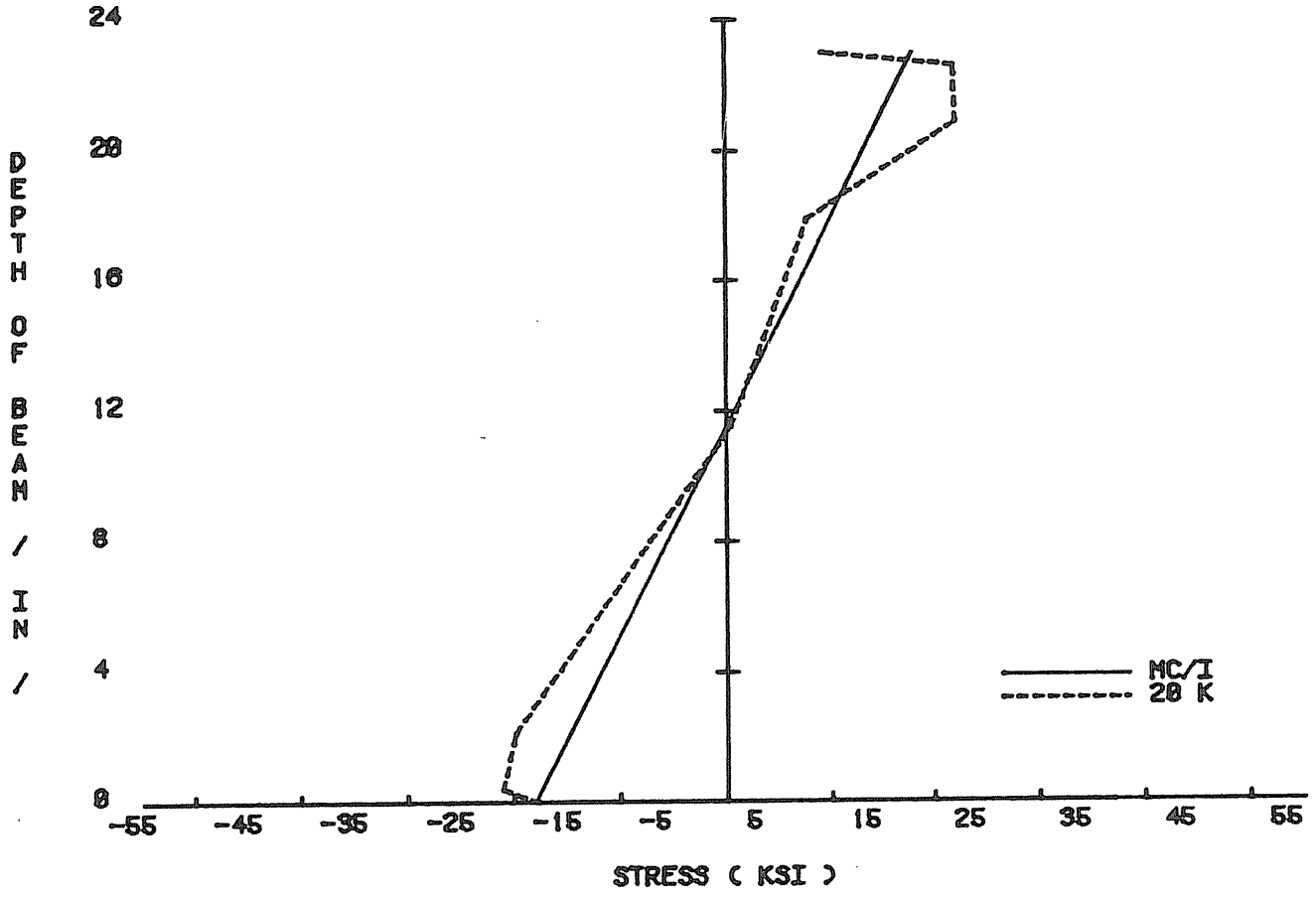

Figure J.6 **LOAD VS STRESS, F02-3/4-1/2-23**

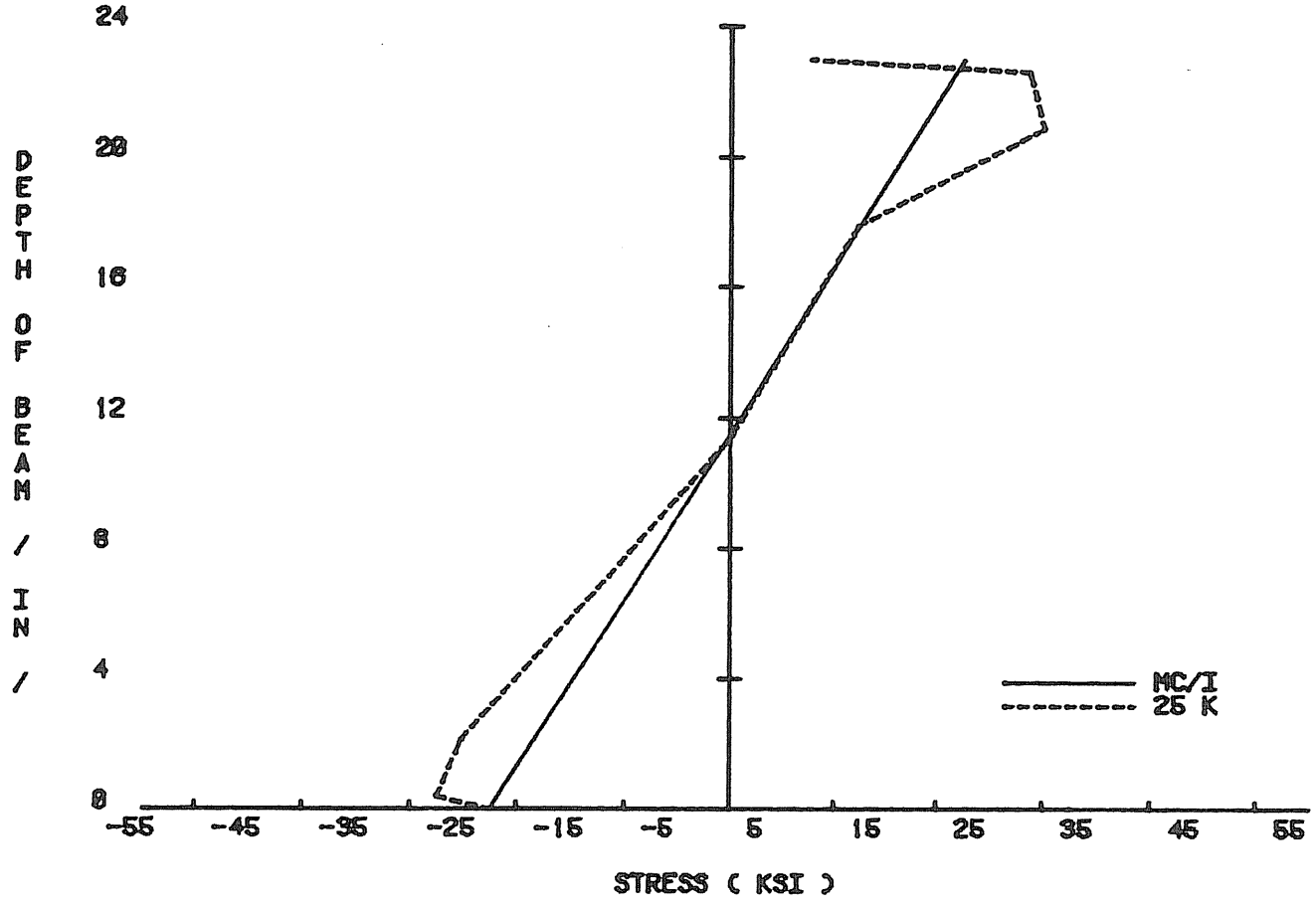

Figure J.7 **LOAD VS STRESS, F02-3/4-1/2-23**

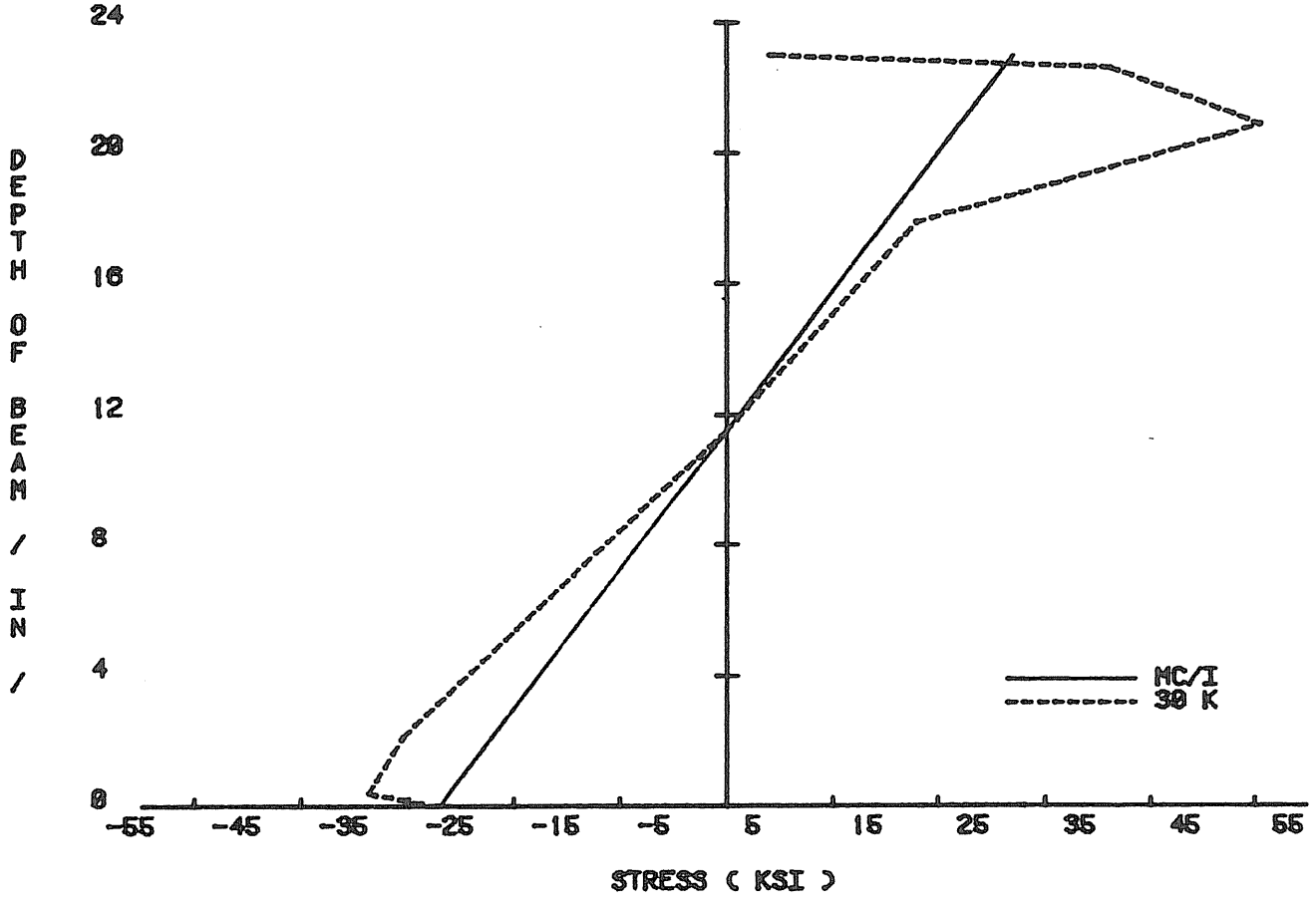

Figure J.8 **LOAD VS STRESS, F02-3/4-1/2-23**

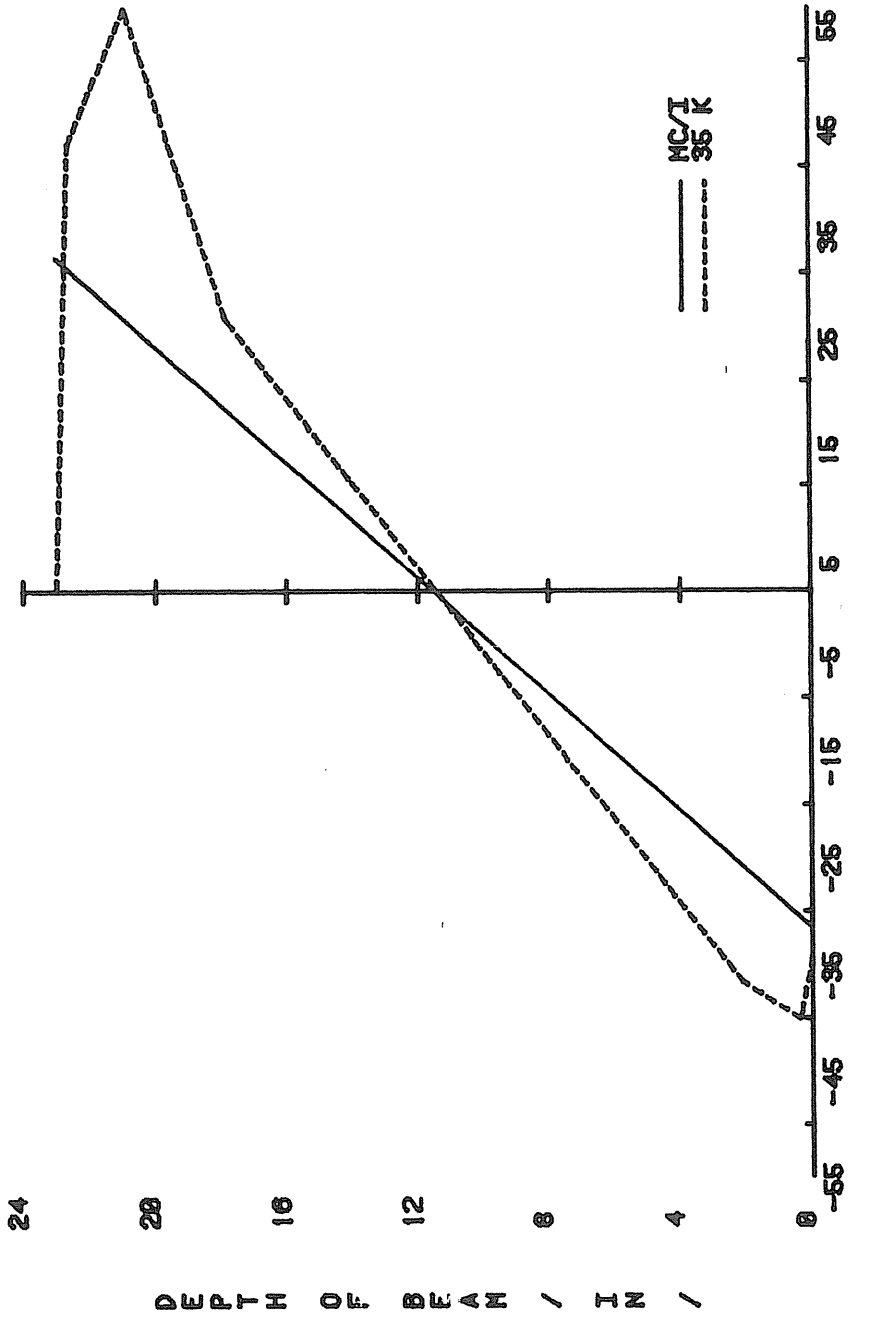

Figure J.9 LOAD VS STRESS, F02-3/4-1/2-23